



Contract Number: 622177

## Deliverable D3.2

# Wireless data transmission systems for repository monitoring

Work Package 3, Task 2

Project Acronym	Modern2020
Project Title	Development and Demonstration of Monitoring Strategies and Technologies for Geological Disposal
Start date of project	01/06/2015
Duration	48 Months
Lead Beneficiary	AMBERG
Contributor(s)	<i>T.J. Schröder (ed., NRG), E. Rosca-Bocancea (NRG), J.L. García-Siñeriz (AMBERG), G. Hermand (ANDRA), H.L. Abós Gracia (ARQUIMEA), J.C. Mayor Zurdo (ENRESA), J. Verstricht (EURIDICE), P. Dick (IRSN), J. Eto (RWMC), M. Sipilä and J.-M. Saari (VTT)</i>
Contractual Delivery Date	29/09/2018
Actual Delivery Date	27/03/2019
Reporting period:	3
Version	Final

***Project co-funded by the European Commission under the Euratom Research and Training Programme on Nuclear Energy within the Horizon 2020 Framework Programme***

Dissemination Level		
<b>PU</b>	Public	X
<b>PP</b>	Restricted to other programme participants (including the Commission Services)	
<b>RE</b>	Restricted to a group specified by the partners of the Modern2020 project	
<b>CO</b>	Confidential, only for partners of the Modern2020 project and EC	



History chart			
Type of revision	Document name	Partner	Date
First set-up	<i>Modern2020_T3_D3.2_Final Report_v01.docx</i>	NRG	20.11.2017
2 <sup>nd</sup> set-up	<i>Modern2020_T3_D3.2_Final Report_v02.docx</i>	NRG	8.2.2018
Contribution	<i>Modern2020_T3_D3.2_Final Report_v02a_RWMC_r1.docx</i>	RWMC	10.4.2018
Contribution	<i>Modern2020_D3.2_VTT Final_report_Wireless data.docx</i>	VTT	13.4.2018
Integration of contributions	<i>Modern2020_T3_D3.2_Final Report_v03.docx</i>	NRG	3.5.2018
Update contribution	<i>Modern2020_D3.2_VTT Final_report_Wireless data_09 05 2018.docx</i>	VTT	9.5.2018
Contribution	<i>Modern2020_T3_D3.2_Final Report_ARQ_v0.docx</i>	Arquimea	9.5.2018
Contribution	<i>Modern2020_T3_D3.2_Final Report_v02a_RWMC_r1_Andra_v0r1.docx</i>	Andra, RWMC	14.5.2018
Integration of contributions	<i>Modern2020_T3_D3.2_Final Report_v04.docx</i>	NRG	28.5.2018
Contribution	<i>Modern2020_T3_D3.2_Final Report_v02a_PDi.docx</i>	IRSN	31.5.2018
Integration of contributions	<i>Modern2020_T3_D3.2_Final Report_v05.docx</i>	NRG	28.5.2018
Update/contribution	<i>Modern2020_T3_D3.2_Final Report_v04_PDi.docx</i>	IRSN	4.6.2018
Update/contribution	<i>Modern2020_T3_D3.2_Final Report_v04_Arq_update.docx</i>	Arquimea	4.6.2018
Update	<i>Modern2020_T3_D3.2_Final Report_v04_RWMC_r.docx</i>	RWMC	11.6.2018
Update	<i>Modern2020 D3.2 chapter 5.3_VTT_12 06 2018.docx</i>	VTT	12.6.2018
Contribution	<i>Modern2020 D3.2 chapter 5.4_VTT+ARQ_12 06 2018a.docx</i>	VTT & Arquimea	12.6.2018
Update	<i>Modern2020 D3.2 chapter 5.4_draft_VTT_14 06 2018.docx</i>	VTT	13.6.2018
Integration of contributions	<i>Modern2020_T3_D3.2_Final Report_v06.docx</i>	NRG	14.6.2018
Review	<i>Modern2020_T3_D3.2_Final Report_v06_JCMAYOR.docx</i>	ENRESA	18.6.2018
Review & contribution	<i>Modern2020_T3_D3.2_Final Report_v06_revGH_18june.docx</i>	Andra	21.6.2018
Review	<i>Modern2020_T3_D3.2_Final Report_v06_RWMC.docx</i>	RWMC	21.6.2018
Updated final draft	<i>Modern2020_T3_D3.2_Final Report_v07.docx</i>	NRG	25.6.2018
Review	<i>Modern2020_T3_D3.2_Final Report_v06_ARQ.docx</i>	Arquimea	25.6.2018
Review	<i>Modern2020_T3_D3.2_Final Report_v06_VTT comments_26 06 2018.docx</i>	VTT	25.6.2018
Review	<i>Modern2020_T3_D3.2_Final Report_v07_s_RWMC.docx</i>	RWMC	26.6.2018
Review	<i>Modern2020_T3_D3.2_Final Report_v07_JCMAYOR.docx</i>	ENRESA	26.6.2018
Final draft	<i>Modern2020_T3_D3.2_Final Report_v08.docx</i>	NRG	28.6.2018
Update	<i>Modern2020_T3_D3.2_Final Report_v08_final draft_ARQ.docx</i>	Arquimea	29.6.2018
Contribution	<i>D3.2Chap7.1Andra.docx</i>	Andra	6.8.2018
Review & contribution	<i>Modern2020_T3_D3.2_Final Report_v08a_Amberg.docx</i>	AMBERG	04.8.2018
Final draft after internal review by WPL	<i>Modern2020_T3_D3.2_Final Report_v10.docx</i>	NRG	15.9.2018
Update	<i>Modern2020_T3_D3.2_Final Report_v10_JLGS.docx</i>	Amberg	26.10.2018
Update final draft for review by EB	<i>Modern2020_T3_D3.2_draft_Final Report.docx</i>	NRG	26.10.2018
Contribution	<i>contribution_7_2.docx</i>	EURIDICE	9.11.2018
Review by EB (B. Frieg)	<i>Modern2020_T3_D3.2_draft_Final Report_Fbe.docx</i>	Nagra	20.12.2018
Final draft after EB review	<i>Modern2020_T3_D3.2_draft_Final Report_Fbe_TJS.docx</i>	NRG	10.1.2019
Update	<i>contribution_7_2_TJS_JVe.docx</i>	EURIDICE	25.3.2019
Final version	<i>Modern2020_T3_D3.2.docx</i>	NRG	27.3.2019



**Reviewed by:**

Berng Frieg (Nagra).

**Approved by:**

This report has been approved by:

- José-luis Garcia-Sineriz, Work Package 3 Leader, *27/03/2019*
- Johan Bertrand, the Modern2020 Project Co-ordinator (on behalf of the Modern2020 Project Executive Board), *31/05/2019*



## Abstract

This report represents the final technical report and summarizes the work performed in Task 3.2, *Wireless data transmission systems for repository monitoring*, of the EU H2020 project Modern2020. It integrates contributions from Amberg, Andra, Arquimea, ENRESA, EURIDICE, IRSN, NRG, RWMC, and VTT and is prepared and compiled by NRG.

Wireless systems allow transmitting monitoring data over natural and engineered barriers without the use of cables that may impair the safety function of those barriers. The barriers of interest could be anything from the concrete buffer of a supercontainer design, a borehole plug, sealings of disposal sections or a shaft sealing: wireless solutions are necessary that can bridge distances from less than a meter up to several hundred meters.

For the wireless transmission of data, electromagnetic waves are used nowadays in many applications, as they can be transmitted easily over long distances in air. However, the presence of solid media as the host rock and its contained water or different components of the engineered barrier system can impede their propagation. Conventional data transmission solutions make use of high-frequencies (hundreds of MHz to GHz), which limits their applicability in a geologic waste disposal facility to short distances (few meters). This has raised the need to develop specific solutions for repository monitoring based on lower frequencies (kHz to few MHz).

Building on the results of the preceding MoDeRn project, Task 3.2 aims to address gaps with respect to wireless technologies as indicated in [1]. Task 3.2 is divided into three subtasks:

- Subtask 1: Improve existing short range (tens of meters) wireless systems based on high or medium frequencies
- Subtask 2: Improve existing long range (hundreds of meters) wireless systems based on low frequencies
- Subtask 3: Evaluate the use of a combination of different range wireless systems to provide a complete data transmission solution

This report summarizes the work of all partners contributing to Task 3.2:

- Implementation of a Wireless Testing Bench (WTB) at the Tournemire URL (IRSN, ENRESA & Aitemin)
- Increase of the range of short range data transmission system through hydrating sealing material (Aitemin & Arquimea)
- Development of a 125-kHz-based short range data transmission system (VTT)
- Understanding and improvements of a long range data transmission system (Andra)
- Implementation of signal hopping strategies to provide robust data transmission over longer transmission distances (RWMC)
- Evaluation of an adapted wireless Through-the-Earth commercial technology (Amberg & ENRESA)
- Test of a miniaturized transmitter for vibrating wire sensor in the WTB (Andra)
- Link of the *m/NT* interrogator behind a supercontainer buffer with a wireless transmitter (EURIDICE)
- Evaluation of a combination of wireless data transmission systems that allow transmitting sensor readings from the inside of a disposal cell to the surface on top of the Tournemire URL (Amberg, Arquimea, IRSN, and NRG)

Within Task 3.2, a major step has been achieved in understanding, designing and demonstrating specific solutions that allow transmitting data through components of the EBS or the host rock. Different technological solutions covering transmission distances between 0.1 and more than 275 m have been developed and tested, covering a variety of application situations, disposal concepts, and host rocks. A greater understanding of the underlying technical and physical principles has been achieved, and the provided solutions have been tested under realistic conditions, e.g. in the Tournemire Wireless Testing Bench (WTB), from the Tournemire tunnel to the surface plateau, or in the VTT underground laboratory. The performance of the developed technologies depends on a number of factors, allowing data transmission over distances of 275 m through the underground with a power consumption per



transmitted bit below 5 mWs, or over 4 m or more of a (partially) saturated barrier with a power consumption below 1 mWs/bit.

The experience gained at the Tournemire URL, the Hades URL and the Andra URL raises confidence that long range transmission over distances larger than 300 m can be achieved as well. Methods have been developed and successfully applied to quantify transmission behaviour from in situ measurements, allowing the estimation of data transmission power needs for each location of interest with relatively small effort. In addition to direct transmission of data from an underground disposal to the surface in a single stage, a system is presented featuring data transmission from the disposal facility to the surface in several stages, by means of several sequential relays.

With regard to short range data transmission over distances of 1 to 30 m, several options are available, operating at frequencies between 4 kHz and 2.2 MHz. Each one of those technologies has its own advantages, and successful data transmission through solid media has been demonstrated for all of them. Versatile, "all-in-one" solutions, integrating different analog and digital sensors, have been developed and tested under realistic conditions at the WTB facility in Tournemire. Along with earlier works at a frequency of 10 kHz, a variety of options and transmission frequencies for various application cases of interest are available on the short range.

In an integrated approach, the possibility of an overall transmission chain allowing data transmission from the inside of a disposal cell to the surface on top of the Tournemire URL was assessed.

By combining different short and long range expertises and solutions, a wireless transmission chain in two stages was projected and will be demonstrated in the second half of 2018 as part of Modern2020's WP4.3.



## Table of content

Abstract.....	4
List of Figures .....	8
List of Tables .....	10
Glossary.....	11
1. Introduction.....	12
2. Objectives of Task 3.2.....	13
3. Scope of this Report .....	14
4. Wireless data transmission in repository monitoring .....	15
4.1. Principles of wireless data transmission.....	15
4.2. Current status of wireless technologies in repository monitoring.....	16
5. Short range wireless data transmission systems .....	18
5.1. Implementation of a Wireless Testing Bench (WTB).....	18
5.1.1. WTB layout.....	18
5.1.2. Installation and first tests.....	20
5.2. Increasing operating range in hydrating sealing material .....	20
5.2.1. Concept description and methodology .....	20
5.2.2. Feasibility tests .....	21
5.2.3. Experimental set-up.....	23
5.2.4. Final design.....	25
5.2.5. Summary .....	26
5.3. Wireless data transmission system at 125 kHz.....	27
5.3.1. Background and objectives .....	27
5.3.2. Data reception from weak signals .....	28
5.3.3. Developed hardware .....	28
5.3.4. Signal modulation and data encoding .....	29
5.3.5. Results .....	30
5.3.6. Summary .....	31
5.4. Adaptation and testing of wireless Through-the-Earth commercial technology .....	31
5.4.1. Background and objectives .....	31
5.4.2. Specifications for the TTE system.....	32
5.4.3. Field testing in the Tournemire WTB .....	35
5.4.4. Future developments .....	36
5.4.5. Summary .....	37
5.5. Discussion and conclusions.....	37
6. Long range wireless data transmission systems .....	39
6.1. Understanding and improving long range wireless transmission system .....	39
6.1.1 Aims of the long-range wireless data transmission .....	39
6.1.2 Theoretical transmission distance versus in situ measurements.....	41
6.1.3 Summary .....	44
6.2. Improvement wireless monitoring system and development of a relay system .....	44
6.2.1. Concept of the wireless relay system .....	44
6.2.2. Power saving by introducing multi-stage wireless relay system .....	45
6.2.3. Transmission test of relay device .....	46



- 6.2.4. Securing redundancy by introducing multi-route wireless relay system .....47
- 6.2.5. Endurance test for relay device .....47
- 6.2.6. Summary .....48
- 6.3. Discussion and conclusions..... 48
- 7. Combination of wireless techniques on different ranges ..... 50
  - 7.1. Test of miniaturized transmitter for vibrating wire sensor interface in the WTB ..... 50
    - 7.1.1. Results .....52
  - 7.2. Evaluation of a wireless monitoring system behind a supercontainer’s concrete buffer ..... 53
    - 7.2.1. Introduction .....53
    - 7.2.2. General set-up.....55
    - 7.2.3. Experimental testing.....55
    - 7.2.4. Summary .....57
  - 7.3. Evaluation of a combination of wireless techniques on different ranges..... 57
    - 7.3.1. Description of the Tournemire site.....57
    - 7.3.2. Short range data transmission .....61
    - 7.3.3. Long range data transmission.....63
    - 7.3.4. Data acquisition and data link between short and long range transmission systems...68
  - 7.4. Discussion and conclusions..... 69
- 8. Overall conclusions..... 70
  - 8.1. Introduction ..... 70
  - 8.2. Short range data transmission..... 70
  - 8.3. Long range data transmission..... 71
  - 8.4. Combined solutions ..... 71
  - 8.5. Current state-of-the-art..... 71
  - 8.6. Outlook ..... 73
- 9. References..... 75



## List of Figures

Figure 5-1: WTB location .....	18
Figure 5-2: Layout of WTB facility .....	19
Figure 5-3: Retaining plate keeping the GBM already emplaced in the MB (left) and PVC casing in front of the highly compacted block layer (right).....	20
Figure 5-4: Block diagram of the wireless node.....	21
Figure 5-5: “Clean-site” measurements points. Red spots indicate the position of the transmitter nodes while green spots indicate the location of the receiver nodes. The numbers relate to the different transmission tests performed (see Table 5-1). .....	22
Figure 5-6: Test configuration at WTB. ....	23
Figure 5-7: Test configuration at WTB during hydration phase. ....	24
Figure 5-8: Water inflow in the buffer and attenuation during the beginning of the hydration phase....	24
Figure 5-9: Sensors connexion module (left) and final RF module (right). ....	25
Figure 5-10: Final antenna configuration with nylon core.....	25
Figure 5-11: Block diagram of the receiver electronics. The receiver coil in the final setup is tuned in series with the capacitor. ....	28
Figure 5-12: Multiplier/down converter of the receiver electronics.....	29
Figure 5-13: Preliminary layout of the TTE data transmission system .....	32
Figure 5-14: Packaging for borehole deployment.....	34
Figure 5-15: Packaging for galleries deployment .....	35
Figure 5-16: Receiver (left) and transmitter (right) used at FSB .....	35
Figure 5-17: Testing inside the access boreholes (left) and at the access gallery (right) at Tournemire	36
Figure 6-1: Medium range wireless configurations. ....	40
Figure 6-2: Long range wireless configuration. ....	40
Figure 6-3: Large antenna for long range wireless transmission in the Tournemire URL. ....	41
Figure 6-4: Long distance underground transmission configuration for tests in Andra’s URL .....	42
Figure 6-5: Long distance wireless transmission tests done in Tournemire URL.....	43
Figure 6-6: Data from wireless transmission tests done in Tournemire URL. ....	43
Figure 6-7: Conceptual diagram of a multi-hopping data relay. The figure on the right side shows rerouting of the data transmission in case of a malfunction of the relay device. Modified from [17]. ....	45
Figure 6-8: Relay device for the multi-stage / multi-route relay system [19]. ....	45
Figure 6-9: Received voltage from the relay device plotted against the transmission distance. The lines depict the expected signal strength of the relay device (blue) and the transmitter (orange). The shaded area denotes a noise level of 2 mV, where transmission is not possible as learned from past experiments. Modified from [20]. ....	46
Figure 6-10: Conceptual diagram of route change in the case of device malfunction. Modified from [17]. ....	47
Figure 7-1: Miniaturized transmitter and vibrating wire extensometer (on the left) – Portable Receiver connected to the needle indicator (on the right) .....	50
Figure 7-2: Positions of the transmitter and the receiver in WTB.....	51
Figure 7-3: Installation of the transmitter in the middle access borehole.....	51
Figure 7-4: Intensity of the wireless signal read by the receiver and the relative EM noise level .....	52
Figure 7-5: Cross-section of a supercontainer with a cement-based buffer as main component. ....	53
Figure 7-6: Functional diagram (left) and implementation of the first <i>m/NT</i> prototype (right) .....	54
Figure 7-7: Current <i>m/NT</i> demonstrator (45 x 150 x 150 mm <sup>3</sup> ).....	54
Figure 7-8: Second approach to demonstrate wireless readout of the <i>m/NT</i> FBGS interrogator.....	55
Figure 7-9: Preliminary assembly fits in a box 23 x 21 x 7 cm <sup>3</sup> .....	56
Figure 7-10: General geological cross-section along the Tournemire tunnel.....	58
Figure 7-11: 3D diagram of the investigation area.....	58
Figure 7-12: 3D view of the location of LTRBM in the Tournemire URL.....	59
Figure 7-13: Proposed layout of LTRBM .....	60
Figure 7-14: Top-down view on the Tournemire URL. Background map © OpenStreetMap contributors ( <a href="http://www.opendatacommons.org/licenses/odbl">www.opendatacommons.org/licenses/odbl</a> ). ....	61
Figure 7-15: Wireless node in preparation for LTRBM (left), final WSU (right).....	62





Figure 7-16: Conceptual layout of the LTRBM (top). Installation drawing of WSU in the block buffer of the LTRBM (bottom). ..... 62

Figure 7-17: Antennas used in Tournemire: Receiver antennas NRG-5 (top left) and NRG-4 (top right), transmitter antenna NRG-6 (bottom)..... 64

Figure 7-18: Input noise of preamp NRG4v2 and the prototype ultra-low noise input stage ULNv1 for the frequency range of interest..... 65

Figure 7-19: Vertical signal strength at the surface at Tournemire measured with the set-up used in Mol (red, [5]), and an improved receiver set-up (black). The peak at 8723 Hz is a calibration tone. .... 66

Figure 7-20: Frequency-dependent signal attenuation of the vertical and radial fields at Tournemire (diamonds), and model calculations for several electric conductivities (lines). ..... 67

Figure 7-21: Overall set-up of the wireless data transmission chain out of the LTRBM borehole to the surface..... 68



## List of Tables

Table 4-1: Skin depth as function of electrical conductivity and transmission frequency .....	16
Table 4-2: Overview on current experiments on wireless data transmission in URLs .....	17
Table 5-1: Results of the campaign in the “clean site”. .....	22
Table 5-2: Specifications of the wireless units .....	26
Table 5-3: Transmitter power consumption and energy requirements .....	34
Table 5-4: Transmission ranges expected with larger antennas .....	36
Table 6-1: Specifications for the miniaturized transmitter [10] .....	44
Table 6-2: Specifications of the relay device. Modified from [19].....	46
Table 6-3: Results of endurance test for the relay system. Modified from [20].....	48
Table 6-4: Comparison of two-types of transmission system for long-distance .....	48
Table 7-1: Sensors data transmitted.....	52
Table 7-2: Objectives/Specifications .....	55
Table 7-3: Wireless performance of the mINT readout.....	56
Table 7-4: Instrumentation to be installed in the LTRBM .....	60
Table 7-5: Energy consumptions of each WSU based on 1 transmission each 12 hours.....	63
Table 7-6: Antenna parameter .....	64
Table 8-1: Performance of current wireless data transmission systems in URLs .....	72



## Glossary

---

AWG	Arrayed Waveguide Grating
ADC	Analog-to-Digital Converter
AISG	Antenna interface standards group
BPSK	Binary Phase Shift Keying
CCA	Circuit-Card Assembly
CRC	Cyclic Redundancy Check
DAS	Data Acquisition System
dBpT	decibel with respect to 1 pico-Tesla
DFT	Discrete Fourier Transformation
DSP	Digital Signal Processor
EBS	Engineered Barrier System
ERT	Electric Resistance Tomography
FBG	Fiber Bragg Grating sensors
FFT	Fast Fourier Transformation
GBM	Granular Bentonite-sand Mixture
HFW	High Frequency Wireless
HLW	High-Level Waste
LF	Low Frequency
ISM	Industrial, Scientific and Medication
LNA	Low Noise Amplifier
LTRBM	Long-Term Rock Buffer Monitoring demonstrator
LVDT	Linear Variable Differential Transformer
MB	Main borehole
MCU	Micro Controller Unit
MF	Medium frequency
PA	Power Amplifier
PIC	Photonic Integrated Circuit
QPSK	Quaternary Phase Shift Keying
R&D	Research and Development
RF	Radio frequency
SD	Secure Digital memory card
SDR	Software-Defined Radio
TC	Thermocouple
TTE	Through-the-Earth
UPS	Uninterruptible Power Supply
URL	Underground Research Laboratory
VLF	Very low frequency
WMO	Waste Management Organisation
WP	Work Package
WSU	Wireless Sensor Unit
WTB	Wireless Testing Bench



# 1. Introduction

The EU H2020 project Modern2020, as a continuation of the former MoDeRn project [1], deals with the Development and Demonstration of Monitoring Strategies and Technologies for Geological Disposal and is jointly funded by the Euratom research and training programme 2014-2018 and European nuclear waste management organisations (WMOs). The Project is running from June 2015 to May 2019, and a total of 28 WMOs, research and consultancy organisations from 12 countries are participating.

The overall aim of the Modern2020 Project is to provide the means for developing and implementing an effective and efficient repository monitoring programme, taking into account requirements of specific national programmes on geological disposal. The Project is divided in six Work Packages (WPs):

- WP1: Coordination and project management.
- WP2: Monitoring programme design basis, monitoring strategies and decision making. This WP aims to define the requirements of monitoring systems in terms of the parameters to be monitored in repository monitoring programmes with explicit links to the safety case and the wider scientific programme (see below).
- WP3: Research and development of relevant monitoring technologies, including wireless data transmission systems, new sensors, and geophysical methods. This WP will also assess the readiness levels of relevant technologies and will establish a common methodology for qualifying the elements of the monitoring system intended for repository use.
- WP4: Demonstration of implementing monitoring programmes, and related technologies and systems in repository-like conditions. The intended demonstrators, each one addressing a range of monitoring-related objectives, are the Full-scale in situ System Test in Finland, the Highly-Active (HA) Industrial Pilot Experiment in France, the Long-Term Rock Buffer Monitoring (LTRBM) Experiment in France, and the Full-scale Emplacement (FE) Experiment in Switzerland. An assessment and synthesis of several other tests and demonstrators will also be undertaken.
- WP5: Effectively engaging local citizen stakeholders in research and development (R&D) and research, development and demonstration (RD&D) on monitoring for geological disposal.
- WP6: Communication and dissemination, including an international conference, a training school, and the Modern2020 Synthesis Report.

This report summarizes the work performed in Task 3.2 of Work Package 3 of the Modern2020 Project. It integrates contributions from Amberg<sup>1</sup>, Andra, Arquimea<sup>1</sup>, ENRESA, EURIDICE, IRSN, NRG, RWMC, and VTT and is prepared and compiled by NRG.

<sup>1</sup> Aitemin participated from the beginning of the project up to 30/09/2016 and the corresponding tasks were resumed by Amberg and Arquimea afterwards.



## 2. Objectives of Task 3.2

This deliverable represents the final technical report of the Modern2020 project's Task 3.2, *Wireless data transmission systems for repository monitoring*. It synthesizes the progress achieved by all partners contributing to the Task 3.2 R&D activities, and aims to support the evaluation of the readiness level of the investigated data transmission technologies (Task 3.1).

The former MoDeRn project has successfully developed and analysed the capabilities of monitoring technologies for future repository use in the fields of measurement techniques and probes, data transmission methods and energy supply. One of the outcomes of this project was a list of priority technical issues that remain to be further investigated [1]. From the critical gaps identified in MoDeRn, Task 3.2 aims to improve and combine wireless data transmission systems. The improvements are either related to increasing operational ranges through geological media or components of the engineered barrier system (EBS) under relevant conditions (e.g. saturated bentonite), or the optimization of the energy efficiency of the data transmission systems. The latter is crucial - in combination with the development of long term power supply sources (Task 3.3) and the consolidation of these systems (Task 3.6) - to extend their lifetime to decades. With respect to the combination and integration of wireless systems, Task 3.2 aims at evaluating the feasibility of completely non-intrusive systems combining sensors and different wireless data transmission. Another goal of Task 3.2 is to develop a Wireless Test Bench (WTB) in the Tournemire URL that allows the in situ evaluation of the performance of data transmission systems during the development phase of the project.

Task 3.2 is divided into three subtasks:

- Subtask 1: Improve existing short range (tens of meters) wireless systems based on high, medium or low frequencies (Aitemin, Amberg, Arquimea, ENRESA, IRSN & VTT)
- Subtask 2: Improve existing long range (hundreds of meters) wireless systems based on low frequencies (Andra & RWMC)
- Subtask 3: Evaluate the use of a combination of different range wireless systems to provide a complete data transmission solution (Amberg, Arquimea, Andra, ENRESA, EURIDICE, IRSN, NRG, RWMC & VTT)



### 3. Scope of this Report

---

This report summarizes the work performed in Task 3.2 of Work Package 3 of the Modern2020 Project, and provides main conclusions on the ability to transmit monitoring data wirelessly over components of the engineered barrier system or through the host rock and the progress achieved in this task. The report integrates contributions from Amberg, Andra, Arquimea, ENRESA, EURIDICE, IRSN, NRG, RWMC, and VTT and is set out as follows:

- Chapter 4 gives a short introduction on general principles of wireless transmission of data through geological media and components of the barrier system and the current state of the art.
- Chapter 5 describes the works performed in Subtask 1 on short range data transmission technologies as performed by Aitemin and Arquimea (Section 5.2), VTT (Section 5.3), and Amberg and ENRESA (Section 5.4), including a description of the purpose and set-up of the Wireless Test Bench (WTB) of IRSN at the Tournemire Underground Research Facility, France (Section 5.1).
- Chapter 6 describes the works performed in Subtask 2 on long range data transmission technologies. It consists of contributions from Andra on understanding and improvements of long range data transmission (Section 6.1) and of RWMC on the implementation of signal hopping strategies to provide robust data transmission over longer transmission distances within the EBS (Section 6.2)
- Chapter 7 describes the works performed in Subtask 3 on combining wireless data transmission technologies on different ranges. In Section 7.1, Andra summarizes their tests of a miniaturized transmitter for a vibrating wire sensor interface in the WTB. In Section 7.2, EURIDICE discusses the link of the *mINT* interrogator unit (see also Task 3.4) used to monitor concrete structures with a wireless transmitter. In Section 7.3, a combined effort of Amberg, Arquimea, IRSN and NRG to evaluate a combination of wireless data transmission systems is summarized. The overall purpose of the combined effort is to provide and demonstrate<sup>2</sup> a complete wireless solution that allows transmitting sensor readings from the inside of a disposal cell to the surface on top of the Tournemire URL by a combination of short and long range transmitters.
- Chapter 8 provides general conclusions with respect to the overall outcome and the current state-of-the-art of wireless data transmission in repository monitoring.

<sup>2</sup> the demonstration works are part of Modern2020 Task 4.3 and will be reported there



## 4. Wireless data transmission in repository monitoring

Modern2020's Task 3.2, which is further elaborated in the next chapters, is related to wireless data transmission systems. Wireless systems allow transmitting monitoring data over natural and engineered barriers without the use of cables that may impair the safety function of these barriers [2]. The barriers of interest could be anything from the concrete buffer of a supercontainer design, a borehole plug, sealings of disposal sections or a shaft sealing: wireless solutions are necessary that can bridge distances from less than a meter up to several hundred meters.

While wireless communication is nowadays used in many industrial and consumer applications, the high-frequency radio waves used in most of these applications can be strongly attenuated by solid materials as the host rock or components of the engineered barrier system (EBS). This attenuation is strongly dependent on the amount of pore water in the barrier or host rock, and will consequently increase with (re)saturation of the host rock or EBS components.

The strong attenuation of the electromagnetic waves used in many wireless applications raises the need to develop customized solutions for repository monitoring, making use of lower frequencies as typically used for transmission through the air. Another specific challenge for wireless solutions in repository monitoring is the powering of these units: any wireless monitoring system operating behind a barrier requires an autonomous supply of power that allows operating over long periods of time (decades and longer). Different options for long term power supply are addressed in Task 3.3 [3], however, the efficient use of available power is an important design criterion for the wireless transmission systems developed in this Task.

### 4.1. Principles of wireless data transmission

Generally, three principal options exist to transmit data by electromagnetic techniques:

- by generation of a magnetic field;
- by generation of an electric field;
- by current injection.

Little work is done on using *current injection* for data transmission. The vast majority of applications make use of an *electric dipole antenna*, and operating at high frequencies. Due to interactions with the media, data transmission by electric fields is limited to shorter distances (Section 7.1), or to medium distances in case the medium has a low electric conductivity [4].

Because for lower frequencies, an electric antenna is too inefficient, most contributions to this task make use of magnetic fields generated by a *magnetic loop antenna*. Generally, it can be distinguished between 'small' loop antennas, where the loop diameter is much smaller than the wave length (Section 5.3, 6.1, 6.2, and 7.3.3), and loop antennas that are 'tuned' to the wave length of interest (Section 5.2 and 7.3.2). The latter results in a more energy efficient field generation, but are unsuitable for lower frequencies due to the often limited open space in a disposal facility.

While the receiver antenna's efficiency is increasing with frequency, higher frequencies can also result in an increasing attenuation of magnetic fields during propagation through the EBS or host rock. The optimum transmission frequency is thus dependent on the transmission frequency and the electrical conductivity of the medium [5].

A simple concept that allows making first estimations on the principal relevance of interactions with the geologic medium is the so-called *skin depth* that defines the distance, at which a signal is attenuated by a factor of  $1/e$ , equivalent to 8.7 dB ([6], [7]). To estimate the skin depth  $\delta$ , a distinction is made between a "good conductor" and a "poor conductor", dependent on the electrical conductivity  $\sigma$ . For

$$\sigma \gg 2\pi f \cdot \epsilon_0 \cdot \epsilon_r \quad (4-1)$$



and

- $\epsilon_0$  permittivity constant ( $8.9 \cdot 10^{-12} \text{ A} \cdot \text{s/V} \cdot \text{m}$ )
- $\epsilon_r$  relative permittivity [-]

the medium can be considered as a “good conductor”. The skin depth for a “good conductor” can be calculated by

$$\delta[m] = \frac{1}{\sqrt{\pi \cdot f \cdot \sigma \cdot \mu_0 \cdot \mu_r}} \quad (4-2)$$

with

- $\mu_0$  permeability constant ( $1.257 \cdot 10^{-6} \text{ V} \cdot \text{s/A} \cdot \text{m}$ )
- $\mu_r$  relative (magnetic) permeability [-]

In the absence of paramagnetic materials,  $\mu_r$  can be assumed to be equal to 1. For  $\epsilon_r$ , values around 3 - 40 are reported for geological media [8]. The electrical conductivity  $\sigma$  of geological media can vary to a large extent, from  $\mu\text{S/m}$  to  $\text{mS/m}$  range for crystalline rock, and  $\text{mS/m}$  to  $\text{S/m}$  range for argillaceous rock [8]. The water-filled porosity of the geological media or EBS component has an important influence on the conductivity, as well as the pore water composition. The electric conductivity of fresh water is about 10  $\text{mS/m}$  to 1  $\text{S/m}$ , and the conductivity of saline water can be as high as 1 - 10  $\text{S/m}$ . Table 4.1 gives some example values for the skin depth at different frequencies and electrical conductivities.

**Table 4-1: Skin depth as function of electrical conductivity and transmission frequency**

Skin depth $\delta$ [m]						
	Electrical conductivity $\sigma$ [mS/m]					
	1	5	10	50	100	1000
1000 Hz	503	225	159	71	50	16
2500 Hz	318	142	101	45	32	10
5000 Hz	225	101	71	32	23	7

## 4.2. Current status of wireless technologies in repository monitoring

A general overview on the state-of-the-art of wireless systems and its main applications is given in [9]. Three application distances can be distinguished in repository monitoring:

- Short range transmission: up to 30 m
- Middle range transmission: 30 m to 100 m
- Long range transmission: > 100 m

Table 4-2 summarizes successful data transmission experiments in URLs under conditions relevant for underground disposal of radioactive waste. In addition to the data transmission experiments, a number of long range signal transmission experiments has been performed, e.g. experiments by MISL who performed measurements through 225 m of Boom Clay and saturated sandy aquifer at the HADES URL [9] and through 80 m of granite and 100 - 250 m of access tunnel at the Grimsel URL [9], or by Andra who demonstrated signal transmission through 275 m of limestone and shales at the Tournemire URL and over 300 m in a surface-surface configuration at the Tournemire URL and the Andra URL (Section 6.1).





**Table 4-2: Overview on current experiments on wireless data transmission in URLs**

Distance	Transmission mode	Frequency	Host rock/barrier (location)	Organization	Reference
0.1 m	Resonant cavity antenna	2.4GHz	Concrete buffer	EURIDICE	Chapter 7.2
4 m	Electric dipole antenna	169 MHz	Bentonite/shotcrete (Grimsel URL)	AITEMIN	[4]
4 - 6 m	$\lambda/4$ loop antenna	2.2 MHz	(Partially) saturated bentonite (Tournemire URL)	Arquimea	Chapter 5.2
5 - 10 m	Magnetic loop antenna	8.5 kHz	(Partially) saturated bentonite (Tournemire URL)	Andra	Chapter 7.1
23 m	Magnetic loop antenna	125 kHz	Granite + Air (Espoo research hall)	VTT	Chapter 5.3
25 m	Magnetic loop antenna	8.5 kHz	Sedimentary rock (Meuse/Haute Marne URL)	RWMC/Andra	[10]
30 m	Magnetic loop antenna	4.0 kHz	(Partially) saturated bentonite (Tournemire URL)	Amberg	Chapter 5.4
30 m	Magnetic loop antenna	575 Hz	Bentonite/shotcrete (Grimsel URL)	MISL	[11]
225 m	Magnetic loop antenna	1.8 kHz.	Boom Clay & saturated sandy aquifer (Hades URL)	NRG	[5]
250 m	Magnetic loop antenna/relay system	8.5 kHz	Sedimentary rock (Horonobe URL)	RWMC	[12]
275 m	Magnetic loop antenna	8.7 kHz	Limestone & Shale (Tournemire URL)	NRG	Chapter 7.3.3

Since high frequencies lead to high signal attenuation when transmitting through a (partially) saturated barrier, all current wireless techniques, except for very short distances (<1 m) make use of the very low frequency (VLF) to – medium frequency (MF) range (3 KHz to 3 MHz).

For long range data transmission, frequencies below 10 kHz are used, although under unsaturated conditions as present in e.g. the Tournemire URL, higher transmission frequencies may be applied as well.

On the small to medium range, a variety of frequencies are used in Modern2020, ranging from 4 kHz to 2.2 MHz. Deciding which one of these frequencies is the most suitable one will depend on the transmission distance to be achieved, the electrical conductivity of the EBS and host rock and the presence of magnetic permeable materials. Another consideration for the selection of the transmission frequency over short and medium ranges could be the lower complexity of the transmission system when using the same technology on all distances.

In summary, successful data transmission has been demonstrated on ranges between less than a meter and about 300 m, and six of the application cases in Table 4-2 are presented in the next three chapters. An important performance figure for wireless solutions is their energy need, certainly for the long distance. The current research initiatives in WP3.2 are directed to understand and develop the energy efficiency further by extending and improving the energy efficiency of existing solutions. Experiments were performed in relevant environments, in order to account for interactions with the host rock or EBS of interest. The overall performances achieved by the different data transmission systems (data rate, energy need) will be presented in the next chapters, and are summarized in the overall conclusions (Chapter 8.6, Table 8-1).



## 5. Short range wireless data transmission systems

### 5.1. Implementation of a Wireless Testing Bench (WTB)

A Wireless Testing Bench (WTB) was implemented in IRSN's Underground Research Laboratory (URL) in Tournemire in the South of France (Aveyron) to provide the possibility of evaluating signal transmission parameters from different wireless technologies for short and long range data transmission under representative in situ conditions.

The WTB setup consists of a large diameter main borehole filled with an engineered barrier system (EBS) composed of 2 bentonite cores, one cement plug and 3 access boreholes (drilled perpendicularly to the main borehole axis) in which wireless units can be placed and tested (Figure 1). The experiment design enables wireless units to be introduced and removed at will within the bentonite buffer. A watertight access to the bentonite cores (transparent to radio waves), allows testing and continuous improvement of the wireless units under different saturation conditions.

The radio transmission units to test do not require incorporating sensors, given that the sensors signal is converted to digital data before being transmitted, but to send equivalent data that will be received at different locations around the emission point to determine the transmission parameters of interest (length, quality, strength of signal, etc.).

The installation works were performed by Aitemin, ENRESA and IRSN during the first half of 2016.

#### 5.1.1. WTB layout

Figure 5-1 shows the location of the WTB at the Tournemire URL.

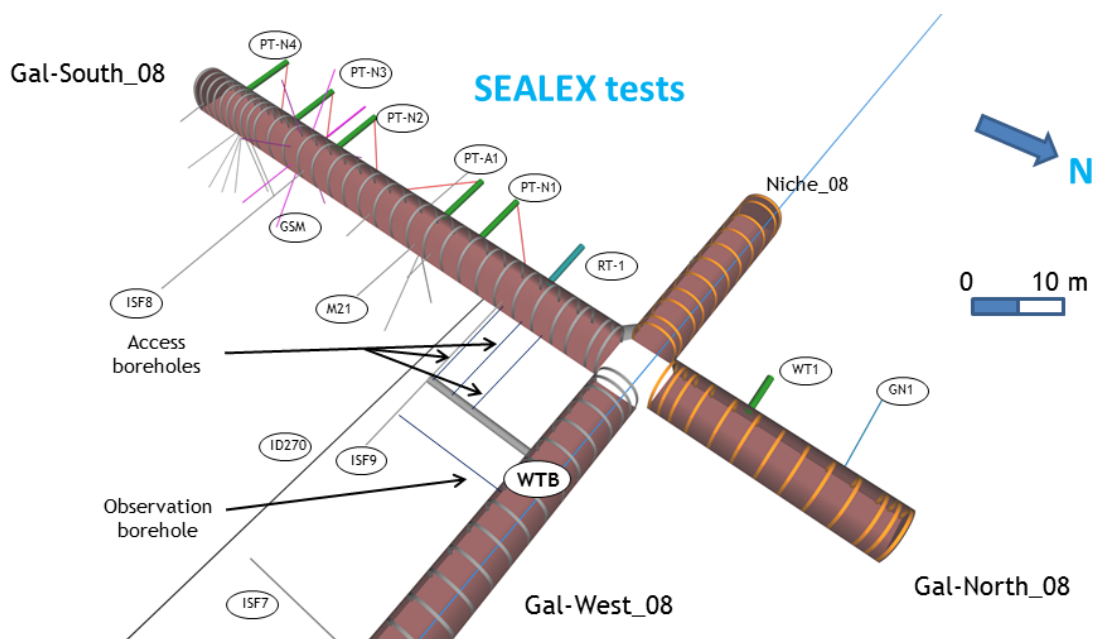


Figure 5-1: WTB location

The WTB is composed of:

- A main horizontal borehole (MB) measuring 60 cm in diameter and 10.13 m in length (Figure 5-2)
- A bentonite buffer, 4.52 m long occupies the rear part of the MB and is divided in two segments:
  - A 2.3 m long segment located at the rear end of the MB, filled with a Granular Bentonite-sand Mixture (GBM - 75 % sand and 25% bentonite). The GBM was inserted in the MB by means of a screw conveyor and a vibrating needle installed in the inner part of the MB. The aimed target for

the dry density was 1.49 g/cm<sup>3</sup>. However, this was not reached due to technical problems. The final dry density of the GBM was 1.34 g/cm<sup>3</sup>.

- A 2.19 m long segment located in front of the GBM buffer filled with 14 layers of highly compacted blocks: 13 layers of a MX80 bentonite/sand mixture, in a ratio of 60/40 and one layer of pure bentonite blocks (Figure 5-3). The natural bentonite used in this work was the American Colloid Co. type MX-80 (Wyoming Na-bentonite).
- Both buffers are separated by a cemented resin plate (30 mm thick and 580 mm in diameter). The plates function is to contain the GBM used for the filling of the rear part of the borehole, thus allowing the passage of a screw conveyer and a vibrating needle during the buffer emplacement. The resin plate is perforated homogeneously in order to allow the passage of water between both buffers (Figure 5-3).
- An artificial hydration system was installed to accelerate buffer saturation. The artificial saturation system is composed of three circular shaped sections of geotextile hydration mats covering the full section of the borehole. The amount of water injected through each wetting surface is continuously monitored.
- A 2.58 m long cement plug has been installed at the outer end of the bentonite buffer. The function of the cement plug is to confine the swelling of the bentonite buffer along the hydration phase.
- Three access boreholes (Figure 5-1 and Figure 5-2) have been drilled perpendicularly to the MB axis (Figure 5-1), the first one at the rear end of the buffer, the second one at its middle section and the third one at its front end. Each borehole, with a diameter of 131 mm, houses a 114 mm diameter inner blind end lining PVC tube. The last section of PVC tube ends in a threaded plastic conical cap. This cap has been filled with resin (Sikadur 52) to assure its integrity and set a flat surface that will stop the wireless unit at its required final position. The chamber for the wireless units overpasses the MB axis by 150 mm (Figure 5-2). All sensors cables and hydration tubes have been driven along the annular gap between the lining tube and the rock, which has been cemented with epoxy resin Sikadur 52 in the outer 2 m of borehole.

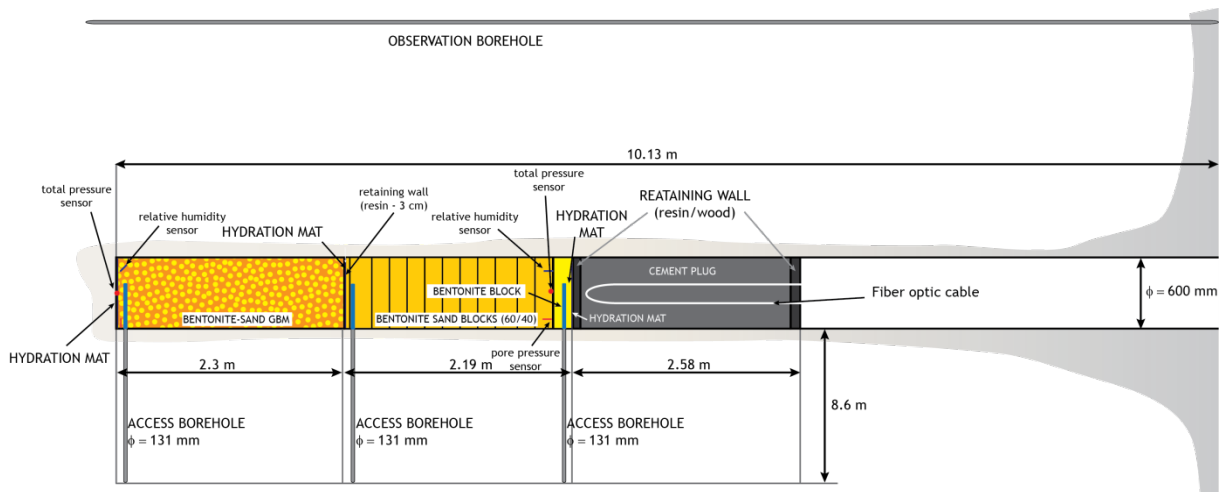
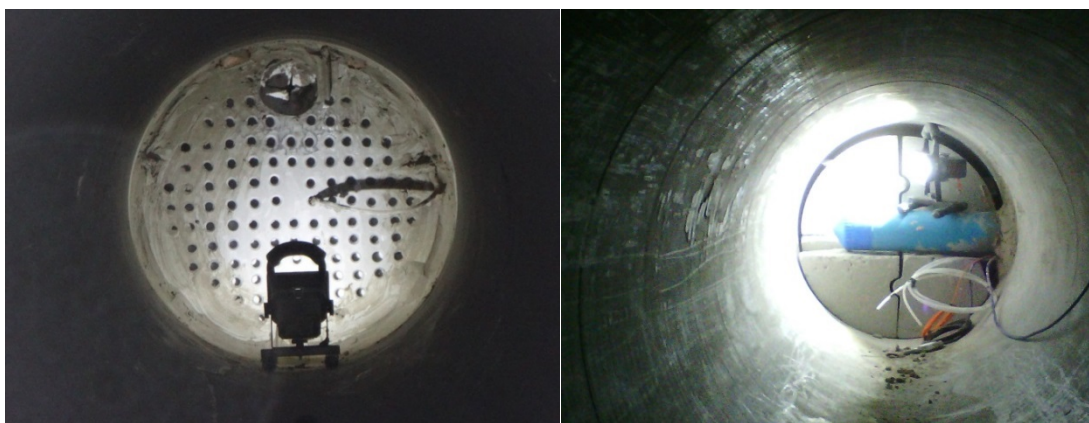


Figure 5-2: Layout of WTB facility

The buffer and the cement plug have been instrumented with wired sensors in order to measure:

- Total pressure at the rear and front ends of the bentonite buffer.
- Pore pressure in the GBM and in the blocks buffer body.
- Relative Humidity in both sections of the buffer.
- Displacement, deformation and temperature of the cement plug.
- Water inflow.



**Figure 5-3: Retaining plate keeping the GBM already emplaced in the MB (left) and PVC casing in front of the highly compacted block layer (right)**

### 5.1.2. Installation and first tests

The installation of the WTB was carried out in three steps: the first one from 1/02/2016 to 5/02/2016, the second one from 18/04/2016 to 22/04/2016 and finally the third one from 28/06/2016 to 01/07/2016. The installation of WTB took longer than expected (3 months overdue), due to problems related to the screw conveyor devices and to the failure of the resin filling operation between the two front lids.

The first wireless tests in WTB were carried out by Arquimea in July and November 2017. This first series of tests were completed before starting the bentonite buffer hydration, whereas the second series of tests was done during the first phase of hydration. The WTB was used by Amberg too for testing their approach to wireless data transmission based on an adapted TTE system. The set-up and results of these tests are summarized in Chapter 5.2 and 5.4.

## 5.2. Increasing operating range in hydrating sealing material

### 5.2.1. Concept description and methodology

The main goal of this contribution from Arquimea is to continue the work initiated by Aitemin to design and develop a new system capable of monitoring the physical parameters inside a sealed repository and to transmit the acquired data over a saturated barrier, based on High Frequency Wireless (HFW) techniques. These techniques, which are totally non-intrusive, do not require physical paths to transport the signal through the sealing elements, which is a clear advantage in the context of a sealed repository compared with wired systems (either optical or electrical), where potential water flow-paths can be more easily produced.

Besides the data transmission through the sealing material, the following requirements are to be accomplished for the HFW node:

- Capability of powering and gathering data from up to four conventional analog sensors and three digital sensors.
- The HFW node must withstand the expected harsh conditions within a disposal cell, and transmit the data obtained to a Master Controller Unit, located in the access gallery.
- The Master Controller unit can be linked to a long range wireless system that allows to transmit the data wirelessly from the access gallery to surface on top of the Tournemire URL (Chapter 7.3).
- The HFW node is powered by a battery.
- Communication is possible in both directions, from the access gallery to the node buried in the disposal cell and the other way around.

Modern2020 – Deliverable D3.2

Dissemination level: PU

Date of issue of this report: 27/03/2019



- The HFW node will remain most of the time in a low-energy consuming sleep mode and will only wake up when reading the sensors and transmit data outside. The timing can be programmed and changed, and when the node wakes up it also spends some time listening.

Starting point for this task is the former MoDeRn project, where Aitemin developed several prototypes of wireless nodes using a 169 MHz radio frequency (RF) transmission module [4]. These units were partly successful, showing some issues regarding antennas geometry, signal losses after hydration of the buffer and energy efficiency.

The wireless node developed by Arquimea in the frame of the Modern2020 project is based on the prototypes previously developed by Aitemin. It keeps the main concepts like core and power supply, but there are several important changes in relation to the data acquisition sensor type and radio transmission mode.

Arquimea has followed an iterative approach consisting of: i) A critical concept review and ii) re-design of the transmitter to 2.228 MHz frequency, iii) testing of prototypes at Arquimea’s facilities and at the WTB in Tournemire aiming at the implementation of improvements. These steps have been iterated 3 times until a final wireless node design has been reached. This final design has been fabricated for the Long-Term Rock Buffer Monitoring demonstrator (LTRBM, Modern2020 Task 4.3).

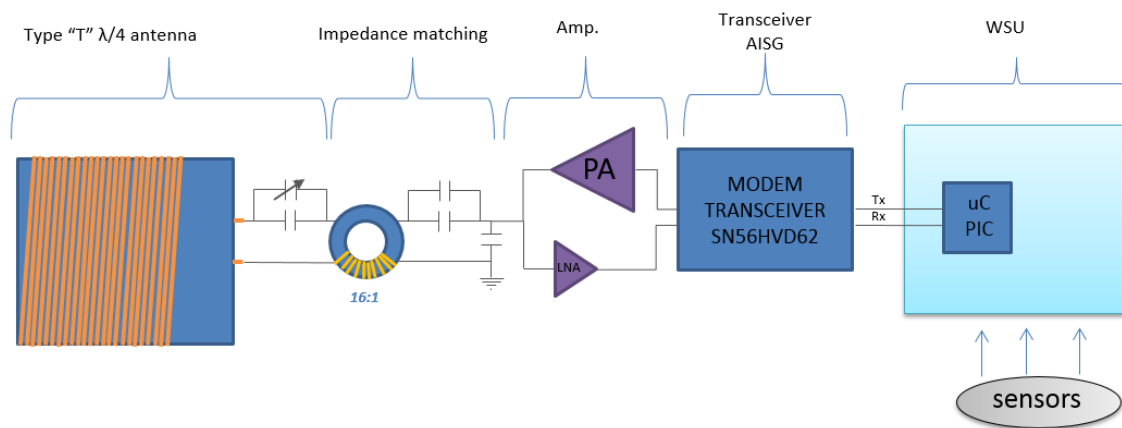


Figure 5-4: Block diagram of the wireless node.

### 5.2.2. Feasibility tests

The first tests carried out have been performed in the WTB facility during 2015 before the installation of the buffer material (“clean site”). These measurements were done to assess the optimum frequency range for the wireless nodes to operate. Measurements have been done placing a transmitter and a receptor node in the access boreholes located at the bottom and at the beginning of the buffer. The intermediate access borehole was not used. Both nodes have been fixed at several distances from the gallery. Figure 5-5 shows the position of the transmitter and the receiver for the performed measurements.

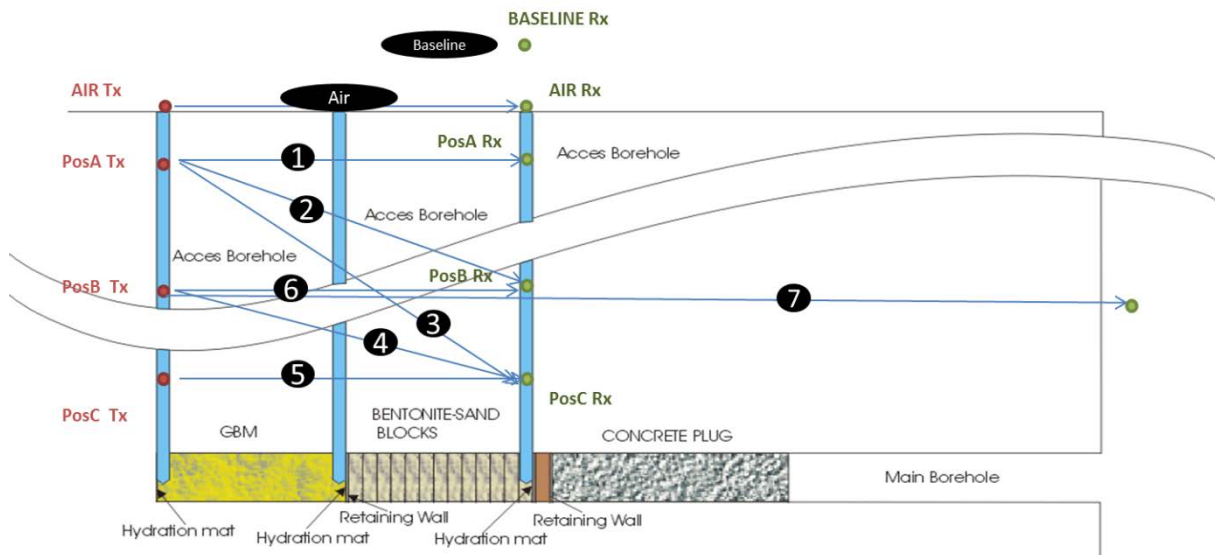


Figure 5-5: “Clean-site” measurements points. Red spots indicate the position of the transmitter nodes while green spots indicate the location of the receiver nodes. The numbers relate to the different transmission tests performed (see Table 5-1).

Based on the analysis of the results (Table 5-1), a frequency band around 1.8 MHz was initially selected. The table represents the peak signal attenuation for each combination of positions in dBm. The base case shows the ambient noise taken by the receptor in the tunnel without transmission.

Table 5-1: Results of the campaign in the “clean site”.

Measurement	Y <sub>1</sub> [m]	Y <sub>2</sub> [m]	dx [m]	D (m)	α [°]	Signal strength [dBm]			
						1 MHz	2,5 MHz	5 MHz	10 MHz
Base	0	0	4	n.a.	n.a.	-104	-106	-111	-108,5
Air	0	0	4	4	0	-82,4	-71,5	-81	-69,4
1	2,5	2,5	4	4	0	-77,2	-70	-83	-67
2	2,5	5	4	4,7	32	-83,7	-77	-90,3	-76
3	2,5	7,5	4	6,4	51	-95	-89	-104	-93,7
4	5	7,5	4	4,7	32	-83,7	-75,9	-89,4	-78,9
5	7,5	7,5	4	4	0	-76,6	-69,2	-81,5	-68,1
6	5	5	4	4	0	-76	-69,2	-82,6	-66
7	5	5	11,5	11,5	0	-99	-102,1	-111	-111

Where:

- Base: One receiver listening (no transmission ongoing)
- Air: Transmitter/Receiver direct sight (separated 4 m)
- Y<sub>1</sub>: Depth for Transmitter
- Y<sub>2</sub>: Depth Receiver
- dx: Horizontal distance between the Transmitter/Receiver planes
- D: Distance between Transmitter/Receiver
- α: Angle between Transmitter/Receiver axes

### 5.2.3. Experimental set-up

After the selection of the frequency band, Arquimea has designed a new wireless communication module *ad-hoc* based on the technology used in AISG standard compliant on and off keying modem transceiver; using it to modulate and demodulate the signal between the core of the wireless sensor unit (WSU) for the implemented transmission frequency (2.228Mhz). The transmission signal is amplified with a power amplifier with a gain of 33dB and in the receiver by a low noise amplifier (90dB). Tests with the new developed transceiver have been carried out in Arquimea installations with several antenna types and amplifiers, selecting the ones that have given the best result regarding both transmission power and low consumption. These tests were done through air.

#### First testing campaign at the WTB (Tournemire)

A first campaign of tests with the new developed transceiver was performed in the WTB at Tournemire during June 2017, when the buffer material was already in place. Main goal was to confirm previous tests carried out in air by combining antennas and amplifiers.

The tests configuration is shown in Figure 5-6, where each capital letter (*A<sub>i</sub>*, *B<sub>i</sub>*, *C<sub>i</sub>*) represent the location of the transmitter, and *D* and *E* indicate the location of the receiver. Signal attenuation between each combination was measured. The results obtained were practically the same than in air, and the overall signal-to-noise ratio was even better due to the absence of external noise and interferences.

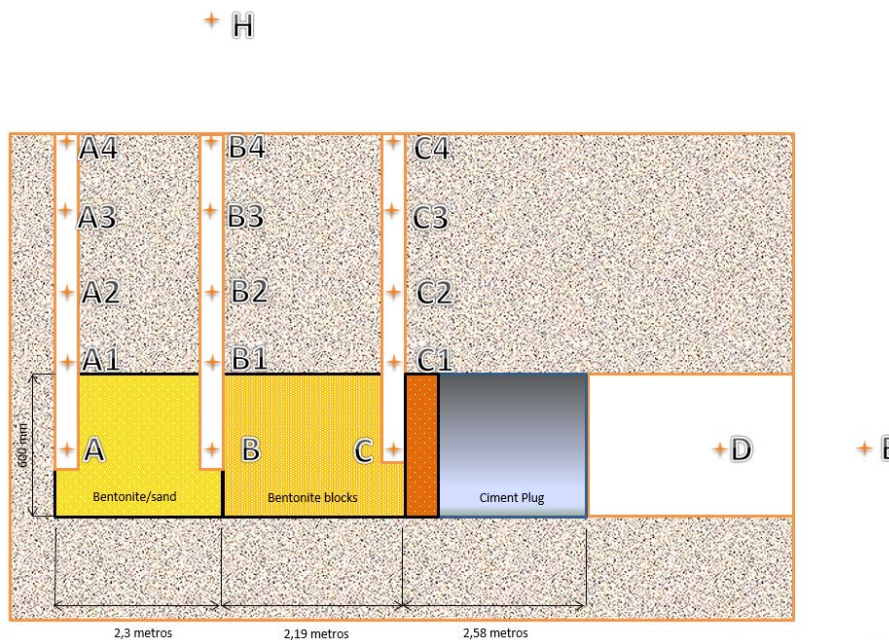


Figure 5-6: Test configuration at WTB.

Finally, a successful radio link was established between *A* and *C*, but it was not possible to achieve it between *A* and *D* and *E* through the retaining wall and the cement plug.

As results of the tests, a “T”  $\lambda/4$  antenna type was selected, getting up to 8 dB of improvement compared to other types and minimizing its dimensions. On the other hand, the impossibility of obtaining a radio link over the whole buffer implied:

- The use of an intermediate node to act as repeater
- A re-design on the amplification stage.

### Second testing campaign at the WTB (Tournemire)

After implementing the changes decided from the previous test campaign, a second test campaign in Tournemire was performed to evaluate the influence of the buffer hydration on the transmission parameters. This campaign was performed from November 2017 to January 2018.

For this campaign, a transmitter was buried in the bentonite buffer (Figure 5-7), emitting 2.228MHz. As receiver, a software-defined radio (SDR) connected to a PC, took several samples daily during the beginning of the hydration period.

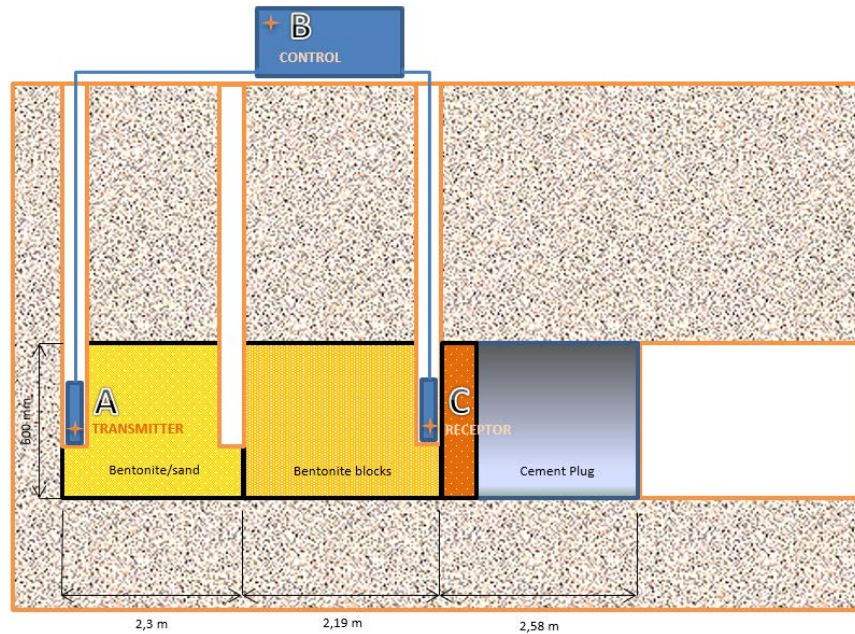


Figure 5-7: Test configuration at WTB during hydration phase.

It was found that during the first month, the hydration has not influenced the transmission between nodes in an appreciable way (differences are less than 5dB, see Figure 5-8).

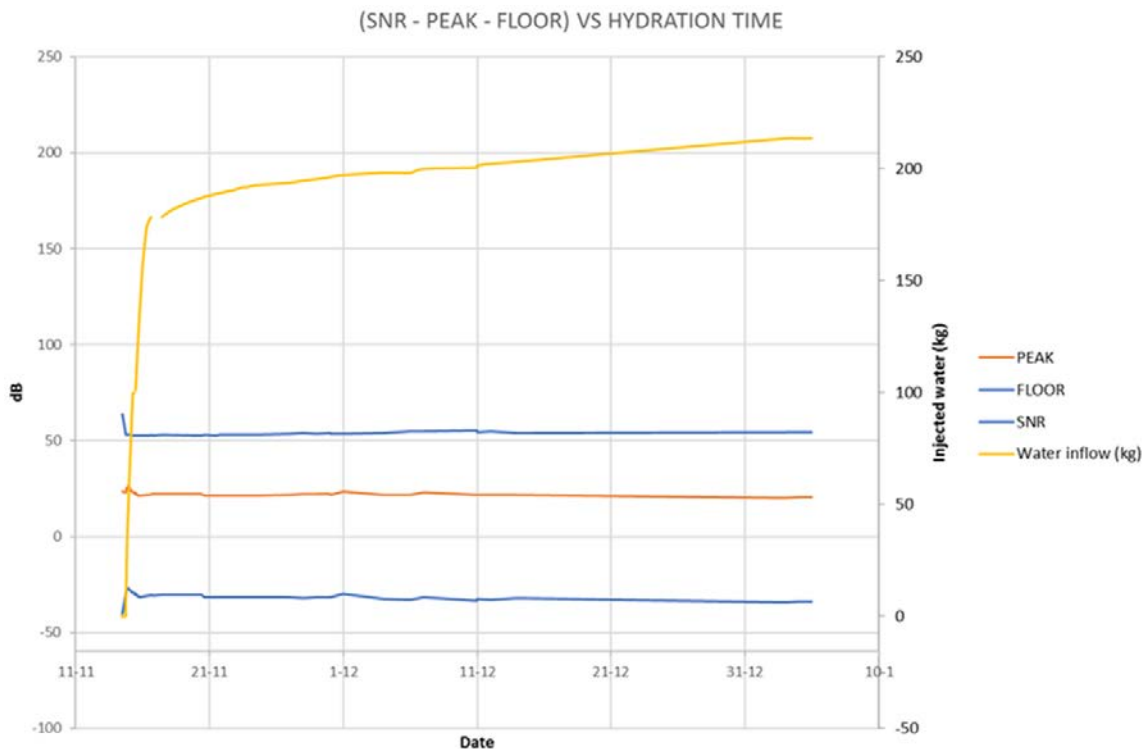


Figure 5-8: Water inflow in the buffer and attenuation during the beginning of the hydration phase.



### 5.2.4. Final design

Results from the second test campaign were used to validate the design of the prototype to be installed at LTRBM, however, two reasons for modifications raised during the final design:

- Having one antenna to receive and another to transmit exceed the desired dimensions. It was decided to share antenna for transmission and reception. Due to the impedance difference of the PA and LNA amplifiers, an impedance adaptation was made for each case. This is done with a balun (1:16) and a RF-switch to select the function.
- Initially, the antenna core was air. The core must withstand the external pressures developed by the bentonite during its hydration, therefore a mineral potting was used as core. Properties of this material shifted the selected frequency for transmission, so finally an inert nylon core has been used to protect the device.

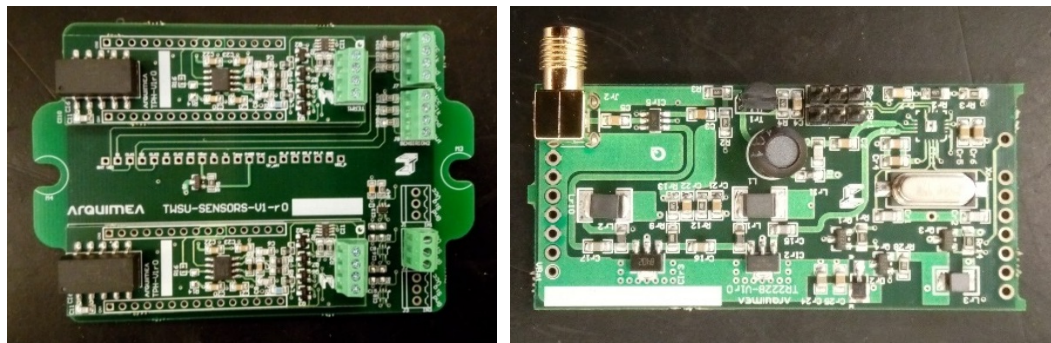


Figure 5-9: Sensors connexion module (left) and final RF module (right).

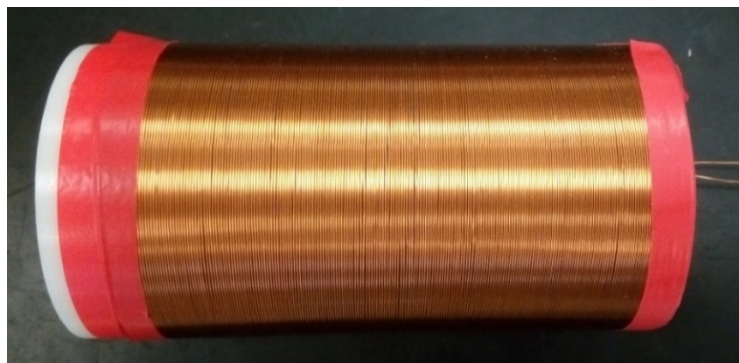


Figure 5-10: Final antenna configuration with nylon core.

Final features for the Arquimea short range wireless data transmission system are given in **Table 5-2**. The device consumes around 1.8 J during the time it is in active mode (that comprises activation, transmission and 'ACK' reception) in each transmission period. Maximal power required by the system is around 400 mA during each data transmission. In inactive mode, the device consumes 0.001 mA at a supply power of 3.6V.

The total system consumption is determined by the number and type of sensors connected to the WSU. In the case prototyped for the LTRBM Demonstrator (WP4) expected consumption is described in Section 7.3.2.

**Table 5-2: Specifications of the wireless units**

Specifications of developed wireless units	
Transmission interval	12 hours
Transmission distance	4 m (Under LTRBM environmental noise)
Durability	About 1 years
Size (diameter x length)	Ø90 mm×355 mm
Frequency	2.228 MHz
Baud rate	38400
Sensors Payload Capacity	<ul style="list-style-type: none"> <li>• 4 Analog sensors (4...20 mA, 0...10 mV, bridge)</li> <li>• 5 Digital sensors type: <ul style="list-style-type: none"> <li>○ SCH-75 (humidity and temperature sensors)</li> <li>○ ARQ Psychrometers</li> </ul> </li> <li>• Built-in temperature and battery monitor</li> </ul>
Power consumption	<ul style="list-style-type: none"> <li>• Sleep mode 0.001 mA@3.6V</li> <li>• Data Transmission 400 mA@9V</li> <li>• ACK reception 0.52mA@3.6V</li> <li>• Active node :5 mA@3.6V</li> </ul>
Scalability	<ul style="list-style-type: none"> <li>• Up to 18 nodes</li> </ul>
Signal hooping	Yes

### 5.2.5. Summary

A new improved wireless transmission system has been developed and will be tested in the LTRBM demonstrator (Modern2020 Task 4.3).

The resulting system presents versatile features to be adapted to different cases of use, providing different working modes and sensors configuration.

The developing process has not been easy, but results are encouraging. The biggest challenges during the development have been caused by the understanding of the transmission attenuation physics, the limitation on power availability and the integration of each module of the device.

There is still room for improvements of the system regarding:

- Reduction of the system size
- Fabrication procedure (antenna subsystem)
- Optimising of the energy management system

These aspects will be re-evaluated after its implementation at LTRBM.

From the energetical point of view, the sensors configuration (number and type) have the greatest influence on the total energy demanded by the system. Neglecting the sensors payload, the total energy demanded during the active mode is around 1.8 J per transmission, demanding a maximum current of 400mA.



## 5.3. Wireless data transmission system at 125 kHz

This chapter summarized the work of VTT on the development of a wireless data transmission system for short ranges.

### 5.3.1. Background and objectives

VTT Technical Research Centre of Finland Ltd has developed short to medium range wireless sensor data communication based on magnetic inductive coupling between two coils. The magnetic communication was first tested for obtaining sensor data wirelessly at 125 kHz from inside bioleaching heaps of nickel ore [13]. The ore heap materials are electrically conductive and attenuate radio waves. This can also be the case with the engineered barrier materials used inside radioactive waste repositories, and the system used in [13] was adapted for this purpose with novel hardware for enhanced capabilities.

The objective of this work was to develop an optimal approach to solve the short distance underground communication problem with state-of-the-art low cost commercial technology. In this system, communication is based on magnetic inductive coupling between the transmitter and receiver coils. This coupling is stronger with larger coils and with more turns in the coils. For a given distance between the coils, the coupling decreases very rapidly with increasing distance between the coils. Also the electrical quality of the coils (Q-values) affects the transmitter efficiency and bandwidth. The maximum coil size is limited by the available space. The maximum applicable frequency is limited by the number of turns in the coils due to the self-resonance of the coils. The self-resonance frequency decreases with an increasing number of turns, and the operating frequency should be considerably lower than self-resonance for the coil to allow a precise tuning of the resonance frequency: operating at or near the self-resonance would make the circuit too sensitive to environmental variations and for example vibrations.

Since the magnetic field decays over distances much larger than the antenna size in an inverse proportion to the third power of distance, the received power decays inversely proportional to the sixth power of distance. This seriously limits the achievable communication distance, it also means that the number of turns and the size of the coil are always a compromise between the transmission distance aimed at and the self-resonance frequency of the coil.

The conductivity losses in the medium, however, increase with frequency. A typical Q-value of a coil in actual environment underground is in the order of 20-50 due to the losses caused by the surrounding conductive materials. Considering the coil material itself, the Q of the coil increases with frequency due to the increased inductive reactance. At the same time the resistance of metal conductors increases proportionally to the square root of frequency because of the skin depth in the metal, lowering the Q. The total effect of frequency on performance is complex, depending on several system parameters and the environment.

The operating frequency of 125 kHz was chosen as a compromise to have low electrical losses with reasonable coupling and to have a reasonable bandwidth available for frequency modulated signals (~1-2 kHz). As an Industrial, Scientific and Medication (ISM) frequency band it is free to use for wireless sensor data transfer, and electrical components are also readily available.

Because of pursuing a longer transmission range new methods were needed to overcome the distance and frequency induced limitations. The hardware was developed with carefully chosen and matched low noise preamplifiers and high performance AD-converters together with three tone frequency modulation method and Fourier transform mathematics.



### 5.3.2. Data reception from weak signals

As the maximum available signal levels approach the noise floor of the reception components, the whole system has to be treated as a unity. Every component in the signal chain affects the next one and the former one, starting from the reception coil and the surroundings together with the transmission coil, which couple to it.

All impedances have to match to the noise properties of the amplifiers, and only the minimum bandwidth needed should be used by tuning the reception coil circuitry. The dynamic range of the preamplifiers and other stages has to be maximised by choosing appropriate components. As the component properties are close to the theoretical limits, mathematics can and shall be used to improve the capabilities of the electronics. Using averaging methods improves the signal to noise ratio, but also decreases the available signal bandwidth. As in all communication systems, the lower the data rate, the weaker signals can be received by averaging (integration), this also corresponds to narrower noise bandwidth, as the bandwidth of the signal is also smaller.

Measuring the frequency components of the signal instead of the amplitude is one way to improve signal to noise ratio, and frequency modulation is commonly used in FM radios around the world. Frequency measurements offer several orders of magnitude higher dynamic range than amplitude measurements.

In low power transmission and reception of weak signals, however, large modulation depths may be a problem if the signal has a small bandwidth due to the relatively high Q-value of the receiving coil. This issue can be solved by using phase modulation, which is close to frequency modulation. In the current study frequency shift keying (FSK) with small modulation depth was used.

### 5.3.3. Developed hardware

The setup used a 3 m x 3 m loop antenna in the transmitter side. The hardware of the current setup developed for the reception side is shown in Figure 5-11.

A two-stage low noise amplifier (Analog Devices, AD797) was matched to the receiving coil impedance at 125 kHz with a capacitor. The receiving coil is a five-turn rectangular loop antenna of 3m x 3m in dimension and with 0.45 mm wire diameter. The receiving coil has an inductance  $L_s = 448\mu\text{H}$  and a resistance  $R_s = 8\Omega$  at 125 kHz. The self-resonance frequency of the coil is about 530 kHz and the unloaded Q-value approximately 44.

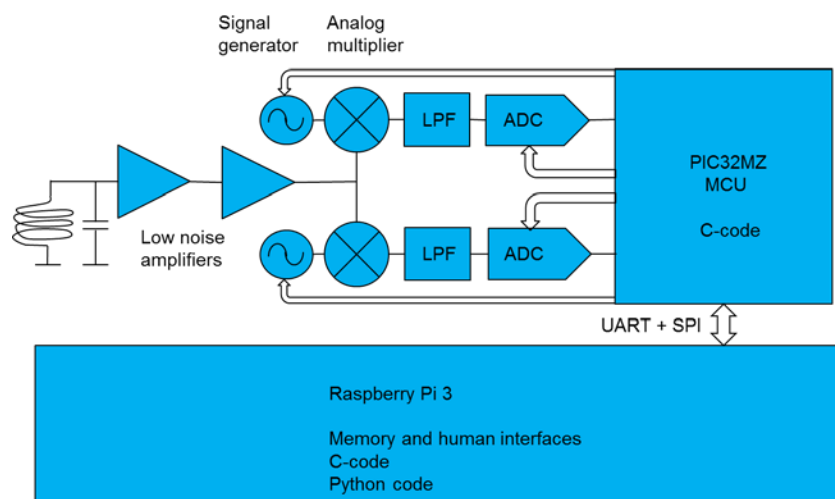


Figure 5-11: Block diagram of the receiver electronics. The receiver coil in the final setup is tuned in series with the capacitor.

The preamplifier voltage gain is about 64 and the second stage gain is 10. The bandwidth of the amplifiers is 16 kHz. After the amplifiers the signal is multiplied with two analogue multipliers (AD835ARZ) in quadrature phase. The local oscillator signals for the multipliers are generated with two signal generators (AD9833BRMZ), which use the same 24 MHz quartz crystal stabilized frequency as the controlling microprocessor (PIC32MZ2048). The frequency resolution of the signal generator is 0.089 Hz. The multiplier/down converter schematics are shown in Figure 5-12.

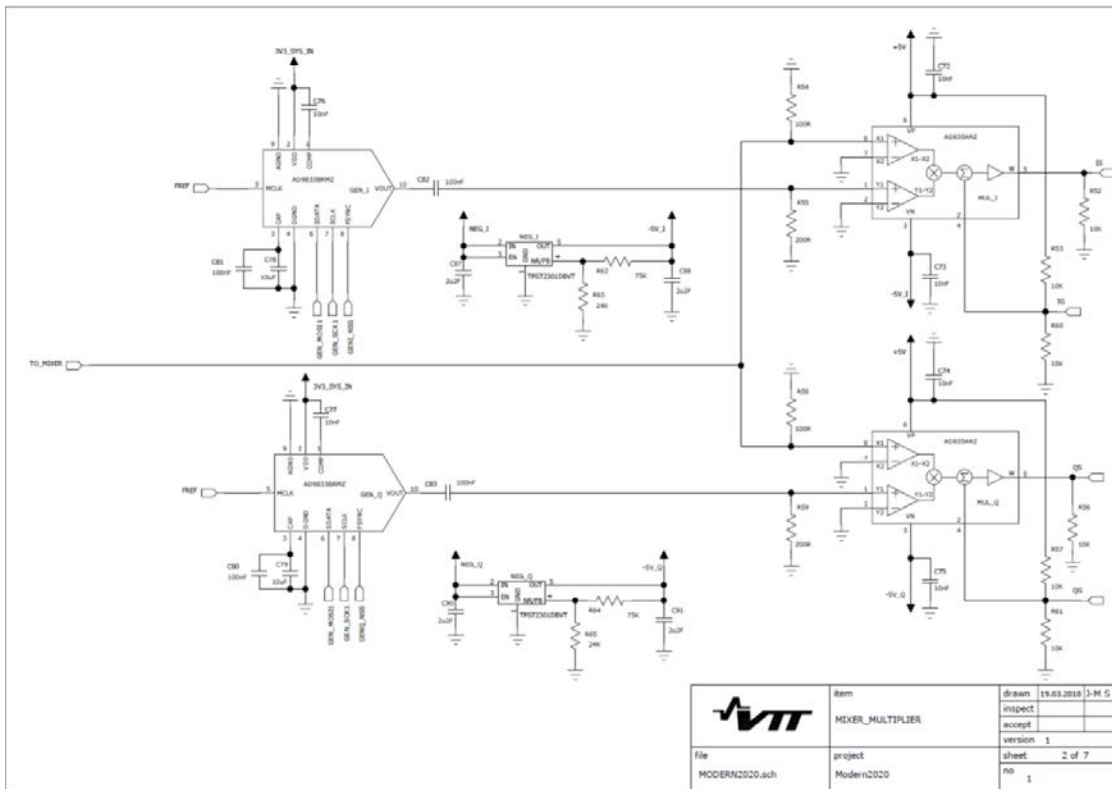


Figure 5-12: Multiplier/down converter of the receiver electronics.

After the IQ-multiplication/down conversion the signal is filtered with a fourth order Butterworth low pass filter with a 5 kHz bandwidth and unity gain. Next an AD-conversion is performed with state-of-the-art 24-bit AD-converters (LTC2380-24) with 20 kSps rate. Data is collected via a 25 MHz SPI-bus to the internal 8 kByte double-buffered storage of the processor. Data acquisition is accomplished with interrupt-controlled hardware and direct DMA-transfer all the way to the final storage in the system controller, Raspberry Pi 3.

The Raspberry Pi 3 is a 64-bit 1.2 GHz four-core ARMv8 Cortex-A53 miniature PC running Linux operating system with various digital interfaces and 32GByte storage capabilities. It has enough processing power for small scale data-analysis due to the 1.2GHz core. A few programs were coded in C- and Python-languages for data transfer and analysis.

The transfer path was demonstrated in VTT’s Otaniemi Research Hall I in Espoo, Finland, in November 2017. A transmission distance of 23 meters with 15 meters of crystalline rock was achieved there. In the Otaniemi demonstration the available space together with the metallic structures restricted the transmission range.

### 5.3.4. Signal modulation and data encoding

Transmitter side modulation is accomplished by phase modulation of the 125 kHz carrier. A three tone modulation is used: the middle tone is used as an end-of-bit marker, which always follows the bit one or bit zero tones. Bit zero tone is the highest tone and bit one the lowest tone. The middle tone was chosen as the bit end marker due to the highest possible signal strength and signal-to-noise ratio in the middle of the transmission coil resonance.

Modulation is performed as a linear ramp of phase, since it is easy to implement in simple electronics. Phase is shifted from 0° to 180° in one tone. The rate at which the phase changes determines the value of the bit. The change of phase is simply accomplished by delaying the start of a new cycle of the carrier by one clock pulse in the transmitting microcontroller. Everything can be transformed into hardware flip-flops and counters, if needed.

In the receiving end of the signal path the down-conversion frequency is 124 kHz, instead of the 125 kHz carrier. This is due to 1/f-noise of the amplifiers, which starts to increase with decreasing frequency from 1 kHz down. The base-band signal is in the 1 kHz range with tones of a few tens of Hertz. Bit length in time is in the order of one second.

A Fourier transform of the gathered data is used for decoding the received signal into spectral frequency and tone components. Since the Fourier transform is of averaging type, it still further enhances the signal-to-noise ratio. As temperature variation is not a problem deep inside the rock, a very narrow bin structure for the Fourier transform could be used. When using very narrow frequency bins, temperature variations could cause the signal to drift away from the assumed bin. In the tests, the whole 10 kHz wide bin structure was used.

### 5.3.5. Results

Underground data transmission over a distance of 23 metres including 15 metres of rock has been achieved. A frequency of 125 kHz was used in the demonstration, the data rate was approximately 1 bit/s. The demonstration was held in VTT's Otaniemi Research Hall I in Espoo, Finland, in November 2017.

The wavelength of the radio signal was 2400 metres, very large compared to the size of the antennas. Therefore the efficiency of the transmitting antenna is necessarily very low, with only a small and unknown portion of the input power actually radiating, this is another way of saying that the communication method was actually near-field. The input transmitter power from power supply during transmission was 1.02 watt. A peak-to-peak voltage of 165 volts was determined at the antenna. The inductance of the receiving antenna was 448 µH and the consumed energy per bit approximately 1 Ws. The bit error rate was not measured, but from the received data it could be seen that a practically error-free transmission was achieved.

The low data rate is the result of the extremely challenging radio link conditions, operating near the noise limit and needing to integrate for a longer time to receive and correctly detect the transmitted bits. The system noise level at the receiver input is approximately -135 dBm, corresponding to about 7 fT magnetic flux density, the signal needs to be at least 10 dB stronger than that for successful reception. The goal was to maximize range, not data rate. On the other hand, the low data rate is not a significant disadvantage, not even combined with the low duty cycle, because the quantities to be monitored only change very slowly.



### 5.3.6. Summary

With the developed medium frequency system, underground data transmission over a distance of 23 metres including 15 metres of rock was achieved. A frequency of 125 kHz was used in the demonstration, the data rate was approximately 1 bit/s.

The signal was transmitted essentially by the magnetic field coupling between transmitter and receiver coils. That field is not much affected by non-metallic materials within the path. The disadvantage is a rapidly increasing attenuation versus distance. The power supply energy per bit was approximately 1 Ws. This may seem to be a large amount, but the maximum communication distance is proportional to the sixth root of the transmitting power. Assuming a constant efficiency, a reasonable distance of 7.3 metres would still be achieved with a much smaller bit energy of 1 mWs. The bit error rate was not measured.

The low data rate is the result of the extremely challenging radio link conditions, operating near the noise limit and needing to integrate for a longer time to receive and correctly detect the transmitted bits. The signal needs to be strong enough with respect to radio frequency noise from the equipment and environment. The goal was to maximize range, not data rate. The low data rate is not a significant disadvantage, not even combined with the low duty cycle, because the quantities to be monitored only change very slowly.

The developed technology is still at a demonstrational stage, having a distance to go into a prototype and a mature product. One of the problems to be solved is the automatic tuning of the antennas. After the antenna has been buried into the filled-up tunnel, the surrounding materials and metal parts will change the delicate tuning of the antenna coil. A method and implementation to re-tune the antenna without a wired connection to the outside world is not yet available, but can be developed in further work after the present project. Some ideas for further development after Modern2020 include: Automatic antenna tuning (as already mentioned), improved packaging, testing and enhancing long term stability and reliability, increased automation and raising the maturity of the design.

## 5.4. Adaptation and testing of wireless Through-the-Earth commercial technology

This chapter summarizes the work of Amberg and ENRESA on the adaptation and testing of a commercial wireless Through-the-Earth technology for short range data transmission under repository conditions.

### 5.4.1. Background and objectives

Low frequency magnetic induction technology, also called wireless Through-the-Earth or TTE, penetrates concrete, rock and other obstructions enabling communication and position determination in some of the most challenging environments in the world, including: mines, caves, subways, utility tunnels, buildings, and parking garages. Equipment based on such technology is currently commercially available and used in mines, military operations, tunnelling communications, etc.

The objective of the work performed by Amberg was to adapt this kind of equipment to the requirements of the Modern2020 project and test it under realistic conditions to ascertain if it could offer a valid approach for the future use in underground repository monitoring. A first prototype was initially tested in a Spanish underground mine to assess the applicability of this potential solution. Due to the good results obtained from this test, it was decided to test it as well in the WTB of Tournemire.



## 5.4.2. Specifications for the TTE system

The operational requirements imposed for the equipment were as follows:

- The TTE transmitter will have a maximum diameter of 10cm
- The receiver may be located at least 10 to 20 m away from the transmitter
- The transmission path will run through solid rock as clay formations (argillites) and sealing materials (concrete, bentonite plugs)
- The transmitter includes a power supply and allows to connect several sensors (WSU).
- Data transmission shall be set at a low duty cycle (one or two transmissions per day)
- The transmitter battery shall have a target lifespan of 10 years.

The preliminary layout of the desired data transmission system is given by Figure 5-13 and the different building blocks are described hereafter.

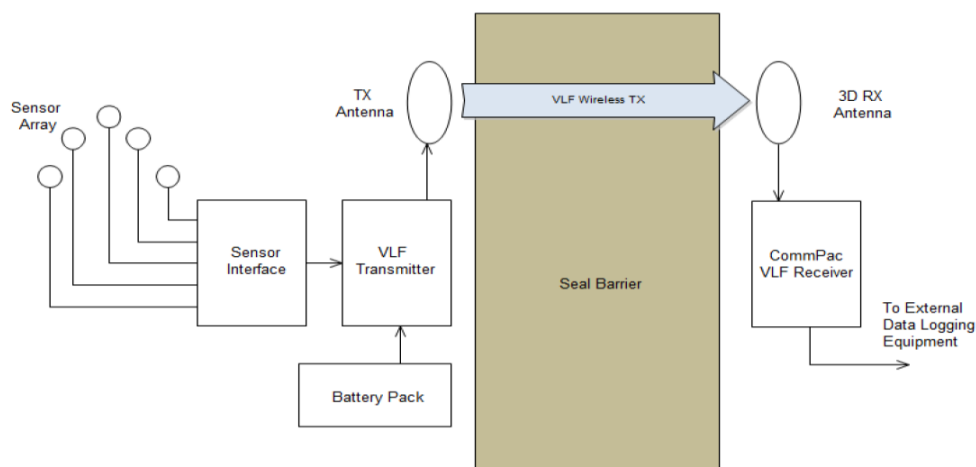


Figure 5-13: Preliminary layout of the TTE data transmission system

**Sensor Array:** The sensor array comprises several sensors from different manufacturers. Each sensor is powered and controlled (if required) by a Circuit-Card Assembly (CCA, see next description).

**Sensor Interface:** This is a custom Circuit-Card Assembly designed to acquire output signals from the sensor array and redirect them to the transmitter. The CCA allows to measure several parameters and to use a wide range of different sensors, with each type of sensor having its own excitation requirement and output signal:

- Temperature (analog TCs & 4-wire Pt100/Pt1000 resistance types)
- Mechanical pressure (mA, mV, Vibrating wire, Wheatstone bridge)
- Hydraulic pressure (mA, mV, Vibrating wire, Wheatstone bridge)
- Water content/saturation (mA, V, Digital Sbus or I<sup>2</sup>C)
- Displacement (mA, mV, Vibrating wire, LVDT)

As already mentioned, each kind of sensor has either a digital or analog interface. Each analog interface has a different excitation requirement and output signal (analog voltage, 0-20 mA current loop, etc.), which must be converted to a digital value for transmission over the VLF data link. The sensor interface uses a micro-controller (MCU) to perform these functions. The microcontroller is also used to track time during sleep mode, when the transmitter and sensors are completely powered-down.

**VLF Transmitter:** The VLF transmitter comprises two circuit board assemblies, the Transmitter CCA and the DSP CCA, which plugs onto the transmitter and houses the VLF radio firmware.



**TX Antenna:** The transmitter antenna has a ferrite core with dimensions of 19 cm x 8 cm and fits into a 90 mm diameter tube.

**RX Antenna:** This is a standard off-the-shelf receiver antenna enclosed in a waterproof housing and connected to the VLF receiver through a cable and MIL connector.

**VLF Receiver:** This is a standard off-the-shelf item. Data received from the sensors is sent to the Data acquisition system over an RS-485 interface (through a connector). This interface has high noise immunity and can negotiate cable lengths of 300 m or longer, if required. It can be easily converted to other serial data formats compatible with e.g. RS-232 or USB interfaces by adding an external converter; these are widely available and low cost components.

**Data Package:** On the sensor interface board, data from each sensor will be converted by the MCU to a standard numerical format and compiled into a data packet together with the Sensor ID and error detection bits (CRC). Each packet length including ID and CRC is assumed to be no longer than 16 bytes, resulting in an overall data batch of maximal 96 bytes (768 bits) per data transmission cycle. Two previous data batches will also be stored in the MCU non-volatile memory; these will be added to the current batch to provide redundancy in the data transmission process.

**Data Transmission:** A sequential transmission number and a unique word will be inserted at the beginning of each data packet, resulting in a total batch of about 300 bytes (2400 bits), which can be transmitted one way only over the VLF link in 1.5 seconds at an average rate of 1600 bit/s using inter-harmonic modulation.

**Data Reception:** The receiver, the batch will be demodulated and sent out as a serial data stream which can be parsed by an App running on an external computer to extract the sensors data.

**Power Supply:** operation over a time span of up to 10 years can only be achieved by operating the radio in a sleep mode for most of the time. Sleep mode will be controlled by the MCU on the Sensor Interface, which is able to maintain a timer running while in a very low power state. Based on previous experience with similar applications, the power consumption will be kept under 0.5 mW while in sleep mode, resulting in a total energy consumption of during the inactive state of 12 mWh per day.

## Overall energy budget

When the transmitter is started up from sleep mode, a number of operations must be done:

- First the transmitter DSP processor must boot and load its program code (5 seconds).
- Then the transmitter must send a sequence of frames so that the receiver can synchronize its internal clocks to the transmitter (30 seconds)
- While these operations are running, the MCU enables each sensor, read the analog signals and create the data batch as described above. This can be done in parallel with the DSP boot and receiver synchronization (up to 35 seconds). Time averaging of the data can be performed during this interval.
- The data batch is then transmitted to the receiver (less than 2 seconds).

For each transmission cycle, the total time in “on” mode for the transmitter is therefore 37 seconds.

The total power consumption while the transmitter is on duty is 9.3 W (0,7 W of sensor interface, 7 W of DSP and Transmitter CCA plus 1,6 W of transmitter antenna). Considering the 37 s time span in “on” mode per transmission cycle, the energy consumed per transmission cycle is 96 mWh. The resulting energy consumption with one transmission cycle per day, including the power consumption during sleep mode, is 107 mWh, or ~ 39,3 Wh per year.

In order to provide more than 10 years of operation, the power supply must have a capacity of at least 393 Wh. Hence, this application requires a primary battery with very low self-discharge rate, to maintain sufficient power over 10 years. The best battery technology for this application is Lithium Thionyl Chloride (Li-SOCl<sub>2</sub>), which is available in different commercial cell sizes with a nominal voltage of 3.6V. A battery comprising 8 cells supplies an output voltage of 28.8V, which is at the upper range for the transmitter, where efficiency is the highest. The main trade off in this technology is between discharge rate and current output capability (see also [3]).



The transmitter power consumption and energy requirements are summarized in Table 5-3.

**Table 5-3: Transmitter power consumption and energy requirements**

Condition	Power consumption [W]	Energy per bit [mWs/bit]
Overall wireless sensor node	9.3	143
Transmitter	1.6	1
Efficiency of data transmission	1000 bits/Ws	

Because the MCU will keep track of the number of transmissions, it is also possible to program it to adjust the rate of transmissions over time, i.e. starting with several transmissions per day (as required for test purposes) and afterwards reducing the transmission rate over time to one or two transmissions per day.

### Mechanical design

Two different deployment scenarios were planned for the transmitter: emplaced within a borehole and emplaced within a larger diameter repository gallery. A common packaging approach was decided for each deployment seeking to minimize development works and manufacturing costs.

- Borehole Deployment (Figure 5-14):** this design is similar to that of the first prototype unit tested in Spain, in which both the transmitter antenna, electronics and battery are all sealed together into a compact single tube. The new ferrite core antenna is much smaller than the prototype air cored loop, so the length of the tube has been drastically reduced, from 200 cm to 69 cm. The tube diameter has also been reduced to 89 mm to anticipate irregularities in the boreholes. Thus the new enclosure results in a volume of 4050 cm<sup>3</sup>.

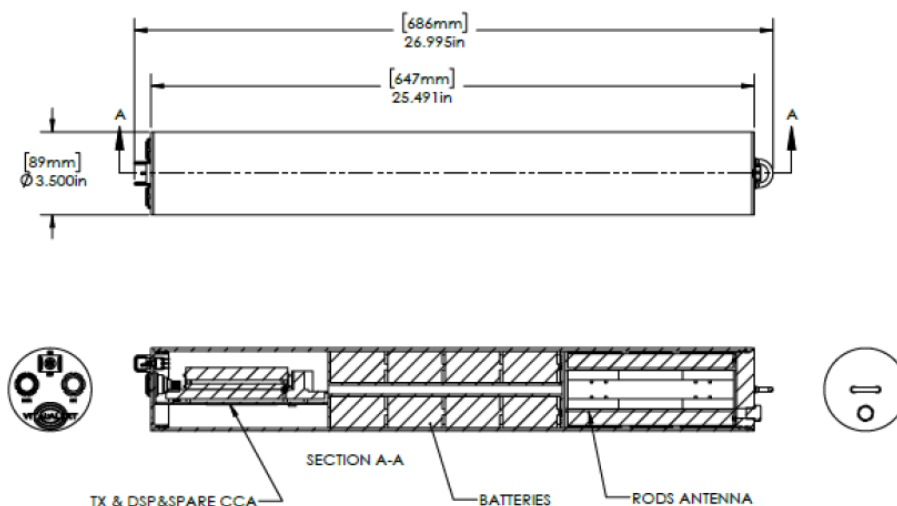


**Figure 5-14: Packaging for borehole deployment**

- Galleries Deployment (Figure 5-15):** for applications where the form factor of the Borehole packaging is not suitable, we propose packaging the battery, transmitter antenna and electronics as three separate sub-systems, each one enclosed in a separate 89 mm diameter tube. Hence, the basic design of the tubes, internal brackets and end caps is the same as for the borehole application. In this configuration, the tubes for transmitter antenna and for electronics are roughly 20 cm long, while the battery tube is 27 cm long. The total volume taken by the electronics in this configuration is 4170 cm<sup>3</sup>. The battery power and antenna are



connected to the radio through a single “Y” cable. The tubes can be emplaced on demand as a compact package or distributed separately.

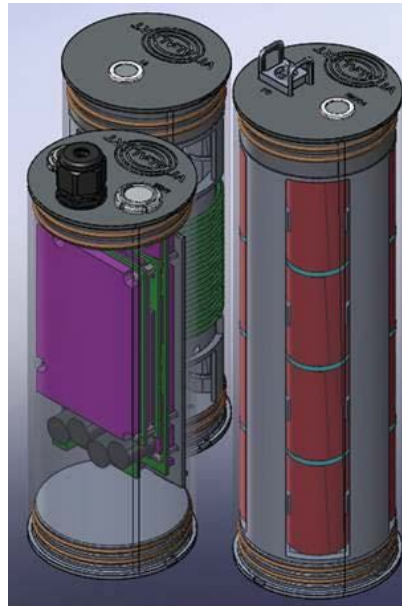


Figure 5-15: Packaging for galleries deployment

### 5.4.3. Field testing in the Tournemire WTB

A first testing was carried out on 7<sup>th</sup> of March 2018 with a prototype of the TTE system at Mina Escuela Bierzo (FSB), an old underground coal mine in Leon (Spain) that is re-used for preparing technical staff for civil underground works. The equipment (Figure 5-16) was tested in three different scenarios: (1) two quasi-parallel galleries that diverge at an angle of 60°; (2) two opposite galleries, currently under excavation, which will meet/join in the future to merge into only one, but at the time of the testing separated by 23 m of rock in between and (3) two parallel galleries separated by 30 m of rock. Results for scenario (1) were 25 and 26 dB signal relative to noise level for a distance of 25 m, while for scenario (2) the signal ranged from 25 to 29 dB and for (3) the signal was 25-26 dB.



Figure 5-16: Receiver (left) and transmitter (right) used at FSB

The second testing was carried out at the WTB of Tournemire on 10<sup>th</sup> April 2018, using the same prototype (see specifications at 5.4.2). The results of the tests over a distance of up to 10m were better than expected; in fact the test using the access boreholes oversaturated the receiver input (signal too strong when both the transmitter and the receiver were located inside the boreholes, Figure 5-17 left). It was then decided to install the transmitter in the access boreholes and the receiver along the access gallery that leads to SEALEX gallery (Figure 5-17, right) to take signal measurements in the readable range. Results were similar to those gathered at FSB, and the maximum range achieved with this arrangement was 30 m.

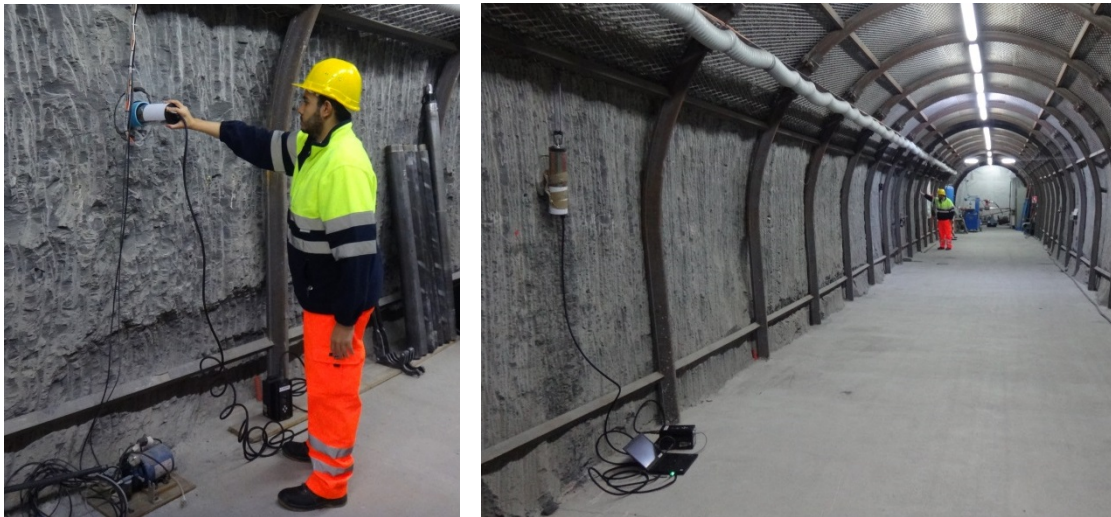


Figure 5-17: Testing inside the access boreholes (left) and at the access gallery (right) at Tournemire

#### 5.4.4. Future developments

If required in future applications, the receiver antenna can also be packaged to fit within a 90 mm diameter tube. This involves replacing two of the three orthogonal ferrite antennas with air cored wire loops, so that they will fit inside the tube, together with the receiver amplifier. This configuration was used in the prototype design, providing the same performance as the standard receiver antenna. As the design has already been proven, the effort required to produce this version of the receiver antenna will be small, but the cost of manufacturing this custom design will be higher than the “off-the-shelf” antenna. The range of the system can be increased by using larger antennas if the available working space allows it. The table below indicates the operating range expected in a low noise repository environment, based on an receiver level of 30 dBpT.

Table 5-4: Transmission ranges expected with larger antennas

Antenna Type	Maximum range
90 x 200 ferrite core	30 m
1m diameter loop (N=4)	60 m
5m diameter loop (N=2)	120 m
10m diameter loop (N=1)	200 m

To extend the battery life the power consumption of the transmitter can be reduced in a number of ways; these are briefly described below:

- a) Reducing the maximum transmission distance to 15 m. This would allow the transmitter current to be lowered (via software configuration setting), which in turn would reduce the power consumption of the existing transmitter design from 9.3 W to 8.1W.
- b) Reducing the number of sensors. The sensor units power consumption of 0.7 W is roughly proportional to the number of sensors used; for applications requiring only a single sensor the power consumption may be reduced to 0.2W
- c) Re-designing the DSP CCS for low power operation. This would require a new hardware and software design, specifically to support this transmitter-only application, and would be based on the use of lower DSP core and memory clock speeds. According to a preliminary estimate, this approach, together with other circuit changes, could reduce the DSP power need by 50 %, to 3.5W.

Implementing together all these changes would reduce the transmitter power consumption to ~4W, which would extend the battery life significantly.

While VLF radio equipment is generally more immune to the effects of ionizing radiation than high frequency RF devices, the transmitter hardware will also need to be hardened to prevent damage to memory and other sensitive components when embedded in a repository containing nuclear waste. These design changes may be incorporated at the same time as the low power design changes discussed in paragraph c) above.

#### 5.4.5. Summary

Results show that the TTE equipment used is suitable to transmit data over distances of up to 30 m under conditions similar to those expected at the future repository. The signal was transmitted by the magnetic field coupling between transmitter and receiver coils. A frequency of 4 kHz was used and the data rate was 1600 bit/s with an energy efficiency of approximately 1 mWs/bit.

However, there is room for much more improvement, as described in 5.4.4. Besides, it should be noted that the same approach could be applied for longer transmission ranges, just by changing the antenna.

### 5.5. Discussion and conclusions

To demonstrate the technological feasibility of underground wireless data transmission, VTT, Arquimea and Amberg have developed short range solutions and have demonstrated them over distances of 4 m (Arquimea) and 30 m (Amberg) in partially saturated bentonite + clayish rock, and over 23 m (VTT) in granite environments.

As shortly discussed in Section 4.1, wireless system capability to transmit across the repository materials and components decreases with increasing frequency. Related to that, three schemes were planned and implemented within the Modern2020 project: Arquimea has improved short range wireless systems based on high frequencies, VTT focused on the use of systems based on medium frequencies, and Amberg has provided a solution based on low frequencies. Furthermore, IRSN has implemented the WTB in the Tournemire Laboratory (see Chapter 5.1) to provide an environment for testing and developing communication systems under relevant conditions.

Regarding the high frequencies approach, the starting point was the outcome of the former MoDeRn project, where prototype wireless sensor units using a 169 MHz radio frequency (RF) transmission were developed by Aitemin. These units were partly successful, showing some issues regarding antennas geometry, signal losses after hydration of the buffer and energy efficiency. A new improved wireless transmission system has been developed by Arquimea using 2.2 MHz as transmission frequency (Chapter 5.2). This work has resulted in performance improvements, by the adaptation of the already existing WSU to a new short loop antenna designed *ad-hoc* for the application. The transmission system was



tested during 2017/2018 showing a radio link node to node over a distance of 4 m inside the bentonite-based buffer installed at the WTB facility. Results from these tests were used for the final design of the three nodes used in the LTRBM (Modern2020 WP4.3).

Regarding medium frequency systems, underground data transmission was achieved over a distance of 23 metres, including 15 metres of rock. A frequency of 125 kHz was used in the demonstration, the data rate being approximately 1 bit/s. The demonstration was held in VTT's Otaniemi Research Hall I in Espoo, Finland, in November 2017 (Chapter 5.3).

Concerning low frequencies, the approach tested by Amberg was capable of transmitting up to 30 m at the WTB in Tournemire using 4025 Hz with a data rate of 1600 bit/s (Chapter 5.4).

In these three studies, understanding of the general principles and applicable technology of short range underground data transmission have been obtained and demonstrated. The general theory of wireless transmission, based on electromagnetic theory, applies to the underground environment. Electromagnetic properties of the associated natural and engineering materials in the transmission path shall of course be taken into account. Problems that arise concern engineering, not basic physics. Engineering work has been done in Modern2010 to apply the general principles to develop data transmission solutions for the underground environment.

These solutions have reached different states of maturity, with Arquimea's WSU and Amberg system providing versatile solutions allowing the integration of different analogue and digital sensors. Arquimea's WSU is ready for testing in the LTRBM. This, together with earlier work of RWMC on 10 kHz, allows to choose between a variety of options and transmission frequencies for various application cases of interest.

The real application case may differ from the demonstration environment in some important aspects. In particular, metallic objects (reinforcements, nets etc.) change significantly the wireless transmission environment, causing additional attenuation and possibly preventing any communication by blocking the signal completely. Enclosures fully surrounded by metal walls do not allow at all this kind of wireless communication from the inside. Although differing in details, this limitation applies in general to all the frequency bands in question. Hence, to ensure successful communications, it is necessary to test the system in the actual environment during repository construction.

To bring the underground short range wireless technologies into products and practical industrial applications, engineering development more than basic research is needed. For the application of 125 kHz, some problems specifically need to be solved, concerning automatic antenna tuning, packaging, reliability and energy consumption. Regarding further development of the 2.2 MHz WSU, main improvements should be focused in system size reduction, fabrication procedure and energy management. The same kind of improvements are pending for Amberg TTE system. These problems are not new, as they have been faced before in other areas of electronic system development. They just need somewhat different approaches in this previously little explored application area. Regarding the engineering work a multidisciplinary approach is necessary, combining expertise from such diverse fields as radio frequency circuit technology, electronics (including reliability engineering), antennas, mechanics and applied electromagnetics. It seems quite certain that the problems can be solved with time and adequate funding, thus raising the technology readiness level relatively rapidly. As part of the development work, testing in actual environments such as WTB (Chapter 5.1) would be essential, and the successful prototype of Arquimea's WSU and the TTE device of Amberg have benefited from an iterative approach that includes extended field test in the WTB.



## 6. Long range wireless data transmission systems

---

### 6.1. Understanding and improving long range wireless transmission system

This chapter summarizes the work done by Andra for understanding and improving their long-range data transmission system.

#### 6.1.1 Aims of the long-range wireless data transmission

In the French project for a deep underground radioactive waste repository (Cigéo project), monitoring tools need to be as discrete as possible and the ways of transmission as well. Several types of wireless transmission systems have been developed as presented in this report. If the use of wireless transmission devices is decided, an adequate combination of wireless transmission systems needs to be deployed. The current strategy for Andra is to use only low frequency transmission (i.e. about 10 kHz) in order to transmit through the host rocks and repository cells seals.

Sensors are not necessarily allocated evenly in all cells regarding to different cell designs (High Level and Intermediate Level - Long Live Radioactive waste cells). The monitoring strategy relies on different levels of instrumentation. Hence, the wireless transmission systems should be adapted to several configurations. For instance, it may consist of miniaturized wireless transmitters connected to one or two sensors put in monitoring borehole near a HLW repository cell; while it could be an all-in-one wireless transmitter connected to a bunch of sensors inside an IL-LLW repository cell (cf. Figure 6-1).

Between repository cells (outside the cells), no wireless communication system is foreseen in this concept: there is no need of leakage prevention in those areas and wire-based communication systems will perform the job with a better reliability and robustness.

Finally, the need of wireless transmission system will be adapted to the different stages of progression of Cigéo: some wireless transmission systems will be needed when sealing will be setup, others will be required before cells drillings.

More precisely, in case of use of medium-range wireless transmission systems (about 30 m), three objectives could be achieved:

1. Transmission of sensor measurements done in rock boreholes completely sealed (generally connected to only one sensor by transmitter).
2. Transmission of sensors measurements done behind a cell-sealing plug – middle range transmission.
3. Transmission of sensors measurements through the host rock layer.



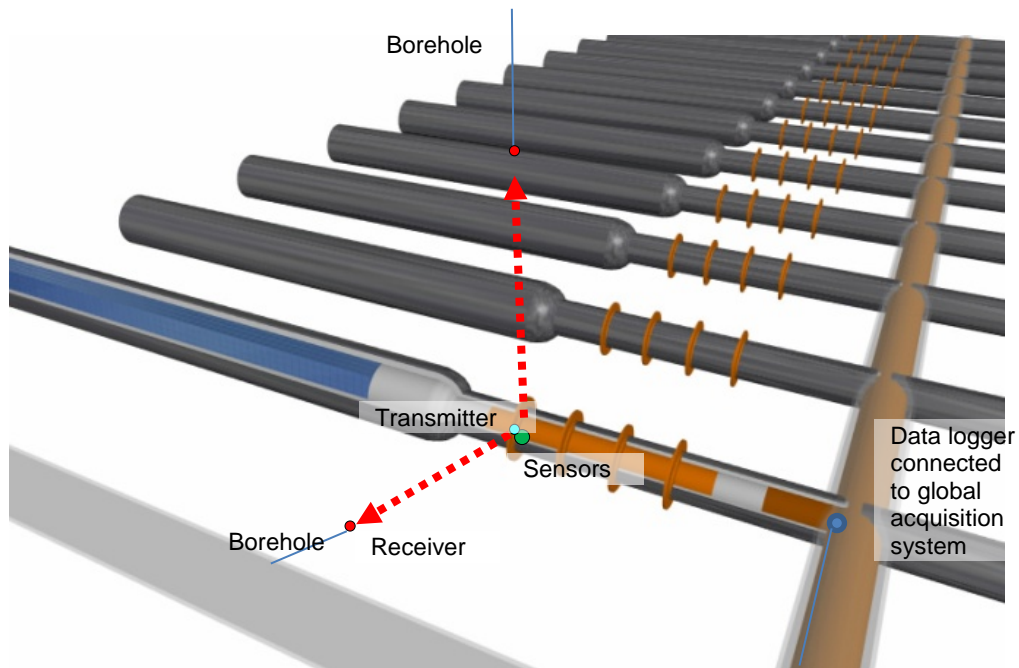


**Figure 6-1: Medium range wireless configurations.**

An alternative option to the medium range wireless configuration is considered for Cigéo: a wireless transmission that allow to transmit monitoring data from the repository level directly to the ground surface. That implies a transmission on a distance greater than 500 meters through the geological rocks (cf. Figure 6-2). This system would be especially suitable at the closure stage of the repository. In the end of the repository operational phase, a complete closure of Cigéo site is foreseen including the shafts and the ramp. Wireless monitoring of structural health after this period will be of great benefit for the confidence put in the safety of the site.

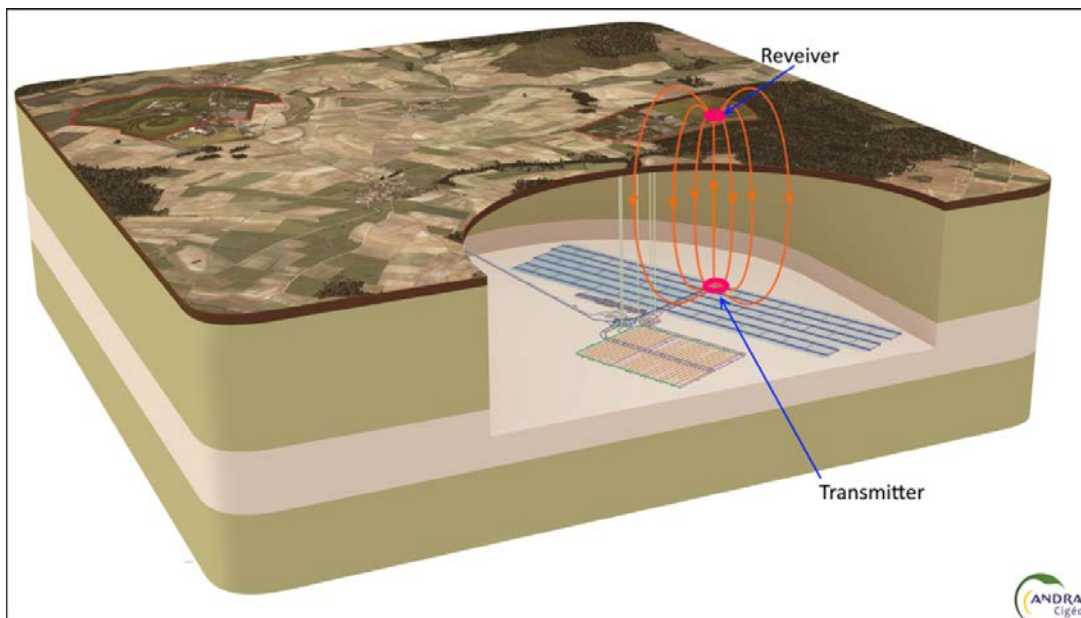


**Figure 6-2: Long range wireless configuration.**



### 6.1.2 Theoretical transmission distance versus in situ measurements

The success of transmission over a great distance such as 500 meters depends on the power and the size of the antenna, and the environmental electromagnetic noise.

A large antenna has been designed in order to be able to transmit a signal at 8533 Hz over hundreds of meters. This antenna is 3.75m by 3.75m large and requests an electrical power of 200 - 300 Watts during transmission (Figure 6-3). A modulated data signal was broadcasted, however, the transmitted data was not analysed: the test campaign focused on the signal strength read on the receiving antenna.



**Figure 6-3: Large antenna for long range wireless transmission in the Tournemire URL.**

In spring 2015, two long distance transmission test campaigns have been performed in Andra's URL. These test campaigns include transmission tests between the transmitter (with the large antenna) positioned on the ground surface and a receiver positioned on the surface at several distances to the transmitter. Furthermore, additional tests were performed with a receiver placed at the surface and the transmitter located in a borehole of the underground URL (cf. Figure 6-4).

The set-up succeeds to transmit wirelessly a modulated signal in a coplanar surface-surface configuration up to 310 meters, but not further. A transmission between the URL and the surface was not successfully established. Two main reasons can explain the failure of transmissions over long distance for these tests: the noise level was too high and the geological properties of the underground medium (rocks) attenuated the signal too much. In fact, the noise level was higher than in other tests due to near human activities (and the presence of buildings) but not extraordinary excessive: about ten times higher than in quiet places. The geological properties of the nearfield rocks around the large antenna could explain an attenuation but there is a lack of very precise information on this medium. In any case, surface-surface transmission was limited to distances of less than 400m, consistent with the finding that no transmission between the ground surface and the URL (500 m) could be established either.

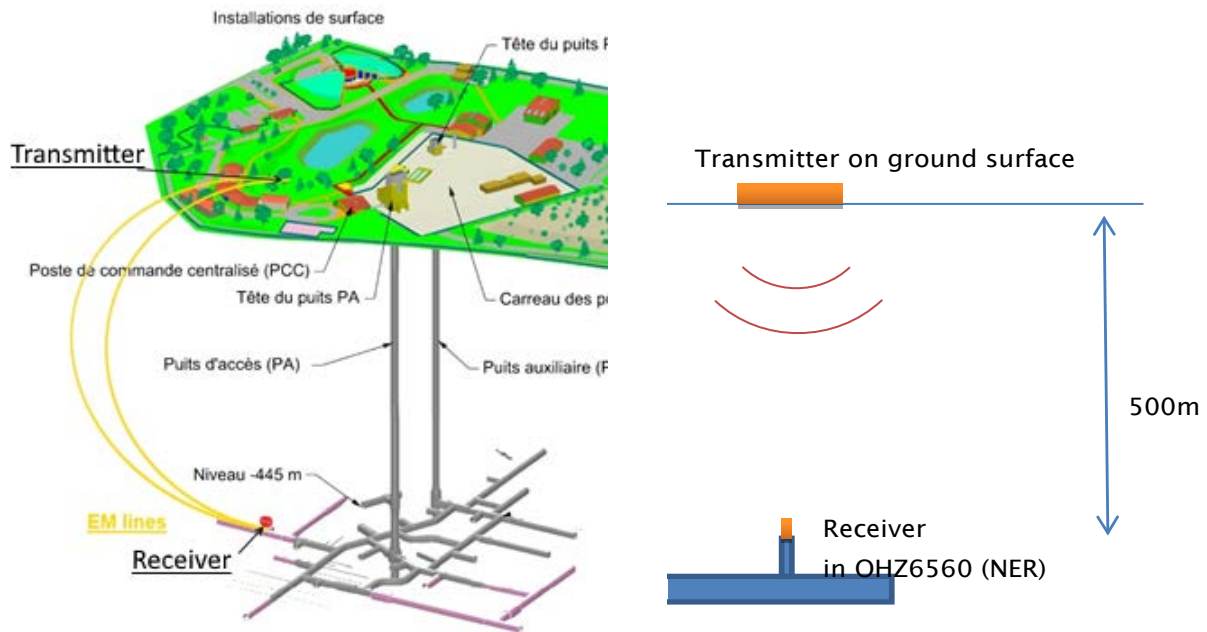


**Figure 6-4: Long distance underground transmission configuration for tests in Andra's URL**

In order to consolidate the results obtained in Andra's URL, the long distance transmission devices have been tested in the Tournemire URL in summer 2017. The ease of access to the tunnel allowed deploying the large antenna in the gallery. Three test campaigns were performed (cf. Figure 6-5):

- Campaign A is a transmission test from the subsurface gallery to top of the mountain.
- Campaign B is a surface-surface transmission test between several locations on the mountain plateau.
- Campaign C is a transmission test from the mountain plateau to the subsurface gallery.

Wireless signal transmission has been achieved for each campaign. Campaign B confirmed the results of the surface-surface test above Andra's URL: the transmission range was limited to 300 meters due to high electromagnetic noise level. In the location of Tournemire, it has been tested up to 300 m and should have worked theoretically at 500 m due to the lower EM noise level.

In the campaign C, wireless transmission was successful over a distance of 270 to 290 m as well: even with the noise level in the gallery 5 to 10 times higher than on the top of the mountain, the received signal strength was two times higher than the noise level. The receiver was placed on several locations in the tunnel, but the received signal level on top was the same at all places. The tunnel is a former railway tunnel, and the rails evened the signal over more than 200 m in the gallery.

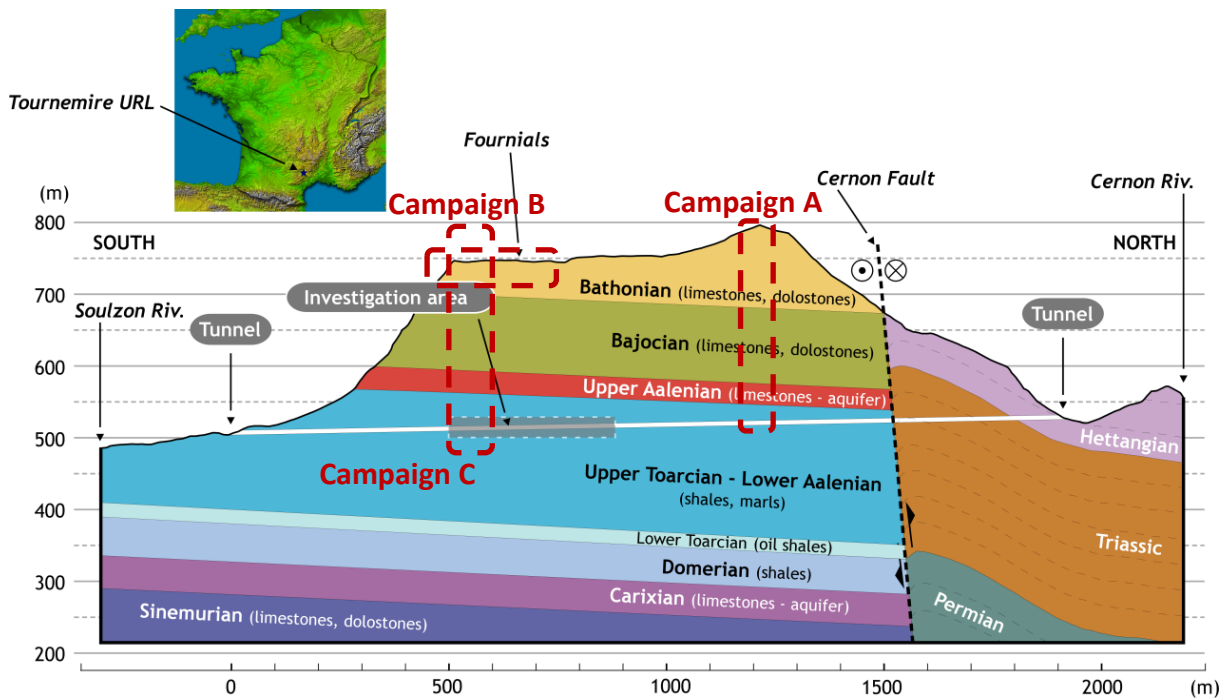


Figure 6-5: Long distance wireless transmission tests done in Tournemire URL

The major result was obtained with campaign A. The transmission from the gallery to the top of the mountain is the most relevant configuration with respect to the objective to transmit wireless data from the Cigéo gallery to the surface. In Tournemire, a transmission through 270 meters of rocks was tested. The signal strength was about four times above the EM noise level on the top of the mountain (cf. Figure 6-6). It demonstrates also that the transmission from the gallery of Andra’s URL to the ground surface cannot be achieved with the current set-up, due to higher EM noise level and greater distance.

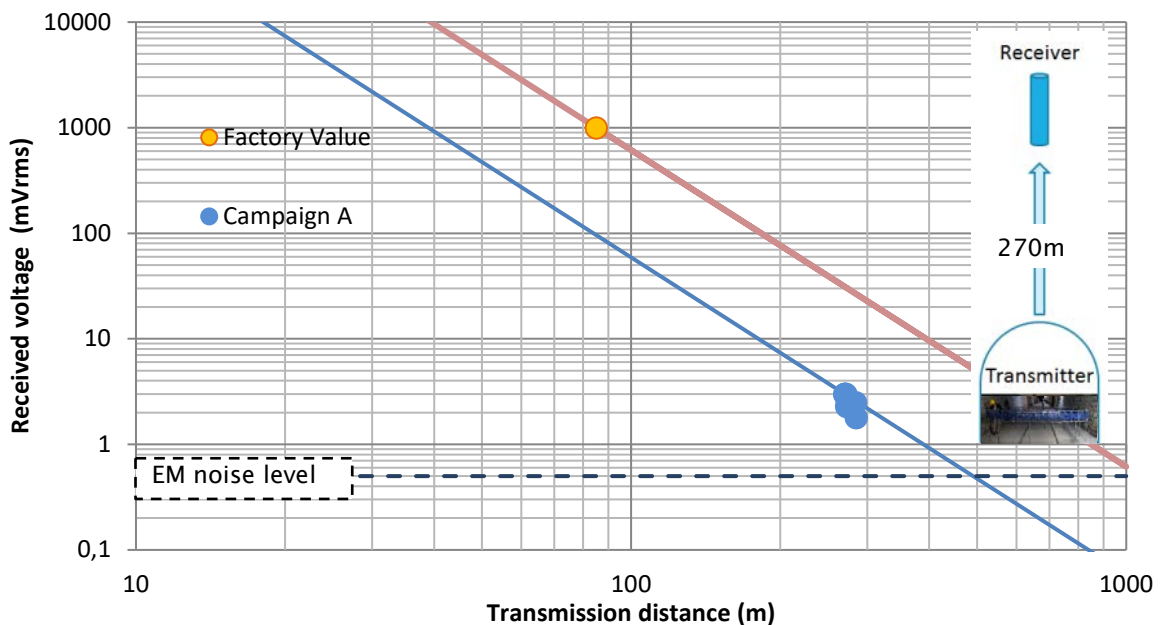


Figure 6-6: Data from wireless transmission tests done in Tournemire URL.

### 6.1.3 Summary

The use of a larger antenna has permitted to extend the previous range of wireless transmission devices from tenths of meters to hundreds of meters. It demonstrates also that the transmitted signal is weakly attenuated by the rocks and strongly deviated by metallic parts such as rails. Nevertheless, the developed system was not able to achieve to transmit data from the Andra's URL to the ground surface. As it is hardly possible to reduce the environmental EM noise level or increase the size of the antenna, the best option to realize a transmission over 500 meters of distance under the given conditions will be to increase the power put in the antenna. This would probably bring safety issues. The use of relay seems more adequate at this stage of developments.

## 6.2. Improvement wireless monitoring system and development of a relay system

### 6.2.1. Concept of the wireless relay system

Since 2002, RWMC is working on wireless data transmission systems as part of their monitoring system that is being developed to avoid detrimental effects of the monitoring system on the quality and performance of the seals in a geological repository [14], [15]. RWMC's underground wireless transmission technology uses electromagnetic waves with frequencies of several kHz to minimize attenuation in the ground and in water. In order to enable monitoring in a limited space such as inside buffer materials or the near-field environment, and to enable receiving the monitoring data on the surface, RWMC has developed a miniaturized transmitter [10] (see Table 6-1), and middle-range and long-range transmission antennas [16] in a collaborative study with Andra<sup>3</sup>. The miniaturized transmitter can be used for the monitoring system, including wireless relay system.

**Table 6-1: Specifications for the miniaturized transmitter [10]**

Transmission interval	1 week
Transmission distance	25 m
Output power	0.54 W
Transmission speed	75 bit/s
Transmission efficiency	7.2 mWs per bit
Durability	About 10 years
Size (diameter x length)	Φ60 mm×240 mm
Frequency of electromagnetic wave	8.5 kHz
Pressure resistance	10 MPa
Operating temperature	0 - 40°C

A wireless relay system for a long distance using the long-range transmission antenna has been developed, and a transmission test for a distance of 250 m has been successfully carried out at the Horonobe URL using an external power source [12]. A large power supply is necessary for long-distance transmission by underground wireless transmitters and relay devices, based on the inverse relation between magnetic field strength and transmission distance [15]. However, the supply of power is a limiting factor. To reduce power consumption, RWMC has proposed a multi-stage relay system to shorten the transmission distance between devices (see Figure 6-7). Also, RWMC has worked to improve redundancy by introducing a multi-route relay system to secure transmission routes in case of malfunction (see Figure 6-7). The goal of the multi-stage/multi-route relay system is to establish alternative transmission routes in case of failures, and to reduce power consumption by combining data

<sup>3</sup> The research in RWMC was a part of "Development of Advanced Technology for Engineering Components of HLW Disposal" under a funding from the Agency for Natural Resources and Energy (ANRE) of the Japanese Ministry of Economy, Trade and Industry (METI).



from more than 10 transmitters in a relay, with the same power consumption as is used by one of these transmitters.

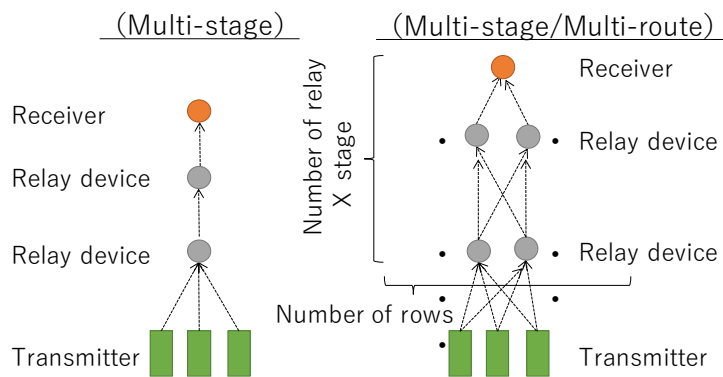


**Figure 6-7: Conceptual diagram of a multi-hopping data relay. The figure on the right side shows rerouting of the data transmission in case of a malfunction of the relay device. Modified from [17].**

### 6.2.2. Power saving by introducing multi-stage wireless relay system

The relay system described above can reduce the power consumption when one transmitter is connected to a relay only. However, the power consumption can increase when the relay device manages several transmitters due to the increase of the time for the ‘reception standby’ mode, i.e. when the relay waits to receive a complete set of data from all transmitter nodes. Analysing the power consumption status for each mode of the relay device, it was found that the power consumption during the reception standby mode is significant: about 70 % of the overall power consumptions. To reduce the power consumption of this mode, a low consumption activation code (GOLAY code; [18]) was introduced that optimizes the receiving circuit usage state. A software was implemented that successfully reduced the power consumption of this mode from the 123 mA to 4 mA, allowing the relay system to be connected to the intended number of transmitters with only 4% of the power.

In a next step, antennas, power supplies, and a container to protect the whole relay device were designed and manufactured (Figure 6-8). The specifications are summarized in Table 6-2.

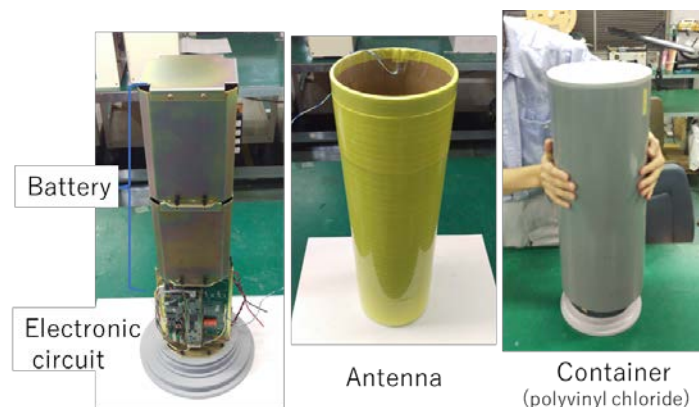


**Figure 6-8: Relay device for the multi-stage / multi-route relay system [19].**

**Table 6-2: Specifications of the relay device. Modified from [19].**

Transmission interval	1 week
Transmission distance	100 m
Output power	10.1 W
Transmission speed	75 bit/s
Transmission efficiency	135 mWs/bit
Durability	About 10 years
Size (diameter x length)	Φ216mm×565mm
Frequency of electromagnetic wave	8.5 kHz
Pressure resistance	5 MPa
Number of transmitters managed	10

### 6.2.3. Transmission test of relay device

Transmission tests for a transmission distance up to 95 m were carried out at the surface, and the received signal strength were measured (see Figure 6-9). All measured signal strengths were above the noise level, as well as on or above the theoretical attenuation line, confirming that the stable transmission was secured [20]. The maximum transmission distance was constrained by the experimental facility.

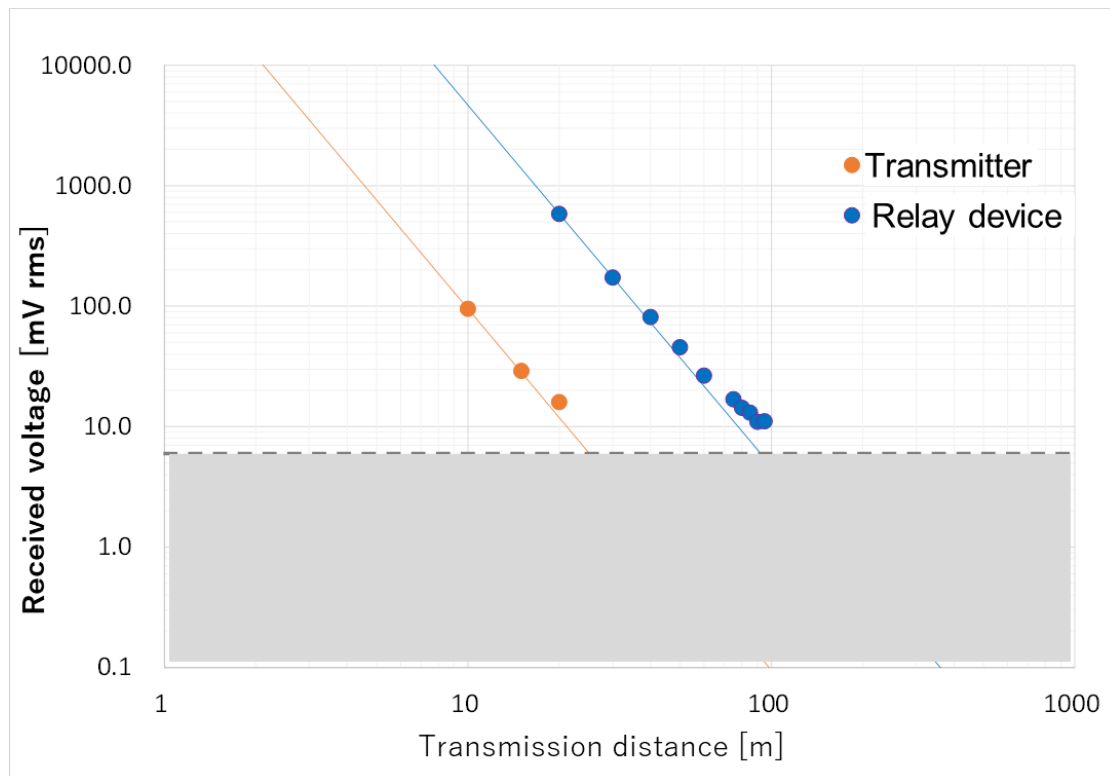


**Figure 6-9: Received voltage from the relay device plotted against the transmission distance. The lines depict the expected signal strength of the relay device (blue) and the transmitter (orange). The shaded area denotes a noise level of 2 mV, where transmission is not possible as learned from past experiments. Modified from [20].**

### 6.2.4. Securing redundancy by introducing multi-route wireless relay system

Furthermore, with the aim of securing the redundancy of the relay system in the case of malfunction, RWMC carried out data rerouting tests using three relay devices with a distance of several meters in a laboratory by the following sequence (see Figure 6-10):

- Step 1: Transmitter 1, 2 → relay device 1 → relay device2 → receiver
- Step 2: Malfunction of relay device 2
- Step 3: Instruction signal from receiver manually sent to relay device 3 to transmit data to the receiver
- Step 4: Transmitter 1, 2 → relay device 1 → relay device 3 → receiver

As result, data from the transmitter were successfully delivered to the receiver even when the data was rerouted from the relay device 2 to 3.

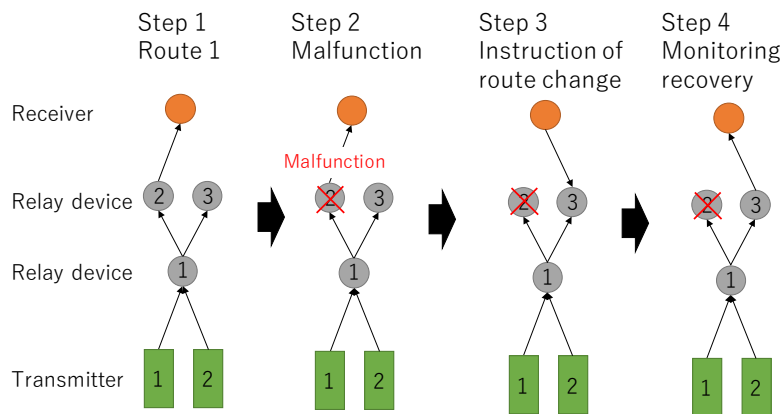


Figure 6-10: Conceptual diagram of route change in the case of device malfunction. Modified from [17].

### 6.2.5. Endurance test for relay device

To validate the durability of the relay system and to evaluate early infant mortality failure rates, an endurance test with the configuration in Figure 6-10 has been performed with a distance of several meters in a laboratory. The test has been continued for 6 months, and more than 4,000 transmissions have been executed without loss of monitored data (see Table 6-3). The number of transmissions for relay devices 1 and 2 were larger than the number of transmissions planned for a 10-years-monitoring (520 times, see Table 6-2). The number of transmissions of relay device 1 was the sum of those of relay device 2 and relay device 3, because the data rerouting test (see Figure 6-10) was carried out during the endurance test.

**Table 6-3: Results of endurance test for the relay system. Modified from [20]**

	Monitored parameters	Measurement interval	Transmission interval	Recorded items	Number of transmissions (actual/planned)	Period of testing
Transmitter 1	<ul style="list-style-type: none"> <li>Temperature</li> <li>Battery voltage</li> </ul>	1hr	1hr	<ul style="list-style-type: none"> <li>Transmission time</li> <li>Signal intensity</li> </ul>	4,353/4,353	1/9/2017, 0h00 to 1/3/2018, 8h00 (181 days or 4,353 hrs)
Transmitter 2						
Relay device 1	-	-		<ul style="list-style-type: none"> <li>Transmission time</li> <li>Battery voltage</li> <li>Current consumption</li> <li>Signal intensity</li> </ul>	4,293/4,293	
Relay device 2						
Relay device 3						
Receiver			-	<ul style="list-style-type: none"> <li>Monitored parameters</li> </ul>	-	

### 6.2.6. Summary

RWMC has developed and tested an underground wireless relay system (multi-stage/multi-route relay system) during the Modern2020 project. This system will enable relay of data sent from miniaturized wireless transmitters to the surface, and the redundancy of the relay system was improved by introducing a function to change the transmission route in case some of the devices fail.

## 6.3. Discussion and conclusions

There are at least two options to send monitoring data from transmitter(s) with sensors from an underground disposal facility to the surface as described in Sections 6.1 and 6.2: the direct transmission over long distances, or the use of multistage relay systems. These systems may have advantages and drawbacks as indicated in Table 6-4.

**Table 6-4: Comparison of two-types of transmission system for long-distance**

Type of transmission system	Advantages	Drawbacks
Long-range transmission system	<ul style="list-style-type: none"> <li>Simple system eases installation</li> <li>Small number of units reduces probability of malfunction</li> </ul>	<ul style="list-style-type: none"> <li>Large antenna requires large space</li> <li>Large power consumption requires large-capacity power source(s)</li> <li>No redundancy if single-route is used</li> </ul>
Multi-stage/multi-route relay system	<ul style="list-style-type: none"> <li>Relatively smaller antennas required</li> <li>Reduced power consumption enables use of conventional battery (for about 10 years)</li> <li>Multi-route secures redundancy</li> </ul>	<ul style="list-style-type: none"> <li>Complicated installation</li> <li>Large number of units increases probability of malfunction</li> </ul>

Taking into the account the experiments feedbacks, it would be more convenient to use relay system at the beginning of the repository’s life. The long-range transmission with unique





transmitter including a large antenna is an option that should be considered afterward in the future of the repository's life.



## 7. Combination of wireless techniques on different ranges

### 7.1. Test of miniaturized transmitter for vibrating wire sensor interface in the WTB

In the Wireless Test Bench (WTB) of the Tournemire URL (see Chapter 5.1), Andra has taken part at an experiment with a short-range wireless transmission system. This system is the result of a RWMC-Andra collaboration and has been realized by the SAKATA Denki Company. The test has been performed from the 23<sup>rd</sup> to the 25<sup>th</sup> of July 2018.

The short-range wireless transmission system consists of the following (Figure 7-1):

- a miniaturized transmitter that contains an antenna, a battery, an interface for sensor measurements and a data logger,
- a vibrating wire extensometer connected to the miniaturized transmitter,
- a portable receiver unit
- a needle indicator for the wireless signal level



**Figure 7-1: Miniaturized transmitter and vibrating wire extensometer (on the left) – Portable Receiver connected to the needle indicator (on the right)**

The aim of the test is to verify that the wireless system is able to transmit sensors data from behind the cell plug of an ILL radiative cell to the entrance of the cell. Hence the test configuration is to put the transmitter and the connected sensor in the access borehole of the WTB and to analyse the signal received by the receiver on the other side of the bentonite plug (i.e. at the entrance of WTB borehole). With the use of the access boreholes, three distances of transmission have been tested from 5 to 10 meters.

This test configuration is described by Figure 7-2.

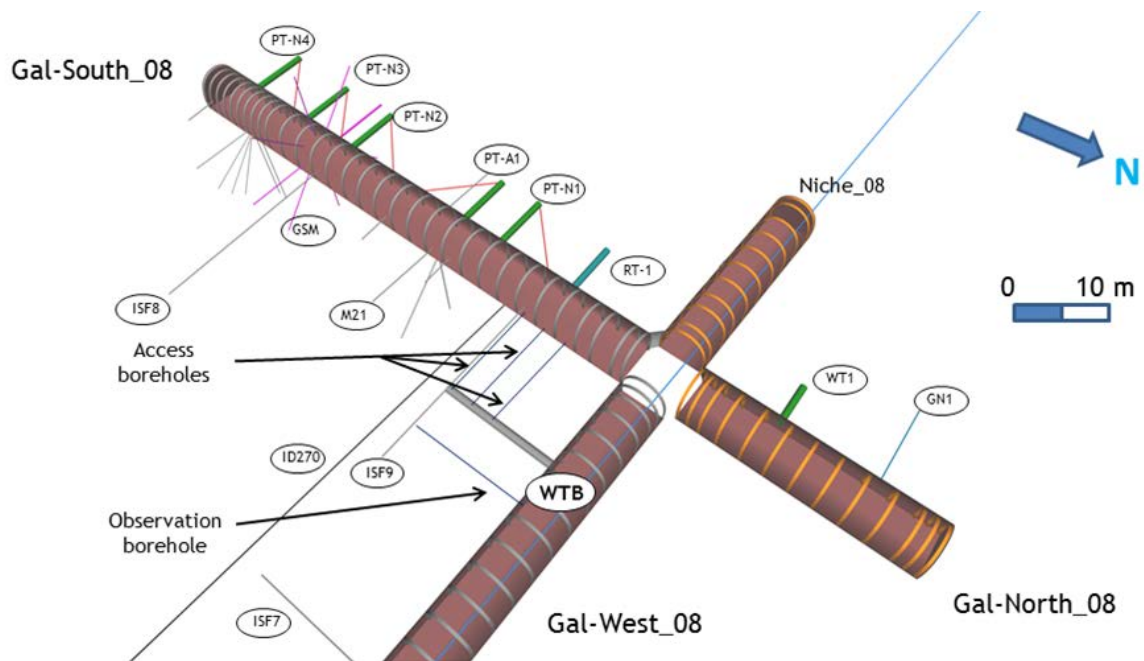


**Figure 7-2: Positions of the transmitter and the receiver in WTB**

The transmitter has a cylinder shape and generates a magnetic flux on the axis of the cylinder. Hence, with the orientation of the access borehole, the signal is transmitted perpendicularly to the WTB borehole. The receiver is positioned at the entrance of WTB borehole with its axis parallel to one of the transmitter. The transmitter (including the antenna) has been installed successively in the three access boreholes. Only the sensor connected to the transmitter was kept on the gallery (cf. Figure 7-3).



**Figure 7-3: Installation of the transmitter in the middle access borehole**

### 7.1.1. Results

In order to receive the sensors data sent by the transmitter, the signal strength at the receiver must be higher than the ambient electromagnetic noise (EM noise). The EM noise at the entrance of WTB borehole was quite low:  $0.6\text{mV}_{\text{rms}}/\sqrt{\text{Hz}}$  at the transmission frequency of 8500Hz.

At each transmission, the signal level reading on the needle indicator has been manually recorded and is presented in Figure 7-4. The signal received was well above the EM noise and all data transmissions were successful. The transmitter consumes a power of 0.55 Watt during transmission. The transmission takes approximatively 20 seconds for ten timestamped measurements.

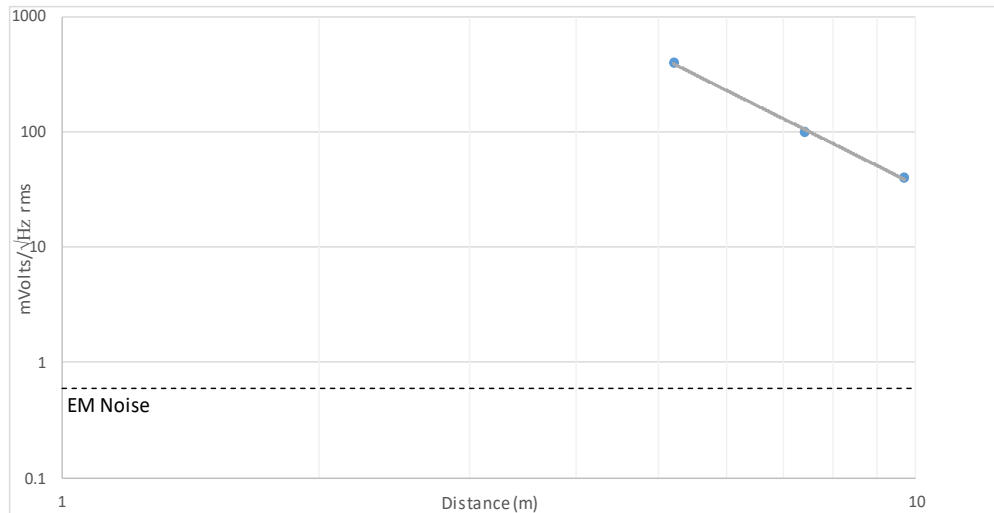


Figure 7-4: Intensity of the wireless signal read by the receiver and the relative EM noise level

The transmitted data recorded on the receiver during the tests has been loaded on a computer. The information transmitted contains a table with the date of measurements, the voltage of the transmitter battery and the sensor data. Two kinds of measurements were done on the vibrating wire extensometer: the natural frequency of the vibrating wire for strain measurement and the electrical resistivity for temperature measurements (Table 7-1).

Table 7-1: Sensors data transmitted

Date	Battery (V)	Data 1 (Hz)	Data 2 (°C)
23/07/2018 06:00	3.285	1014.42	13.77
23/07/2018 12:00	3.305	1014.44	13.82
23/07/2018 18:00	3.275	1014.61	14.08
24/07/2018 00:00	3.285	1014.58	13.91
24/07/2018 06:00	3.285	1014.57	13.86
24/07/2018 12:00	3.275	1014.03	13.99
24/07/2018 18:00	3.29	1013.85	14.16
25/07/2018 00:00	3.275	1013.80	13.85
25/07/2018 06:00	3.285	1013.80	13.81

Table 7-1 present the stable measurements achieved. The temperature difference during the 48 hours of measurements changed less than 1°C in the Tournemire gallery, and the deformation (calculated from the frequencies) is less than 1µm/m (which was expected, because no constrain was applied on it).

The wireless transmission system successfully passed the test at the greatest distance of the test bench. It seems to have also a margin to be able to transmit data 5 meters further.

## 7.2. Evaluation of a wireless monitoring system behind a supercontainer's concrete buffer

This chapter summarizes the work of EURIDICE on evaluating the option to link a new developed fiber optic sensor with a wireless data transmission system that allows monitoring inside a supercontainer waste package design for the disposal of high level radwaste as considered in the Belgian research programme.

### 7.2.1. Introduction

In the current concept, the Belgian waste disposal programme considers the packaging of the high-level radwaste (both spent nuclear fuel assemblies as well as canisters with vitrified waste) in a so-called supercontainer (Figure 7-5). In the supercontainer, the actual waste is first packaged in a thick-walled (few cm) steel overpack, which, in its turn, is covered by a cement-based buffer of about 0.7 m thickness. This buffer has several safety functions, such as radiation shielding, and providing a chemical environment that controls the corrosion of the overpack. The supercontainer is manufactured in a surface facility, which further reduces the complexity of the underground installation works. Due to the inherent radiation shielding, less precautions for the underground works have to be taken. With already a lot of EBS materials integrated in the supercontainer, fewer additional EBS materials have to be installed in situ.

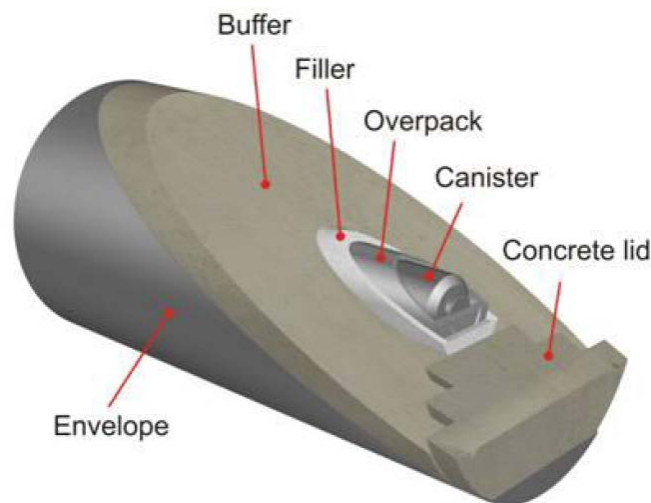


Figure 7-5: Cross-section of a supercontainer with a cement-based buffer as main component.

Monitoring the condition of a supercontainer could be a relevant part of the quality assessment of the supercontainer from its fabrication, over storage up to the final disposal. Although no formal parameter screening has been performed yet for the supercontainer, the attention to the hardening of young concrete, and the chemical buffering by the concrete give an indication for some processes, such as the formation of cracks, and the detection of unexpected corrosion processes. In this context, monitoring of strain, pH, and presence of hydrogen (e.g. due to anaerobic corrosion) could be relevant parameters to monitor. Within Modern2020's WP3.4, some sensors to monitor these parameters have been developed by the University of Mons.

For the implementation of this monitoring, a wireless (or contactless) method is recommended for both safety and reliability reasons. The absence of signal cables through (part of) the buffer of the supercontainer is essential to guarantee the integrity of the concrete buffer. In addition, such signal cables (or optical fibers) are very vulnerable itself where they exit the massive supercontainer structure. And for longer-term monitoring, connecting and disconnecting cables involves additional manipulations that are not desirable when dealing with radioactive waste. A wireless monitoring method could avoid these issues. The idea is then to install a wireless interrogator within the cement-based buffer, at a sufficient depth so that the integrity of this buffer is not compromised. A specific depth could not be

detailed, but it is expected to be comparable to the diameter of the interrogator itself – so at least at a depth of 10 cm from the surface of the supercontainer.

Therefore, after consultation with their subcontractor Com&Sens, EURIDICE decided to aim for a demonstration of a wireless readout of the *mINT* fiber interrogator. The *mINT* device is a miniaturized version of a readout for Fiber Bragg Grating (FBG) Sensors, and has been developed in the frame of the EC SMARTFIBER project (2010-2014; [21]). Miniaturization allows to embed the read-out instrument in the structure to be monitored, and thus to avoid (signal) cabling. A prototype of the *mINT* device, with a diameter of 10 cm and a thickness of less than 1 cm (to affect the structure as little as possible) is shown in Figure 7-6. The wireless interface not only took care of the data transmission, but also of the transmission of power for the device, so no long-life batteries would be needed in this original concept. The wireless technology was based on inductive coupling.

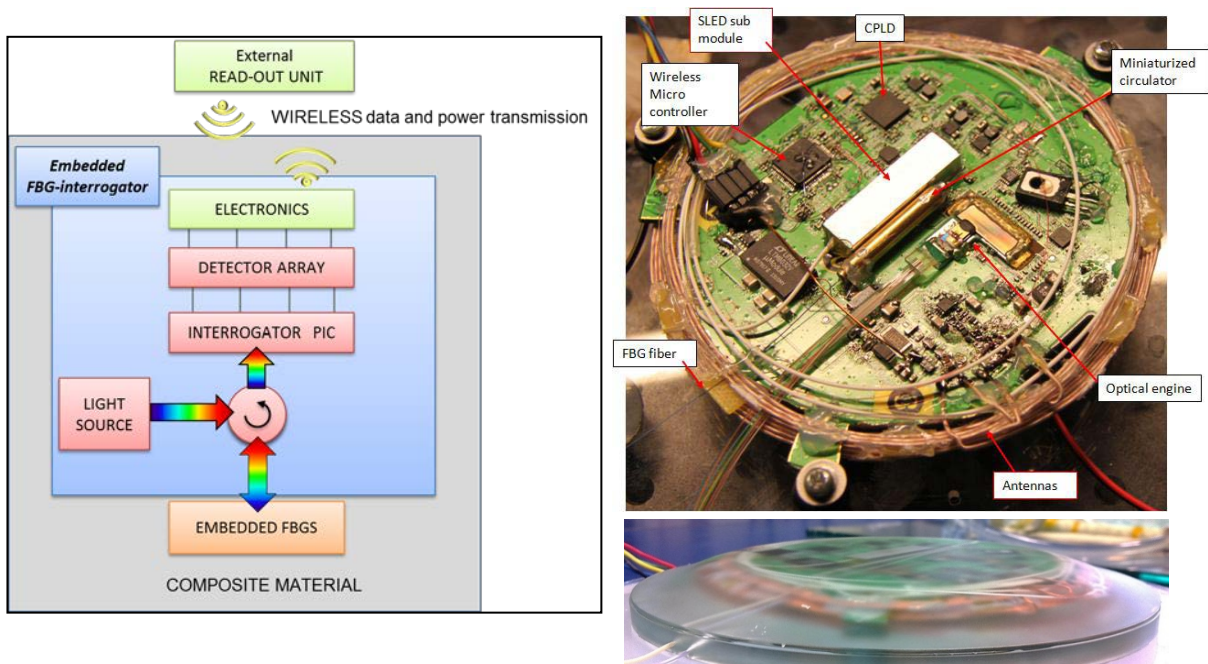


Figure 7-6: Functional diagram (left) and implementation of the first *mINT* prototype (right)

The prototype however did not perform according to the target specifications. Due to non-optimal processing conditions for the Photonic Integrated Circuit (PIC), an important cross-talk between the different Arrayed Waveguide Grating (AWG) spectrometer channels was present. The background power was too high, leading to less accurate measurements. For the *mINT* interrogator itself, a new ‘proof of principle’ version (without the miniaturisation) was assembled (Figure 7-7).

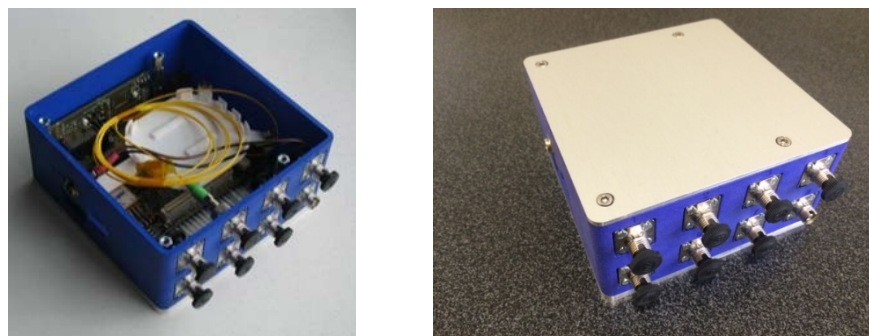


Figure 7-7: Current *mINT* demonstrator (45 x 150 x 150 mm<sup>3</sup>)

The general specifications of the *mINT* appear in Table 7-2.

**Table 7-2: Objectives/Specifications**

Optical Bandwidth	50 nm	Read-out Frequency	1 kHz
Number of Input Channels	1-8	Power consumption	5W
Sensors/channel	5-10	Power supply	5V
Resolution	2.5 pm	Operation temperature	-20°C - +60°C
Absolute accuracy	16 pm	Life time	<i>n.d.</i>

### 7.2.2. General set-up

The objective of this contribution to Modern2020’s Task 3.2 was to link the updated version of the *mINT* to a wireless transmitter. Due to the fixed project budget, the former wireless readout solution could not be kept in the *mINT* technology roadmap. As an alternative, an external solution was considered to demonstrate the feasibility of the wireless *mINT* (in any case without fixed wall power). This was done by connecting an external, commercially available wireless LAN transmitter to the *mINT* through its USB interface.

A first approach using a commercially available USB device server did not work due to the incompatibility between the commercial drivers and the *mINT* readout software necessary to connect over the USB. Therefore, a second approach used a Raspberry Pi Zero W device, with the ‘*VirtualHere CloudHub*’ software installed. The receiving device consisted of a laptop, running the *VirtualHere* client to connect to the *mINT* device, and the *mINT* readout software itself, as shown in Figure 7-8.

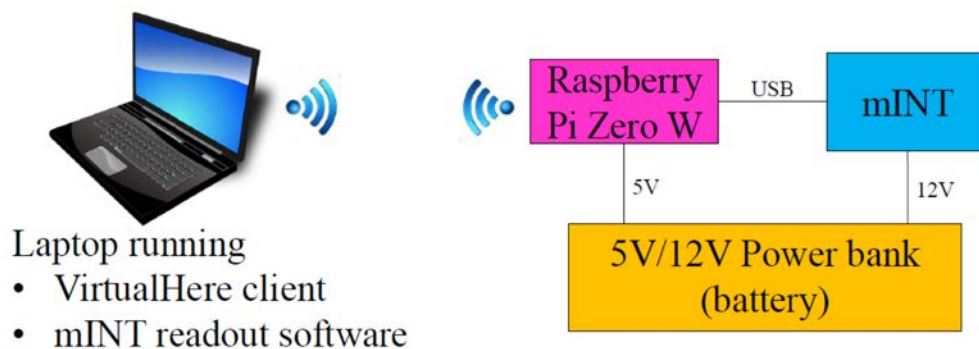


**Figure 7-8: Second approach to demonstrate wireless readout of the *mINT* FBGS interrogator**

### 7.2.3. Experimental testing

This study focused on demonstrating the general feasibility of wireless measurements using the *mINT* interrogator. However, the used set-up was not optimized for low power use, and in a final application, the amount of data to be sent can be clearly reduced by processing with a more powerful hardware than used in this demonstration. Additionally, due to the way the system had to be implemented with the constraints in the available hardware, the entire USB communication with the *mINT* device had to be transferred over the wireless connection, increasing the amount of data that had to be sent quite significantly.

The assembly was not optimized for minimal space/dimensions. The test set-up (*mINT*, Raspberry Pi, powerbank) fits in a 23x21x7 cm<sup>3</sup> box (Figure 7-9).



Figure 7-9: Preliminary assembly fits in a box 23 x 21 x 7 cm<sup>3</sup>

The wireless data transfer uses IEEE 802.11 b/g/n wireless LAN on the 2.4 GHz band, with the corresponding transmission protocols (DSSS for IEEE 802.11b and OFDM for 802.11 g/n). In practical in-house testing using 802.11n, the achieved transmission rates with line of sight at 20 m distance were in excess of 30 Mbit/s. The wireless performance is directly linked to the WiFi characteristics, as the technical solution used (*VirtualHere CloudHub*) creates its own WiFi network. This resulted in a measurement rates that depend on the distances and obstacles, as shown in Table 7-3.

Table 7-3: Wireless performance of the *mINT* readout

Distance		Measurement rate
through air	through concrete	
Close proximity (< 1 m)	-	> 300 Hz
20 m	-	> 50 Hz
20 m	>0.1 m	> 1 Hz

The original transmission distance specified when developing the *mINT* device was 10 cm or smaller. The data rates were not formally measured during the tests, but were more than sufficient to achieve more than 50 FBG measurements per second at these conditions, and more than one measurement per second through a concrete building wall at 20 m distance (Table 7-3). Since all USB communication overhead also needed to be transmitted wirelessly, and not just the raw data, it should be clear that much less energy is necessary if the control software for the *mINT* device would running at an embedded PC, and only the processed data had to be transmitted over the 802.11 b/g/n connection.

A 75 Wh powerbank allowed for about 12 to 25 hours of continuous measurement; the exact time depended on the *mINT* light source intensity. In the case of a discontinuous measurement, longer measurement times are possible (e.g. 1500 days with one measurement/day). The complete measurement system including wireless transfer typically consumes between 3 and 6 W during a continuous measurement (depending on the light source intensity as mentioned above). The wireless transmission as implemented in the project is responsible for approximately 1 W of the power requirements.



A particular design feature of the original *mINT* prototype was wireless energy transmission to power the interrogator (through inductive coupling at 125 kHz). With limited distances in mind, this could also be considered (a possible implementation is then the wireless charging of the embedded battery).

### 7.2.4. Summary

The results indicate that it is feasible to monitor FBGs using a *mINT* device combined with a wireless link and a compact battery to transmit measurements from inside the supercontainer, especially if the required data rate is limited. With an appropriate size battery, it should be possible to monitor stand alone for several years. For very long term monitoring, it will become an economical and practical decision between very large batteries or other power sources without recharging, and a smaller battery that is intermittently topped up using wireless charging.

## 7.3. Evaluation of a combination of wireless techniques on different ranges

In a combined effort, Amberg, Arquimea, IRSN, ENRESA and NRG have evaluated the possibility to provide an integrated solution that links sensor nodes situated in a disposal cell behind a safety relevant barrier (seal) to the surface by a combination of wireless technologies for short and long distance data transmission. In the next sections,

- a short description of the relevant features of the Tournemire site is given by IRSN and NRG (Section 7.3.1),
- main features and performances of the short range data transmission system as provided by Arquimea are summarized (Section 7.3.2),
- main features and performances of the long-range data transmission system as provided by NRG are summarized (Section 7.3.3), and
- a condensed overview of the data acquisition system that is used between both transmission systems is provided by Arquimea and IRSN (Section 7.3.4)

### 7.3.1. Description of the Tournemire site

The French National Radioactive Waste Management Agency (Andra) is responsible for designing, constructing and operating a geological radioactive waste disposal facility. Pending approval, this facility will be opened in eastern France in 2025. With this in mind, Andra has been operating an underground laboratory in Bure (Meuse) since 1999, where it carries out studies and research. To ensure an independent assessment of Andra's project, IRSN has been carrying out its own research at the Tournemire Underground Research Laboratory (URL) in southern France (Aveyron) for the last 30 years.

Located in a former railway tunnel built over 120 years ago, the URL provides access to a shale formation that has geological characteristics similar to the site chosen by Andra. The research carried out at Tournemire enables IRSN to examine certain processes that play an especially important role in ensuring the long-term safety of a geological repository.

#### Geological and structural features

Located on the western border of the Mesozoic sedimentary Causses Basin (Massif Central, Southwest of France), the Tournemire massif is a monocline structure with a mean dip angle of about  $-5^\circ$  towards the North (Figure 7-10). The massif is formed by a 250 meter thick Toarcian shale formation that is interbedded between two aquifers. The lower (Hettangian to Carixian series) and upper (Aalenian to Bathonian series) aquifers are 300 m and 250 m thick respectively, and essentially composed of limestone and dolomite.



The undeformed Upper Toarcian shale formation presents low porosity (8-12%) and low permeability ( $10^{-18}$  to  $10^{-22}$  m<sup>2</sup>) values and was probably buried under 2500±500 m of sediments more than the present day overburden, explaining the over-consolidated state of the shale.

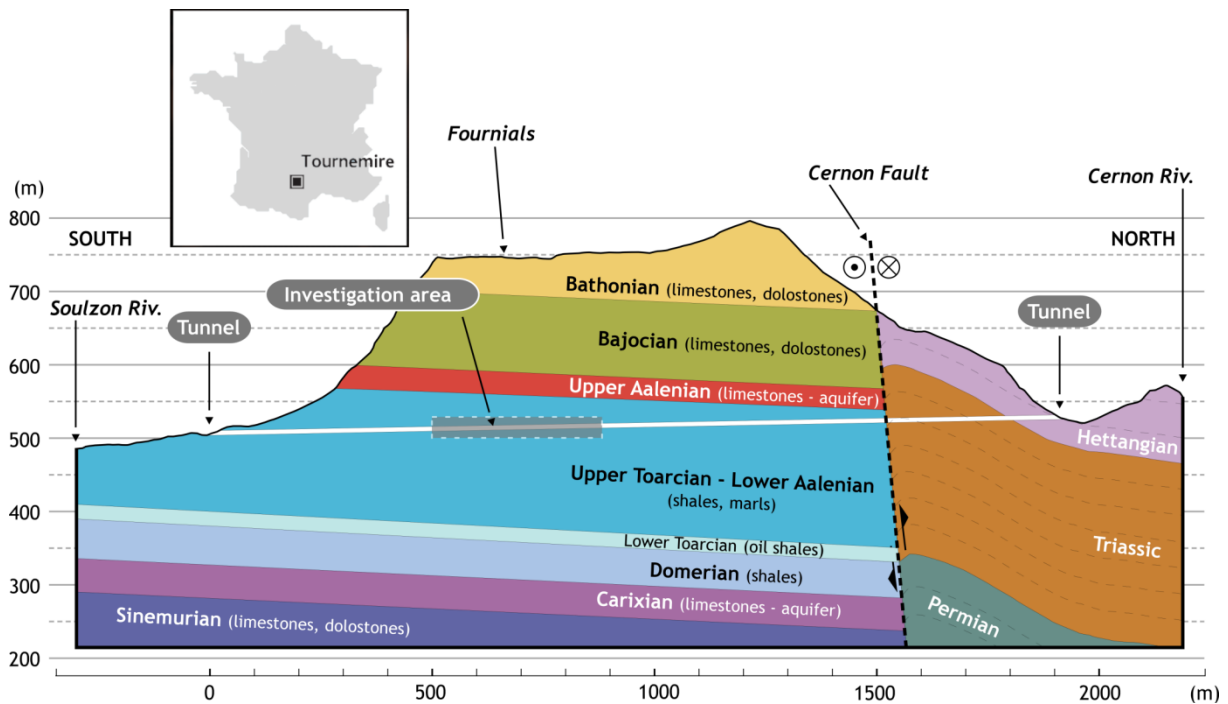


Figure 7-10: General geological cross-section along the Tournemire tunnel

The shale's clay fraction ranges between 20 and 50% of the bulk rock. It is mainly composed of illite (5 to 15%), illite/smectite mixed-layer minerals (5 to 10% with a smectitic proportion of about 10%), chlorite (1 to 5%) and kaolinite (15-20%). The shale also contains 10 to 20% of quartz grains, 10 to 40% of carbonates (mainly composed of calcite with traces of dolomite and siderite) and 2 to 7% of pyrite.

### Tournemire tunnel and URL

Excavated at the end of the 19th century, the old Tournemire railway tunnel is 1,885 metres long. It thus offers a unique opportunity to observe 125 years of disturbances generated by an underground engineering structure excavated in a shale formation.

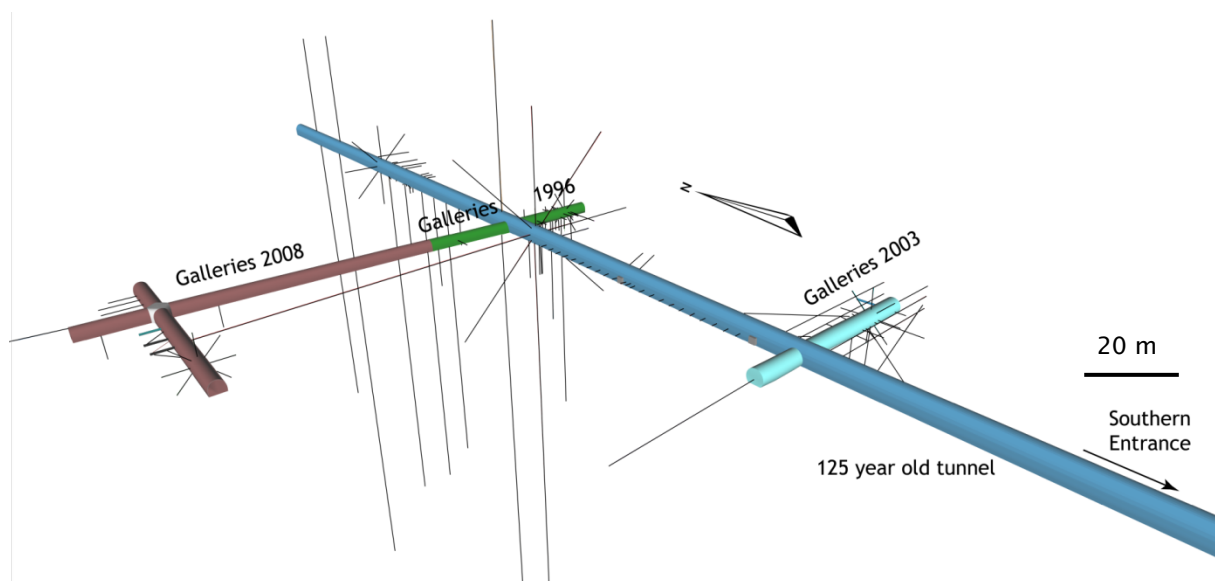


Figure 7-11: 3D diagram of the investigation area

The URL itself is located in a central part of the massif (Figure 7-10 and Figure 7-11). It is made up of the former tunnel, six drifts which are 285 metres in length in total, and over 400 boreholes excavated since 1988, which lead in different directions from either the tunnel or the drifts.

A range of measuring equipment and observation techniques are deployed in the URL to analyse the shale and its behaviour, detect faults using geophysical methods, the water it contains and the rate at which it moves through the formation, as well as disturbances likely to affect this type of rock if it is used for disposal. More recently, the URL has been used to assess the performance of sealing components that may be used in a disposal facility.

### General set-up of the Long-Term Rock Buffer Monitoring (LTRBM)

The Long-Term Rock Buffer Monitoring (LTRBM) is one of the field demonstrators in WP4 of the Modern2020 project. Initially, LTRBM was intended to host part of the new monitoring devices developed in WP3 (mainly wireless devices including long term power supply solutions and new sensors) in order to assess the real performance of the suggested solutions under realistic conditions.

The LTRBM design was based on experience gained from IRSN's in situ SEALEX experiments in the Tournemire URL and the possibility to use the existing infrastructure of these experiments in order to minimise the development costs.

The LTRBM is located close to the other Modern2020 in situ tests: WTB and the electrical tomography test (ERT-IP, see Modern2020 WP3.5) as well as the SEALEX experiments in the Tournemire URL (Figure 7-12). The geographical grouping of these tests was done in order to take advantage of the services already available there: power supply, communications and a new data acquisition system that will be implemented by the end of 2018.

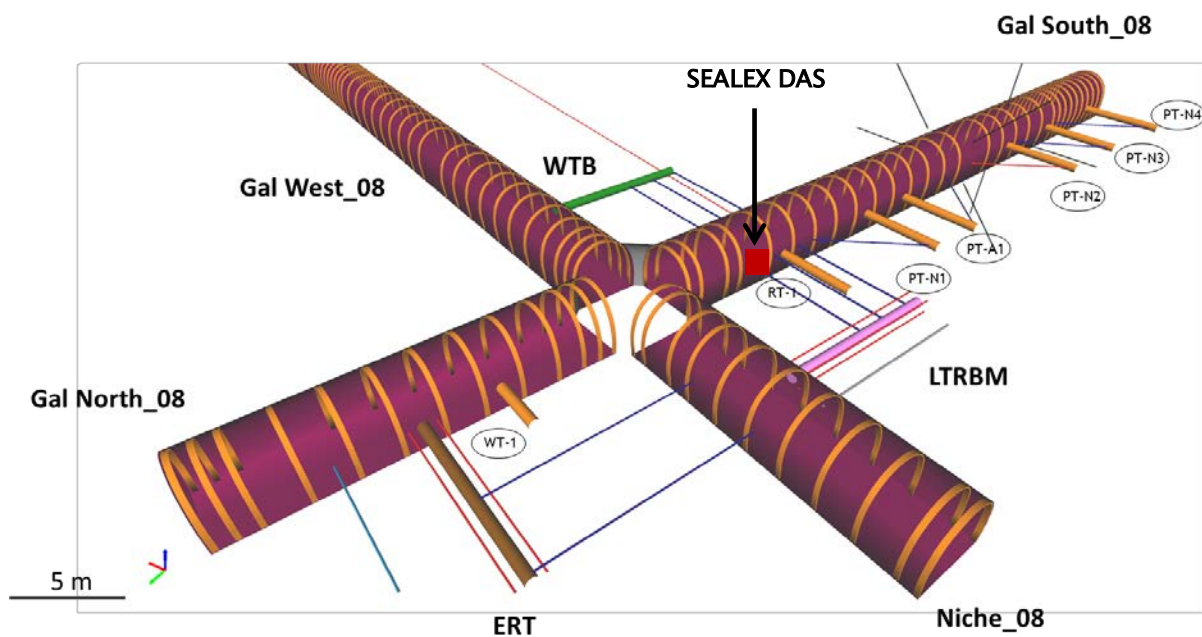


Figure 7-12: 3D view of the location of LTRBM in the Tournemire URL

The initial layout is given in Figure 7-13, using WTB as reference (Section 5.1), and has the following specifications:

- The main horizontal borehole (MB) measures 60 cm in diameter and up to 10 m in length and is parallel to the gallery *South\_08*. The MB will be filled with a bentonite-sand buffer (highly compacted bentonite-sand blocks and granular material based on bentonite pellets) confined by means of a low-pH concrete plug lid. The buffer will be equipped with an artificial saturation system, composed by several hydration mats inside the MB connected to a water injection system, to accelerate the saturation of the buffer.

- The length and composition of the bentonite buffer was determined according to the number, types and operational conditions desired for the prototypes. All the bentonite to be used is a natural sodic Wyoming bentonite MX-80 type. The ratio bentonite/sand, initially 60/40, could be adjusted in function of a scoping calculation on the buffer performance to be done by IRSN to determine expected saturation times and hydromechanical parameter evolution.

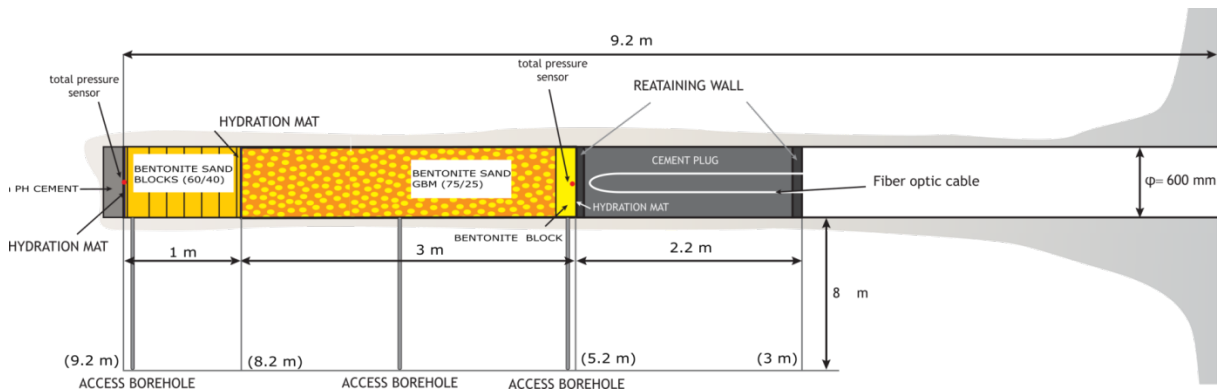


Figure 7-13: Proposed layout of LTRBM

The instrumentation to be installed is summarized in Table 7-4:

Table 7-4: Instrumentation to be installed in the LTRBM

New measuring instruments from WP3 to be tested:	Chemical sensors based on IrOx (pH, Eh & Cl-)
	New Thermocouple Psychrometers
	A THMC smart sensor provided by CTU
Other new measuring instruments to be tested:	Pore water sensors (VW based) attached to a wireless transmitter
	Total pressure (fibre-optics based)
	Probes of electrodes for developing ERT measures and provided by IRSN
Standard measuring instruments to cross check the performance of the new ones:	A fibre optic cable (measuring deformation and temperature) in the cement plug
	Miniature piezoresistive pore pressure sensors
	Piezoresistive total pressure cells
	Capacitive type hygrometers
	Automatic tensiometers
	FDR type water content sensors
	Wescor Psychrometers
Instrumentation required to control and follow the test evolution:	TDRs in the buffer
	Displacement sensors
	Hydraulic pressure sensors
	Weight sensor
	Temperature sensors

The long distance transmitter is placed in the main tunnel north of the test facility, where no additional mechanical support has been installed. This also avoids large interferences from a high voltage power line on top of the main facility. Figure 7-14 shows a top-down view of the facility and the location of the transmitter antenna ("Tx position"). It also shows the high-voltage power line that runs perpendicular to the tunnel. North of the power line, the ridge of the plateau on top of the Tournemire URL is marked by a yellow dashed line. The receiver antenna location is indicated as "Rx position". For the experiments, it was decided to locate the receiver antenna right on top of the transmitter antenna in a coaxial position, resulting in a transmission distance of about 275 m.

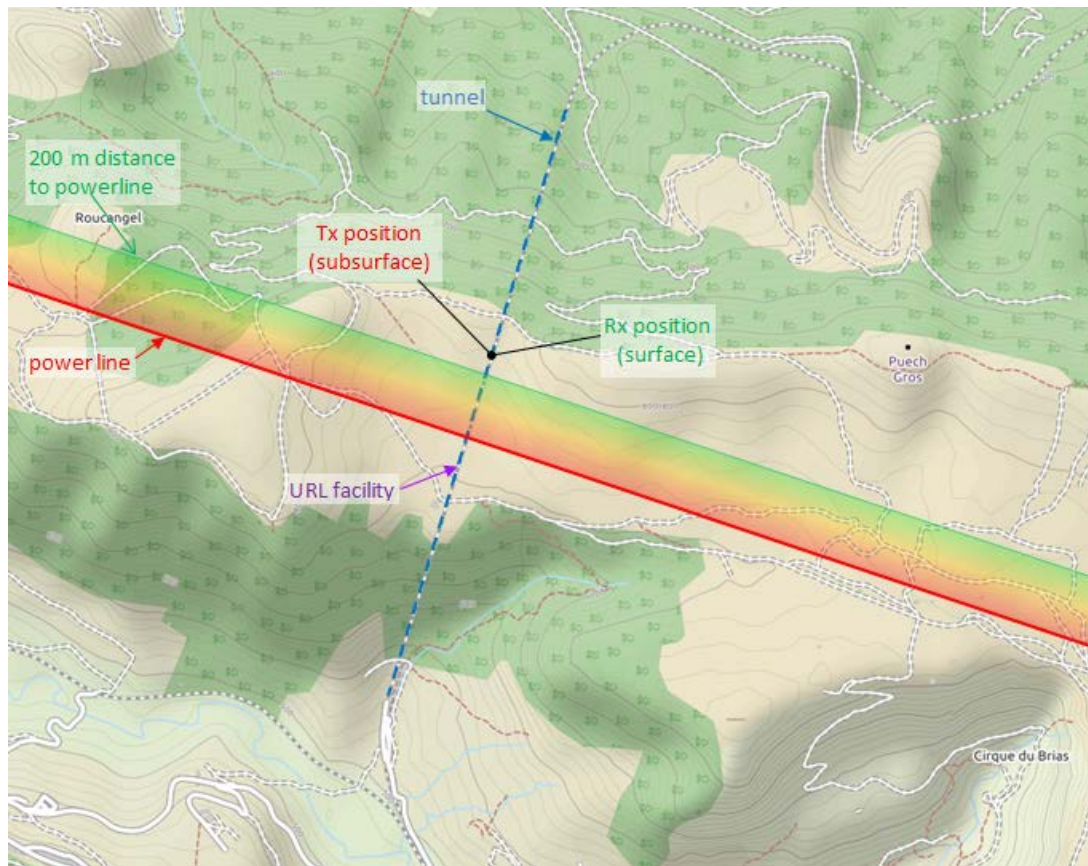


Figure 7-14: Top-down view on the Tournemire URL. Background map © OpenStreetMap contributors ([www.opendatacommons.org/licenses/odbl](http://www.opendatacommons.org/licenses/odbl)).

The planning of the LTRBM implementation foresees the installation of the EBS, hydration system and sensors to take place between June 25 and July 13 2018. The coordination of the activities at Tournemire will be managed by IRSN, whereas the coordination and quality control of the in situ activities will be supervised by Amberg. The demonstration of the combined solution summarized in this chapter will take place in autumn 2018 and will be documented in Modern2020 Deliverable D4.3.

### 7.3.2. Short range data transmission

As part of the combined demonstration in Modern2020's Task 4.3, Arquimea is responsible for the wireless data transmission from the buffered section of the LTRBM to the gallery. Arquimea developed a short range wireless data transmission system based on the prototype used for the tests performed in the WTB that demonstrated transmission through 4 meter of bentonite buffer (Chapter 5.2). The set-up that will be used for data transmission consists of three wireless sensor units (WSUs; see Figure 7-15) described in Chapter 5.2.4 with the following sensors payload:

- 2 new psychrometers developed by Arquimea under Task 3.4.
  - Relative humidity from 95% to 99.96%
- An analog pore pressure transducer
  - 0...10 bar
- A digital capacitive type hygrometer:
  - 0% to 100% Relative Humidity
- Temperature measurements:
  - -40°C to 125 °C

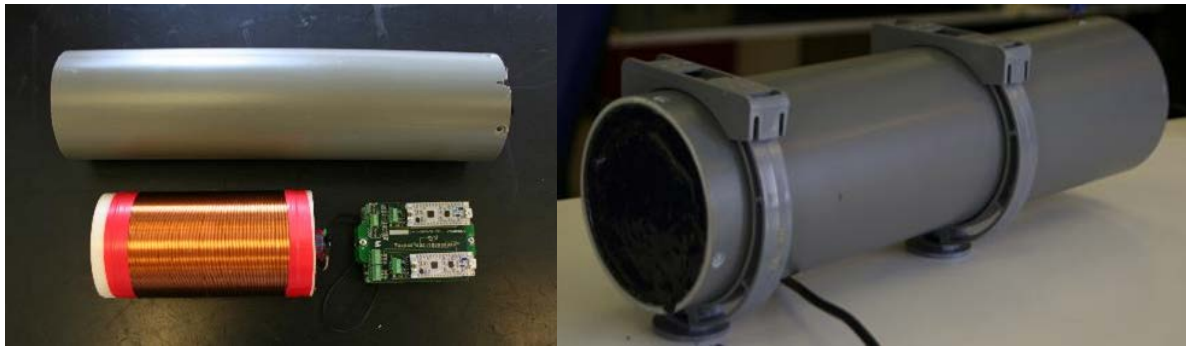


Figure 7-15: Wireless node in preparation for LTRBM (left), final WSU (right).

Two of the WSUs (WSU1 and WSU2) will be installed inside the buffered section of the LTRBM, while the third one (Master WSU) will be installed outside the borehole (see Figure 7-16).

WSU1 and WSU2 shall link with the Master WSU. In case that the Master WSU does not receive a data frame from WSU1 (because of signal attenuation and/or interferences), WSU2 will automatically act as signal repeater for WSU1. In case the Master WSU does not receive any data frame during hydration, the parallel borehole could be used to insert the Master WSU to bring it closer to the buried nodes.

The Master WSU will be on listen mode by default. It will record on a Secure Digital (SD) memory card (readable by serial command) every WSU1 and WSU2 data frame. The Master WSU is in charge for the time synchronization, and its power supply will be supported by a backup uninterruptible power supply (UPS). The Master WSU will be connected to the Data Acquisition System (DAS), so it will be accessible from SEALEX computer for data logging, and - later on - for any computer via a web application (see Section 7.3.4).

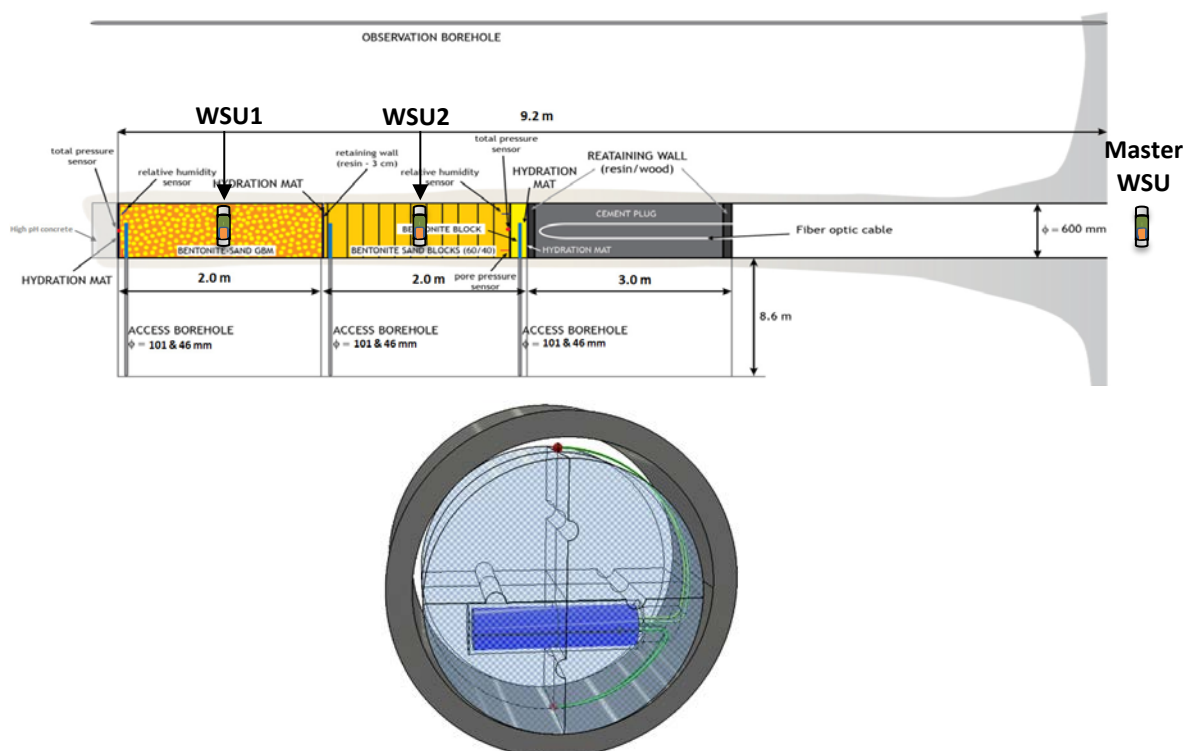


Figure 7-16: Conceptual layout of the LTRBM (top). Installation drawing of WSU in the block buffer of the LTRBM (bottom).

With the sensor configuration chosen for the LTRBM configuration, the energy and currents demanded by each node are shown in Table 7-5. The system is foreseen to measure and transmit data twice a day, and based on that rate, the estimated lifetime of its battery is 4 to 5 years.

**Table 7-5: Energy consumptions of each WSU based on 1 transmission each 12 hours.**

Operation	Power consumption [mW]	Duration per 12 hours time [s]	Daily power consumption [mWh]
Base current	$3.6 \cdot 10^{-3}$	43200	0.086
Data Transmission	3600	0.1	0.2
'Ack' reception	1.84	20	0.02
Active Node	18	120	1.2
Psychrometer (2 units)	850	35	16.53
Pore pressure (4...20 mA) + Capacitive Relative Humidity sensor	180	5	0.05
Total			approx. 18

### 7.3.3. Long range data transmission

NRG developed a long range wireless data transmission system and demonstrated data transmission through 225 m of overburden in the HADES underground research facility at Mol, Belgium [5]. As part of the LTRBM demonstrator (Modern2020 work package 4.3), NRG is responsible for the wireless data transmission from the Tournemire tunnel to the surface plateau on top of the tunnel. The low water table and type of host rock is expected to result in comparable low electrical conductivity that allows using higher (and more efficient) transmission frequencies for long range data transmission than e.g. applied in the HADES URL in Mol [5]. In this section, the general set-up is discussed, and measurement results are presented.

#### Magnetic field propagation

Low frequency data transmission makes use of a magnetic field that is induced by a loop antenna. By forcing a current  $I$  through the antenna, a magnetic moment  $m_d$  can be generated as function of the loop area ( $A$ ), the number of turns of the loop  $N$  and the current:

$$m_d = A \cdot N \cdot I \quad (7-1)$$

In a conducting half-space [22], magnetic field propagation at the surface can be estimated by:

$$H_{radial} = \frac{m_d}{2\pi d^3} T_{radial}; H_{vertical} = \frac{m_d}{2\pi d^3} T_{vertical} \quad (7-2)$$

with

$$\left. \begin{matrix} T_{radial} \\ T_{vertical} \end{matrix} \right\} = \int_0^{\infty} \frac{x^3}{x + \sqrt{x^2 + iG^2}} \exp\left(-\sqrt{x^2 + iG^2}\right) \begin{matrix} J_1(xD) \\ J_0(xD) \end{matrix} dx \quad (7-3)$$

where  $J_0$  and  $J_1$  are Bessel functions of the first kind,  $d$  the axial and  $\rho$  the radial distance to the transmitter,  $m_d$  the magnetic moment,  $G = d \cdot (\sigma \mu \omega)^{1/2}$ , and  $D = \rho/h$ . Additional analyses are published that allow to analyse e.g. horizontal stratified media (e.g. [22], [23]). The validity of these equations is limited to the near-field, under the condition where both  $G$  and  $G \cdot D \ll 1$ . However, as discussed in [5], the optimum transmission efficiency can be found in the extended near-field, and some caution in interpreting the calculated field strength under these conditions is necessary.

#### Experimental set-up

The set-up used for signal and data transmission experiments consists of a signal source, a coil driver for the transmitter antenna, a (tuned) transmitter antenna, a (tuned) receiver antenna, a preamplifier for the receiver antenna, an analog-to-digital converter (ADC), and a (software) demodulator and decoder.



The signal source provided the test signals used for the signal and data transmission experiments. For the data transmission experiments, a battery-based coil driver was developed, that supplies about 60 mW to the transmitter antenna. The transmitter antenna was placed in the northern part of the tunnel, about 1230 m from southern entrance and about 660 m from northern entrance, at a height of about 520 m a.s.l. (Figure 7-17, bottom). The receiver antennas (Figure 7-17, top) were situated at the surface on top of the transmitter, at about 795 m a.s.l. (GPS coordinate: 43°59.312' N, 3°00.920' E), resulting in a transmission distance of 275 m (see also Figure 7-14).



Figure 7-17: Antennas used in Tournemire: Receiver antennas NRG-5 (top left) and NRG-4 (top right), transmitter antenna NRG-6 (bottom)

Several antennas were used in order to perform a variety of measurements. Table 7-6 summarizes the main features of the transmitter- and receiver antennas used in Tournemire.

Table 7-6: Antenna parameter

	NRG-1	NRG-4a + b	NRG-5	NRG-6	NRG-7
purpose	calibration	2D noise & signal attenuation measurement	data transmission (receiver)	data transmission (transmitter)	signal transmission (transmitter)
loop radius $r_l$ [m]	0.042	0.2	2.25	2.25	2.25
number of turns $N$	79	900	7	5	3
inductivity $L_{ant}$ [mH]	0.36	71	0.8	0.42	0.15



The receiver was based on the design used in Mol [5], but was adapted to the higher frequency range considered in Tournemire (5 - 9 kHz). To increase sensitivity, an additional ultra-low-noise input stage was built for the preamplifier, resulting in an improved sensitivity of 0.4 nV/ $\sqrt{\text{Hz}}$  (Figure 7-18).

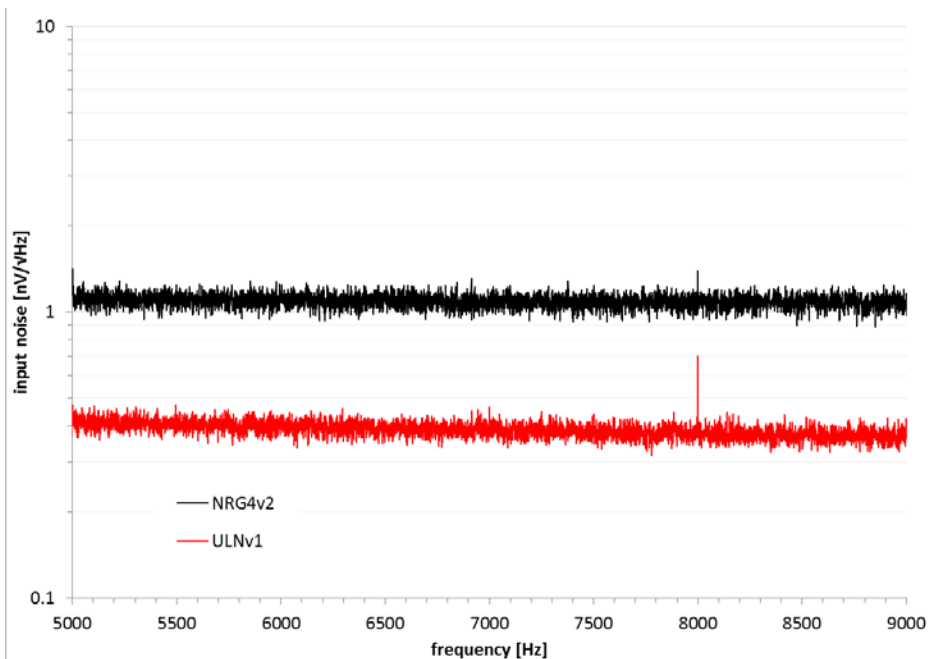


Figure 7-18: Input noise of preamp NRG4v2 and the prototype ultra-low noise input stage ULNV1 for the frequency range of interest.

### Field measurements in Tournemire

Two field measurement campaigns were performed by NRG in Tournemire:

- in the first campaign in July 2017, site characterization measurements were performed;
- in the second campaign in April 2018, data transmission modes were tested.

The objectives of the first measurement campaign were:

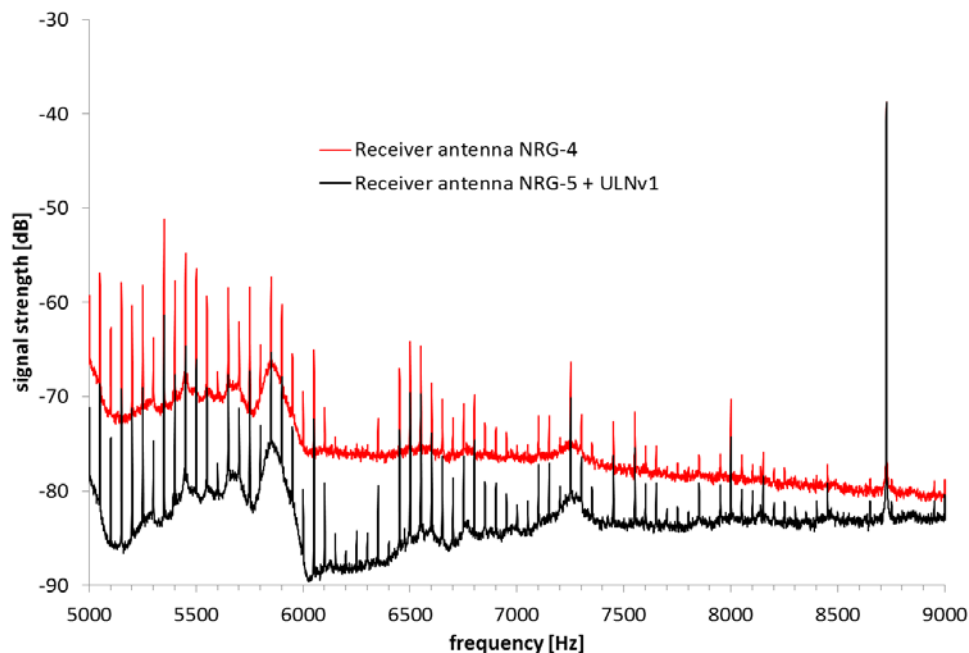
- to quantify the sensitivity of the updated receiver set-up under field conditions;
- to characterize local interferences and background noise levels in vertical and radial direction;
- to characterize magnetic field propagation through the overburden of the Tournemire tunnel;
- to identify potential impact of the rails in (and outside) the tunnel on magnetic field propagation.

In a second campaign, data transmission experiments were performed. Main focus was to study the specific interactions of local interference with the transmitted data stream, and to test different transmission modes (BPSK and QPSK) and data rates (30 - 100 sym/s).

### Results

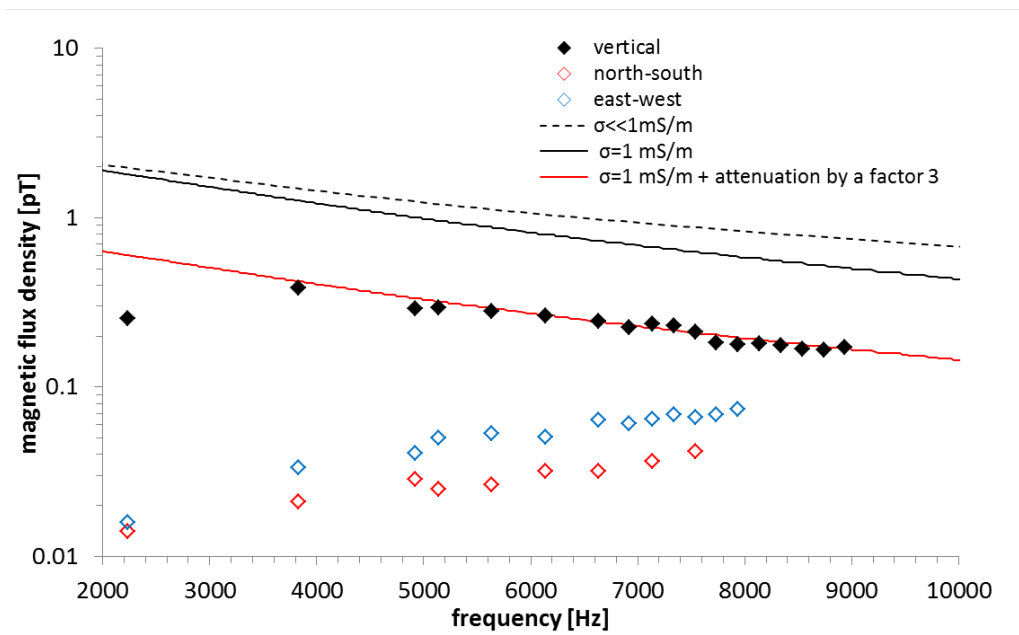
In the first campaign, site characterization measurements have been performed. Interferences from the electric network in vertical direction in Tournemire were found to be much lower than in Mol, with peak values of the harmonics usually less than 20 dB above the background noise (Figure 7-19). Interferences in the north-south direction (perpendicular to the power line) are in a comparable order of magnitude as in the vertical direction (data not shown). Interferences in the radial field in the east-west direction (parallel to the power line) are generally lower than in the vertical field (data not shown).

Figure 7-19 shows also the higher sensitivity of the improved receiver. The vertical background noise between the harmonics is estimated to be about 3 to 7 fT/ $\sqrt{\text{Hz}}$  for the most favourable channels, however, lower background noise ( $<1$  fT/ $\sqrt{\text{Hz}}$ ) could be measured in the Netherlands (data not shown). The background noise in between the peaks consists mainly of bursts, rather than random Gaussian noise. The sensitivity established by discrete Fourier transformation (DFT) has therefore to be interpreted with care when evaluating the necessary power for data transmission.



**Figure 7-19: Vertical signal strength at the surface at Tournemire measured with the set-up used in Mol (red, [5]), and an improved receiver set-up (black). The peak at 8723 Hz is a calibration tone.**

Only a weak frequency-dependent attenuation by the overburden was found, implying an effective electrical conductivity of 1 mS/m or less (Figure 7-20). However, a frequency-independent overall attenuation by a factor of three was found as well. The radial field strength in north-south and east-west directions are much smaller than the vertical field strength, consistent with the low electrical conductivities found. Radial field strengths in north-south direction are lower than in east-west direction. From both can be concluded that the presence of the rails in the tunnel does not favour overall signal propagation, but has an adverse effect on propagation behaviour of the vertical field. This is generally consistent with the attenuation found by Andra during their measurements at Tournemire (Section 6.1). The frequency range of 8 - 9 kHz is identified as most suitable for data transmission. Alternatively, a range with low background noise was found between 6.0 and 6.5 kHz.



**Figure 7-20: Frequency-dependent signal attenuation of the vertical and radial fields at Tournemire (diamonds), and model calculations for several electric conductivities (lines).**

In the second campaign, data transmission experiments have been performed. A critical, low power level of the transmitter has been chosen (60 mW), in order to study the effect of the specific local interferences on the transmission performance. Data transmission has been achieved at a transmission frequency of 8723 Hz, although the application of simple standard demodulation techniques did not allow a flawless reception at the used power level (bit error rate  $\pm 0.1\%$ ). This is - not unexpected - particularly true for higher data rates ( $>60$  sym/s). As part of Modern2020's Task 4.3, the measured and recorded signals will be analysed closer, and more advanced demodulation approaches will be tested. As part of Modern2020 Task 4.3, better demodulation schemes will be implemented, the most suitable modulation modes and data rates will be selected, and - if necessary - the transmitter power will be adapted to allow a reliable data transmission under the conditions in Tournemire.

### Conclusions

The measured attenuation of a magnetic field in the 5 - 9 kHz range due to interactions with the overburden is low in Tournemire, best estimation is an effective electrical conductivity of  $<1$  mS/m. The presence of rails in the tunnel attenuates the field by about a factor of three, equivalent to an increase of the transmission distance to 400 m. Data transmission has been demonstrated successfully at a low power level (60 mW), although a flawless data transmission (bit error rate  $\ll 0.1\%$ ) will require either better demodulation techniques or higher power levels. However, it is expected that data transmission over 275 m of overburden is possible with an antenna power of less than 5 mW/bit of transmitted data. In preparation of the intended demonstration of a combined wireless solution in Modern2020 Task 4.3, additional analyses will be performed on the recorded data transmissions from the second measurement campaign in Tournemire. Based on the outcomes, the most suitable demodulation schemes will be implemented, and the necessary power level will be determined that allows to transmit data with a sufficient low bit error rate ( $\ll 0.1\%$ ).

### 7.3.4. Data acquisition and data link between short and long range transmission systems

Figure 7-21 provides an overview of the overall set-up and data flow in the LTRBM demonstrator: Monitoring data obtained twice a day by the WSUs buried in the LTRBM are transmitted wirelessly to a Master WSU that records the incoming data. The collected data of all WSUs is send via a wired link to a central Data Acquisition System (DAS), which store the data of all wired and wireless sensors located in the LTRBM, and allow to distribute them further via several wired and wireless routes. The long range subsurface transmitter request data from the DAS via a wired interface (RS-485) and transmit these wirelessly to the surface.

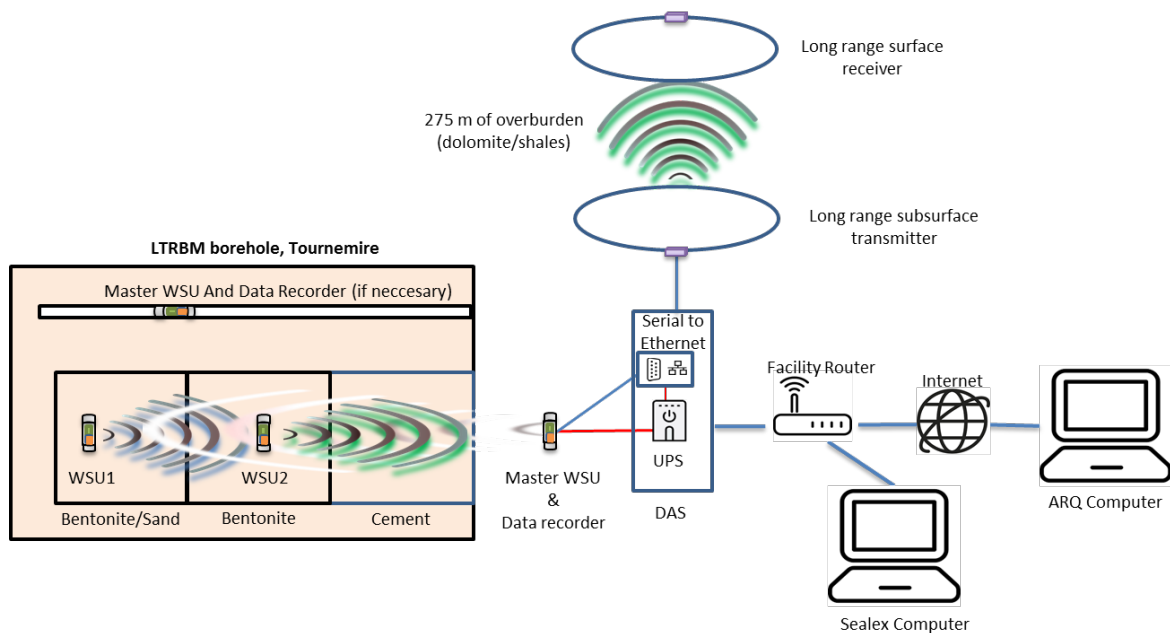


**Figure 7-21: Overall set-up of the wireless data transmission chain out of the LTRBM borehole to the surface**

The LTRBM Data Acquisition System will be temporarily integrated to the existing SEALEX DAS, located at the entry of gallery *South\_08* (see Figure 7-12). Due to a general reorganisation of the Tournemire DAS systems, IRSN will install at the end of 2018 a new DAS in the Tournemire URL. The new DAS will be composed of OMNIALOG data loggers that will be linked together. The data from the loggers will be transferred every 30 minutes to a server/database, a web-software will enable to visualize and download the data. Real time data will be available by connecting directly a PC to the data logger via LAN Ethernet, USB and RS232 connections.

The cabinet for the conventional LTRBM sensors (not shown in Figure 7-21) will be installed at the gallery wall and close to the mouth of the access boreholes driving out the cables of the sensors. The location will be decided upon the final arrangement of the boreholes.

## 7.4. Discussion and conclusions

Within Task 3.2., Andra successfully tested a wireless vibrating sensor in the WTB with a miniaturized transmitter over distances of 5 to 10 m. EURIDICE linked their *m/NT* fiber optic sensors with a commercial wireless LAN transmitter and demonstrated data transmission through the air and a concrete building wall with high data rates (>600kbit/s). Furthermore, a basic set-up and technology was developed and tested to demonstrate a combined solution that allows to monitor in a disposal cell behind a safety relevant barrier, and to transmit the data wirelessly in two stages, through the plug and through 275 m of overburden, to the surface. The combined solution consists of four contributions:

- The LTRBM borehole that has been prepared and constructed at the Tournemire URL by Amberg under the supervision of IRSN. The borehole is backfilled with bentonite and will be hydrated in the second part of 2018, to test under realistic conditions the new sensors and wireless technologies developed in WP3.
- A wireless sensor node developed by Arquimea that allows to monitor inside the borehole and to transmit the data to a receiver node placed outside the borehole. The wireless sensor node was developed and successfully tested with several iterations in the WTB in Tournemire (see also Section 5.2);
- A data acquisition system (DAS), set-up by IRSN and operated by Amberg that collects and stores all data from the wireless sensor node and other (wired) sensors in the LTRBM;
- A long range data transmission system by NRG that transmits data stored in the DAS from the tunnel through 275 m of overburden to the surface. The system was adapted to the local conditions, and signal and data transmission was successfully achieved. Further work will be performed in the next period as part of Modern2020's WP4.3, in order to provide a hardware and software link to the DAS, and to optimize the systems performance under the local conditions.

The overall transmission chain will be demonstrated as part of Modern2020's WP4.3 in end of 2018/beginning 2019.



## 8. Overall conclusions

---

### 8.1. Introduction

Wireless data transmission technologies are used in an increasing number of industrial and consumer applications. Today, wireless technologies that transmit all kinds of data through the air are an abundant part of everyday life. The success of these technologies is related to their robustness and price-effectiveness. In the previous chapters, several solutions for wireless data transmission have been presented, developed as part of the Modern2020 project. These contributions focussed on the transmission of data through solid media: unlike for the transmission in air, high frequencies are considerably attenuated in solid materials. Consequently, distances of more than a meter require specific solutions that are not available on the market today: much lower frequencies are applied than in other established applications, with communication often taking place in a more unfavourable, noisy part of the frequency spectrum. In addition, low frequencies cannot be efficiently generated by electric dipole antennas as used in the vast majority of applications. Therefore many contributions in this report had to apply another, rather uncommon technique: the generation of magnetic fields by loop antennas.

Within the Modern2020 and previous MoDeRn project, major steps has been achieved in understanding, designing and demonstrating specific solutions that allow transmitting data through components of the EBS or the host rock. Different technological solutions covering transmission distances between 0.1 and more than 275 m have been developed and tested, covering a variety of application situations, disposal concepts, and host rocks. A greater understanding of the underlying technical and physical principles has been achieved, and the provided solutions have been tested under realistic conditions, e.g. in the Tournemire Wireless Testing Bench (WTB), from the Tournemire tunnel to the surface plateau, or in the VTT underground laboratory. The performance of the developed technologies depends on a number of factors which, if carefully implemented, allow transmitting data over distances of 275 m through the underground with less than 5 mWs/bit of transmitted data, or over 4 m or more of a (partially) saturated barrier with less than 1 mWs/bit.

### 8.2. Short range data transmission

With respect to short range data transmission over distances larger than 1 m, several options are available, operating at frequencies between 4 kHz and 2.2 MHz. Each one of these technologies has its own advantages, and for all these technologies, successful data transmission through solid media has been demonstrated. The solutions presented in Chapter 5 have reached different states of maturity, with Arquimea's high-frequency WSU (Chapter 5.2) and Amberg's low frequency WSU (Chapter 5.4) providing versatile, "all-in-one" solution allowing to integrate different analog and digital sensors. Both WSU's were tested in IRSN's WTB (Chapter 5.1), raising confidence that WSU readiness will be demonstrated successfully in the LTRBM as part of Modern2020's WP4.3.

VTT's solution, working on a frequency of 125 kHz (Chapter 5.3), enables transmission distances of up to 23 m. Considering the dimensions of current disposal cell concepts ([3], Appendix), this approach addresses the needs of disposal concepts with comparable large plug designs (>10 m length), and provides sufficient range to allow data transmission not only directly through the plug, but in a coaxial, shifted configuration as well. Such a configuration may be of practical interest because it avoids interactions with magnetic permeable materials present in the plug constructions, e.g. steel reinforcements or monitoring devices. Together with the work of Amberg at 4 kHz (Chapter 5.4) and the earlier work of RWMC on 10 kHz, a variety of options and transmission frequencies for various application cases of interest are available on the short range.



### 8.3. Long range data transmission

The experience gained in Tournemire URL, the Hades URL and the Andra URL raises confidence that long range transmission can be achieved over distances larger than 300 m as well: this is necessary because disposal facilities are usually situated at larger depths than URLs. In [5], specific requirements and features of the technology of interest are presented, and custom tailoring of the technical set-up following the outline of these requirements allows developing optimum solutions.

The energy necessary to transmit data can rise up to the 6<sup>th</sup> power of the distance<sup>4</sup>, and one may wonder if transmission distances of 500 m or more are feasible at all. The URLs where the experiments presented in Chapter 6 and Section 7.3.3 have taken place allowed deploying only small, suboptimal antennas of less than 5 m in diameter during the field measurements. However, antenna sizes of 20 m or more are expected to have a performance over a distance of 500 m that is comparable to the performance of small antennas used in the current experiments over 225 to 275 m.

Some concerns are noticed that transmission through a non-homogeneous medium might be more strongly attenuated than implied by the equations used, applying to field propagation through a homogeneous medium. While such concerns are difficult to be answered by numerical model analyses, in Modern2020 and MoDeRn methods have been developed and successfully applied that allow to quantify transmission behaviour by in situ measurements ([5], Section 7.3.3) in a structured and detailed manner. Together with a detailed characterisation of the background noise and local interferences as outlined in Section 7.3.3, these measurements allow the estimation of the power necessary for data transmission in each location of interest with reasonable efforts.

A particular challenge for long range data transmission is to handle the complex interferences occurring at lower frequencies: as shown in [5] and Section 7.3.3, the interference pattern seldom representing random noise, and with standard 'textbook' demodulation and filter techniques, the full potential of this technology might not be achieved. Also in this field, specific solutions are required.

Finally, an interesting contribution to overcome the 6<sup>th</sup>-power-of-the-distance-relation for the energy need was provided in Chapter 6.2: here, a system is presented that transmits data in several stages from the disposal facility to the surface, by making use of several sequential relays, each transmitting over shorter transmission distances. The developed system also allows adapting the transmission route in case of a relay failure. Such a multi-hopping/multi-route relay system introduces additional technical challenges and complexities that, however, where successfully mastered, and an endurance test demonstrated 4000 successful transmissions, even in case of (simulated) failures of single relays.

### 8.4. Combined solutions

In an integrated approach, Amberg, Arquimea, IRSN, ENRESA and NRG evaluated the possibility to offer an overall transmission chain that allows transmitting data measured in the LTRBM demonstrator of Modern2020's WP4.3 to the surface on top of the Tournemire URL (Chapter 7.3). By combining different expertise's and solutions on short and long range, a wireless transmission chain over two stages was projected and will be demonstrated in the second part of 2018 as part of WP4.3.

### 8.5. Current state-of-the-art

**Table 8-1** gives a condensed overview of the performance of the different technologies as achieved in Modern2020, MoDeRn or elsewhere. However, some remarks are necessary to put the outcomes into perspective:

- For long range data transmission, energy efficiency is more critical than for short range transmission. In the latter case, the overall energy budget can be dominated by the sensor's energy need (see e.g. Table 8-1 in [3]). In such a case, further optimization of the data transmission performance would barely improve the overall power need of a wireless sensor node.

<sup>4</sup> This is an (often) used, conservative estimation



- For long range data transmission, results from one location cannot be directly translated to other locations. Energy need depends on transmission distance, electrical conductivity, the maximum antenna size that can be deployed, and local background noise and interferences.
- The use of larger antennas than used for the experiments in Table 8-1 (>5 m) could improve the efficiency and may compensate for larger transmission distances.
- The energy need of the transmitter during 'sleep mode' needs to be known to make up an overall energy budget (see [3]). An inefficient sleep mode might relevantly increase the energy budget and lower the overall performance.
- Currently there is no indication of the minimum data rate necessary for data transmission. However, even with the lowest data rate in Table 8-1, more than 3000 sensor readings can be transmitted per day, assuming 16 bit resolution of the sensor data, and 35% 'overhead' for redundancy, error-detection, and meta information.

**Table 8-1: Performance of current wireless data transmission systems in URLs**

Distance	Transmission mode	Energy efficiency [mWs/bit]	Data rate [bit/s]	Frequency	Host rock/barrier (location)	Reference
0.1 m	Resonant cavity antenna	<0.002	>600'000	2.4 GHz	Concrete buffer	Chapter 7.2
4 m	Electric dipole antenna	~0.5	1200	169 MHz	Bentonite/shotcrete (Grimsel URL)	[4]
4 m	$\lambda/4$ loop antenna	0.75	38'400	2.2 MHz	(Partially) saturated bentonite (Tournemire URL)	Chapter 5.2
5 - 10 m	Magnetic loop antenna	~0.5	75	8.5 kHz	(Partially) saturated bentonite (Tournemire URL)	Chapter 7.1
23 m	Magnetic loop antenna	1000	1	125 kHz	Granite + Air (Espoo research hall)	Chapter 5.3
25 m	Magnetic loop antenna	7	75	8.5 kHz	Sedimentary rock (Meuse / Haute-Marne URL)	[10]
30 m	Magnetic loop antenna	500	20	575 Hz	Bentonite/shotcrete (Grimsel URL)	[11]
30 m	Magnetic loop antenna	1	1600	4.0 kHz	Partially saturated bentonite (Tournemire URL)	Chapter 5.4
225 m	Magnetic loop antenna	1100 - 2000	25 - 100	1.8 kHz	Boom Clay & saturated sandy aquifer (Hades URL)	[5]
250 m	Magnetic loop antenna/relay system	3710	75	8.5 kHz	Sedimentary rock (Honorobe URL)	[12]
275 m	Magnetic loop antenna	2880	75	8.5 kHz	Limestone & Shale (Tournemire URL)	Chapter 6.1
275 m	Magnetic loop antenna	<5	>30	8.7 kHz	Limestone & Shale (Tournemire URL)	Section 7.3.3



## 8.6. Outlook

Wireless data transmission is a promising technology for repository monitoring allowing the use of a variety of sensors placed behind safety-relevant barriers, and major progresses were achieved in Modern2020. In order to bring this technology to a readiness level that allows its application in disposal facilities, additional research is necessary, as outlined in the following bullets:

- A key topic, not only for wireless technologies, is the long-term reliability of wireless solutions. As for all other components of monitoring systems placed behind safety relevant barriers, the life time of the components is essential, because maintenance of the components will be difficult or even impossible. The topic of reliability includes the strengthening of wireless data transmission systems against the harsh environment as present in a geological disposal facility [2], which, however, is expected to be less challenging for data transmission solutions than for sensors. Some work on reliability and radiation hardness has been done in Modern2020's WP3.6, however, more extended testing of wireless solutions e.g. as part of demonstrator activities such as the LTRBM (Modern2020 WP4.3, see also Section 7.3.3) is recommended.
- Another key topic is the energy efficiency, particularly for long range data transmission systems, where it can present a limiting factor the amount of data that can be transmitted. However, also for short range systems, energy efficiency can be of relevance: although analyses of Arquimea's WSU showed that in the current set-up data transmission is only responsible for 1% of the overall energy use (see [3]), improvements of energy efficiency of electronic components are likely, following a general trend in today's electronic industry. Besides, a lower power consumption of WSUs may be necessary considering current options for energy supply (see [3]). More energy efficient solutions are therefore expected to be developed, and if adapted in future WSUs, wireless data transmission may have a larger contribution on the overall energy budget. Furthermore, short range wireless solutions are also in competition with other data transmission systems (i.e. Fiber Optics), and a general understanding of the energy need may support strategic choices on the overall monitoring strategy.
- With the general processes related to long-term data transmission in homogeneous media sufficiently understood, and approaches to evaluate relevant performance parameters of a specific location successfully applied on different locations, it should be possible to adapt existing solutions to other locations of interest as well. However, four topics of interest with respect to future work on long range wireless solutions have been identified:
  - To study the combination of long-term power supply sources as e.g. elaborated in Modern2020 WP3.3 [3], with wireless data transmission systems is seen as an important topic for future research.
  - Potential interactions of transmitter antennas with magnetic permeable materials in a repository (e.g. steel used for gallery support) and the effect of heterogeneities on field propagation through the overburden leave some questions with respect to the transferability of the current results to other locations of interest. With methods to quantify these interactions at hand, site characterization measurements are expected to provide answers with reasonable efforts for a location of interest.
  - Wireless data transmission was successfully demonstrated over a distance up to 275 m, and the relevant parameters that define the overall performance and energy need were determined. While current understanding allows to extrapolate these results to larger distances as well, some need to demonstrate data transmission over larger distances is noted, since the typical repository depth is 500 m or deeper. As noted in the previous bullet, this can be done by a structured approach.
  - The large (man-made and natural) interferences in the 1 - 10 kHz range are a challenging feature of low frequency data transmission. These can be orders of magnitude higher than the receiver sensitivity ([5], 63), and may strongly limit the overall performance. More sophisticated data processing methods are expected to significantly improve the overall performance of a system, and more data on the variability of noise and interferences on day-



to-day level will allow to improve the reliability of the data link under unfavourable conditions (e.g. thunderstorm).

Other topics that need attention in the future include:

- Cost is an important parameter to make the right choice among the different solutions at hand.
- To develop the 125 kHz data transmission technology to a more mature state (Chapter 5.3), the development of an automatic tuning of the antennas is necessary, because surrounding materials and metal parts of an antenna buried in a disposal will change the delicate tuning of the antenna coil. Further topics include improved packaging and increased automation.



## 9. References

---

- [1] MoDeRn, "Monitoring Reference Framework Report," MoDeRn Deliverable D1.2.1, 2013.
- [2] Aitemin, "Technical requirements report," MoDeRn Deliverable D2.1.1, 2011.
- [3] Modern2020, "Long-term power supply sources for repository monitoring," Modern2020 Deliverable D3.3, submitted.
- [4] Aitemin, "Wireless sensor network demonstrator report," MoDeRn Deliverable D3.3.1, 2013.
- [5] T. J. Schröder and E. Rosca-Bocancea, "Wireless Data Transmission Demonstrator: from the HADES to the surface," MoDeRn Deliverable D.3.4.2, 2013.
- [6] P. C. Clemmow, *An Introduction to Electromagnetic Theory*, Cambridge, U.K: Cambridge University Press, 1973.
- [7] G. Lehner, *Elektromagnetische Feldtheorie für Ingenieure und Physiker*. 6th ed., Heidelberg: Springer Verlag, 2008.
- [8] N. J. Cassidy, *Electrical and magnetic properties of rock, soils and fluids*. In: Jol, H.M. (ed.). *Ground Penetrating Radar Theory and Applications*, Amsterdam: Elsevier Science, 2009, pp. 41-72.
- [9] Aitemin, NDA, Andra, NRG, NAGRA, ENRESA, EURIDICE, ETH-Zurich, RWMC, D. TEC, POSIVA, SKB, RAWRA and GSL, "State of Art Report on Monitoring Technology," MoDeRn Deliverable D2.2.2, 2013.
- [10] Suzuki, K., Eto, J., Tanabe, H., Takamura, H., Suyama, Y., Bertrand, J., Hermand, G., "Development of Miniaturized Wireless Transmitter and Borehole type Receiver with Low Frequency Magnetic Waves," in *Proceedings of an International Conference and Workshop of MoDeRn Project, Appendix C, Full Conference Papers*, Luxembourg, 19 - 21 March 2013.
- [11] T. Spillmann, "Application of wired, wireless and non-intrusive standard monitoring techniques. The TEM Project at the Grimsel Test Site - ANNUAL REPORT," Nagra Arbeitsbericht NAB 08-52, Wettlingen, Switzerland, 2008.
- [12] Tsubono, K., Kobayashi, M., Yamakawa, H., Hasui, A., Masumoto, K., Matsushita, T., Sugahara, N., Tanaka, T., Nagai, C., "Development of Wireless Monitoring Systems for Geological Disposal," in *Proc. of the 6th East Asia Forum on Radwaste Management*, Osaka, Japan, November, 2017.
- [13] C. McCaffrey, J. Häkli, M. Hirvonen, I. Huhtinen, K. Nummila, T. Lehtikainen, "Magnetically coupled wireless communication for buried environmental sensor," in *12th International Conference on Environment and Electrical Engineering*, Wroclaw, Poland, 5-8 May 2013.
- [14] Suyama, Y., Takamura, H., Aoki, K., Wada, R., Shimbo, H. and Okutsu, K., "Wireless transmission monitoring in a geological disposal repository (I) Concepts and Advantages," in *Mater. Res. Soc. Symp. Proc., Vol. 1193, pp. 135-141*, 2009.
- [15] Takamura, H., Shimbo, H., Okutsu, K., Suyama, Y., Aoki, K. and Wada, R., "Wireless transmission monitoring in a geological disposal repository (II) Research and Development," in *Mater. Res. Soc. Symp. Proc., Vol. 1193, pp. 143-150*, 2009.
- [16] Eto, J., Suzuki, K., Tanabe, H., Takamura, H., Suyama, Y., Bertrand, J., Hermand, G., "Development of Wireless Monitoring System for Stepwise Backfill/Sealing of Geological



Repository,” in *Proceedings of an International Conference and Workshop of MoDeRn Project, Apendix C, Full Conference Papers*, Luxembourg, 19 – 21 March 2013.

- [17] RWMC, “Development of Advanced Technology for Engineering Components of HLW Disposal, Development of Monitoring Technology,” 2015.
- [18] K. Nishimura, “Data coding technique and basis of error correction: revised edition,” CQ Publisher, pp. 133-134, 2010.
- [19] RWMC, “Development of Advanced Technology for Engineering Components of HLW Disposal, Development of Monitoring Technology,” 2017.
- [20] RWMC, “Development of Advanced Technology for Engineering Components of HLW Disposal, Development of Monitoring Technology,” 2018.
- [21] N. Lammens, G. Luyckx, E. Voet, W. Van Paepegem and J. Degrieck, “SMARTFIBER: miniaturized optical-fiber sensor based health monitoring system,” in *6th International Conference on Emerging Technologies in Non Destructive Testing*, 2015.
- [22] J. R. Wait, “Criteria for Locating an Oscillating Magnetic Dipole Buried in the Earth,” pp. 1033-1035, 1971.
- [23] J. R. Wait and K. P. Spies, “Electromagnetic Fields of a Small Loop in a Stratified Earth,” *IEEE Trans. Antennas and Propagation*, AP-19 (5), 1971.

